UNIVERSIDADE DA BEIRA INTERIOR

Engenharias

Helicopter Flight Modeling and Robust Autonomous Control with Uncertain Dynamics

Sandro Bruno Duarte Alves

Thesis submitted in fulfillment of Master Degree in

Aeronautical Engineering

Supervisor: Prof. Kouamana Bousson

Covilhã, October 2012

"Success is the ability to go from one failure to another with no loss of enthusiasm"

Sir Winston Churchill

Acknowledgements

My first acknowledgment goes to my parents, *Paula Duarte* and *José Alves*, and maternal grandparents, *Mercedes Duarte* and *Mateus Duarte,* the effort, dedication and willingness to provide me, sometimes with great difficulty, with an education of excellence.

I would like also to thank my advisor, Professor *Kouamana Bousson* for is constant support and advice during my thesis work, for sharing with me his knowledge of helicopter dynamics and control, but also is willingness to help me during my academic years at *UBI*.

A special thanks to all the elements that compose and composed the *DCA* for all the support and commitment during my tough years in *UBI*.

To my girlfriend *Marta Baptista*: I would not have accomplished any of this without her presence and support.

I would also like to acknowledge some of the many people which have made enjoyable my life in *Covilhã*: *Carlos Costa, Henrique Matos, Lia Pereira, Marlene Gonçalves, Paulo Mendes, Rafael Santos* and *Tiago Domingues*.

Last, but not least, my appreciation to all members of *"Esquadrilha de Helicópteros da Marinha" (Helicopter Squadron)*, by providing a summer internship in that same unit, triggered an extra motivation for developing this thesis.

Resumo

O controlo de helicópteros tem vindo a adquirir nas últimas décadas maior visibilidade devido à característica desta aeronave. É uma tarefa de elevada dificuldade devido ao próprio sistema ser, já por si, inconstante. O controlo de helicópteros é a junção de várias variáveis como as qualidades de voo e performance, a perícia do piloto, condições atmosféricas, etc. Seja qual for a missão do helicóptero (militar, civil, SAR, etc), precisaremos de parâmetros de controlo precisos, e é nas qualidades de voo que iremos focar a nossa atenção.

O presente trabalho é dedicado então à modelação e controlo autónomo de plataformas de asa rotativa convencional, de forma a que haja uma boa relação entre *robustez* e *performance* do sistema para que, quando hajam perturbações, o sistema possa estabilizar eficazmente e, para se verificar isso mesmo, um helicóptero específico é utilizado para a validação dos métodos elaborados: *DRA research Lynx ZD559* (*Lynx Mk7*), ainda ao serviço do *UK Army Air Corps*.

Na dinâmica do voo do helicóptero, irá ser focada a fase de autorrotação e fase de voo para diferentes velocidades e dois sistemas de controlo irão ser comparados: *LQR normal* e *LQR robusto*.

Projectou-se então os controladores referidos anteriormente comparando os seus resultados através da dinâmica e navegação do modelo já linearizado, para se verificar qual dos dois será mais apropriado para que a plataforma, no momento em que existe uma alteração na dinâmica da aeronave, possa regressar a essa mesma posição o mais brevemente possivel.

Através então dos resultados obtidos, verifica-se em ambos os casos, o sucesso em estabilizar a aeronave e controlar o voo dada uma determinada referência para diferentes velocidades, mas um controlador evidencia-se mais que o outro.

Palavras-chave: *Controlo de helicópteros, robustez, performance, LQR robusto*

Abstract

Helicopter flight control has gained greater visibility in the last decades due to its characteristics. It is a task of high difficulty due to the system being changeable. Helicopter control is the junction of several variables such as the flying qualities and performance, skill of the pilot, weather conditions, etc. For a given configuration of a helicopter (military, civil, SAR, etc.), we need precise control parameters, and is in flying qualities that we focus our attention.

This paper is then dedicated to autonomous modeling and control of conventional rotary-wing platforms, so that there is a good balance between *robustness* and *performance* of the system, so that when there are disturbances, it can stabilize more quickly and effectively and, to verify this, a particular helicopter is used for the validation of the methods elaborated: *DRA research ZD559 Lynx (Lynx Mk7),* still serving the *UK Army Air Corps*.

In helicopter flight dynamics, will be focused autorotation phase and different flight speed phase and two specific control systems will be compared: *normal LQR* and *robust LQR*. Is then designed the controllers previously mentioned, comparing their results through the dynamic model already linearized in order to verify which one is most appropriate for the platform. When there is a change in the balance of the aircraft, it can return to the same position as quickly as possible.

By the obtained results, it's verified in both cases, success in stabilizing the aircraft and controlling it's trajectory given different reference speeds, a controller is most evident than the other.

Keywords: *Helicopter flight control, robustness, performance, robust LQR*.

Contents

List of Figures

List of Symbols

A – state matrix

A_b – blade area (m^2)

B – control matrix

c - chord (m)

cg – center of gravity

g - acceleration due to gravity (m/s^2)

I_{xx}, I_{yy}, I_{zz} - moments of inertia of the helicopter about the *x*-, *y*- and *z*-axes $(kg.m^2)$

I_{xz} - product of inertia of the helicopter about the *x*- and *z*-axes $(kg.m^2)$

I_β – flap moment of inertia $(kg.m^2)$

M_a – helicopter mass (kg)

N_b – number of blades

L, M, N - external aerodynamic moments about the *x*-, *y*- and *z*-axes $(N.m)$

P_e, Q_e, R_e - trim angular velocities in fuselage axes system (rad/s)

p, q, r - angular velocity components of helicopter about fuselage x-, y and z-axes (rad/s)

R - rotor radius (m)

R_{be} - earth frame to body frame matrix

R_{eb} - body frame to earth frame matrix

s – rotor solidity $\frac{N_b \times c}{\pi R}$

S_β – stiffness number $\frac{\lambda_\beta^2 - 1}{\gamma/8}$

T – main rotor thrust (N)

U_e, V_e, W_e - trim velocities in fuselage axes system (rad/s)

u – control vector

u, v, w - translational velocity components of helicopter along fuselage (m/s)

W – helicopter weight

x – state vector

X, Y, Z - external aerodynamic forces acting along the *x*-, *y*- and *z*-axes (N)

X_R, Y_R – components of X and Y from the main rotor (N)

ρ - air density $(kg.m^3)$

Θ_e, Φ_e, Ψ_e- equilibrium or trim Euler angles (rad)

θ, ϕ, ψ – Euler angles defining the orientation of the aircraft relative to the Earth (rad)

β_{1c}, β_{1s} - Lateral and longitudinal flapping angle

Ω – main rotor speed (rad/s)

μ – advance ratio $\frac{V cos\alpha}{\Omega R}$

λ_0 – rotor uniform ΩR

α – disc incidence (rad)

List of Acronyms

AFCS – Automatic Flight Control System
AW – Agusta Westland
BET – Blade Element Theory
DCA – Departamento de Ciências Aerospaciais
DoF – Degrees of Freedom
EMA – Empresa de Meios Aéreos
LQR – Linear Quadratic Regulator
PAF – Portuguese Air Force
PID - Proportional Integral Derivative
RC – Radio Controlled
SAR – Search and Rescue
SISO - Single-Input-Single-Output
UBI – Universidade da Beira Interior

Chapter 1

Introduction

1.1 Motivation

The advantages of the rotorcraft unique flight capabilities have drawn much attention through the years. The main benefit of using a rotorcraft is its ability to perform vertical/short take-off and landing, hover around a specific object and its ability to be controllable when engine failure happens. They have some advantages relative to fixed-wing aircraft: they don't require any relative velocity to produce lift and their vertical/hover flight capability previously mentioned. The main representative of the rotorcraft family is, of course, the helicopter [9].

The number of situations in which helicopters could be deployed and used successfully are various. The following list cites a few of the possible scenarios:

Search and rescue: "*Para que outros vivam*" (That others may live). This is the motto of the 751 Squadron "Pumas". This helicopter squadron of the Portuguese Air Force operates, since 2006, the new *AgustaWestland* AW101 Merlin and their crews have rescued 2757 people since 1978 (Fig.1). These platforms will be able to search quickly and systematically a very large area and could be more readily deployed, unlike fixed-wing aircraft, because of their take-off/landing and hover capabilities and, therefore, saving human lives [17];

Surveillance: Helicopters could perform a variety of surveillance operations and report interesting or unusual activity (fishing fleet control, contraband, etc.)(Fig.2);

Fig.1 – AW101 from PAF during a sea rescue exercise

Fig.2 – Navy commandos during a ship inspection exercise

Law Enforcement: Helicopters could fly overhead to aid police forces in high-speed chases or criminal search operations;

Inspection: Helicopters could inspect high voltage electrical lines (Fig.3), bridges, and dams in remote locations and monitor traffic;

Aerial Mapping: Helicopters could build more accurate topological maps than conventional aircraft with substantial cost savings by flying in smaller and more constrained areas;

Fire Fighting: Helicopters can be fitted with buckets usually filled by submerging or dipping them in lakes, rivers, reservoirs, sometimes in hard to reach areas and perform the fire fight successfully (Fig.4).

Fig.3 - High voltage electrical line inspection

Fig.4 – EMA's Kamov performing a water discharge during a forest fire

Many aviation experts consider the helicopter the most innovative and versatile vehicle known to man. Since helicopters first flew just over sixty years ago, they are without any question one of the most vital aircraft in the world today [9].

1.2 Helicopter Manual Control

The typical configuration of a helicopter is shown in Fig.5. The most important parts of a helicopter are considered: the *main rotor* and the *tail rotor*. The main rotor produces the thrust force for the vertical lift; the tail rotor compensates the torque produced by the main rotor and controls the heading of the helicopter [1].

Due to the strong coupling between the longitudinal and lateral motion, the work of the pilot is harder than an aircraft pilot. In the helicopter pilot case, he must control, simultaneously, four controllers: *collective*, *cyclic*, *anti-torque pedals* and *throttle* (Fig.6) [14]. The *collective* helps the pilot to change the pitch angle of all main rotor blades collectively (i.e., all at the same time). Therefore, if a collective input is made, all the blades change equally, increasing or decreasing total lift or thrust, with the result of the helicopter increasing or decreasing in altitude or airspeed (Fig.5); The *cyclic* can vary the pitch of the rotor blades throughout each revolution of the main rotor system (i.e., through each cycle of rotation) to develop unequal lift (thrust). The result is to tilt the rotor disk in a particular direction, resulting in the helicopter moving in that direction. If the pilot pushes the cyclic forward, the rotor disk tilts forward, and the rotor produces a thrust in the forward direction. If the pilot pushes the cyclic to the side, the rotor disk tilts to that side and produces thrust in that direction, causing the helicopter to hover sideways, performing pitching a rolling moments (Fig.5); The *anti-torque pedals* are located in the same position as the rudder pedals in a fixed-wing aircraft, and serve a similar purpose, namely to control the direction in which the nose of the aircraft is pointed. Application of the pedal in a given direction changes the pitch of the tail rotor blades, increasing or reducing the thrust produced by the tail rotor and causing the nose to yaw in the direction of the applied pedal and yawing moment is performed (Fig.5). The *throttle* controls the power produced by the engine, which is connected to the rotor by a transmission. The purpose of the throttle is to maintain enough engine power to keep the rotor rpm within allowable limits in order to keep the rotor producing enough lift for flight. The throttle is located in the collective lever [15].

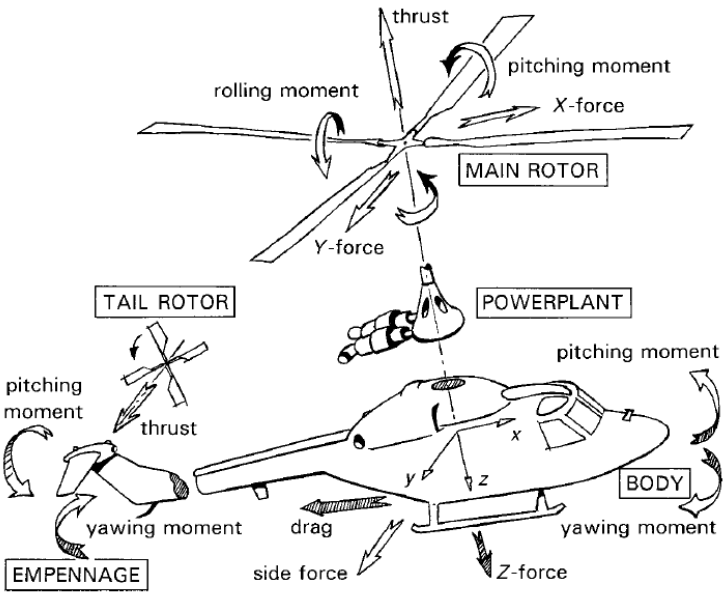

Fig.5 – The modeling components of a helicopter

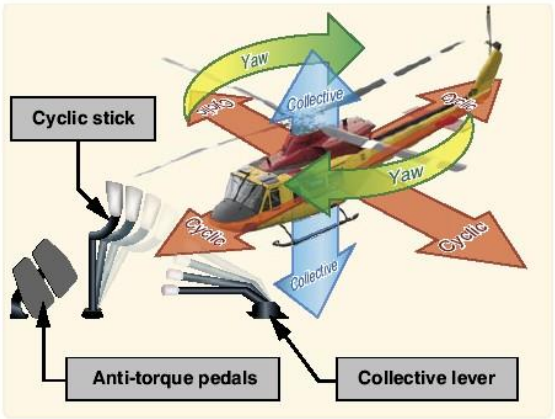

Fig.6 – Helicopter's input controllers

1.3 Helicopter Motion Equations

The behavior of a helicopter in flight is modeled by the combination of the following interacting subsystems: *main rotor*, *fuselage*, *powerplant*, *empennage* (consist of horizontal stabilizer and vertical fin) and *tail rotor* and the resulting forces and moments (Fig.5). The simplified form of orthogonal body axes system is presented in Fig.7 [2].

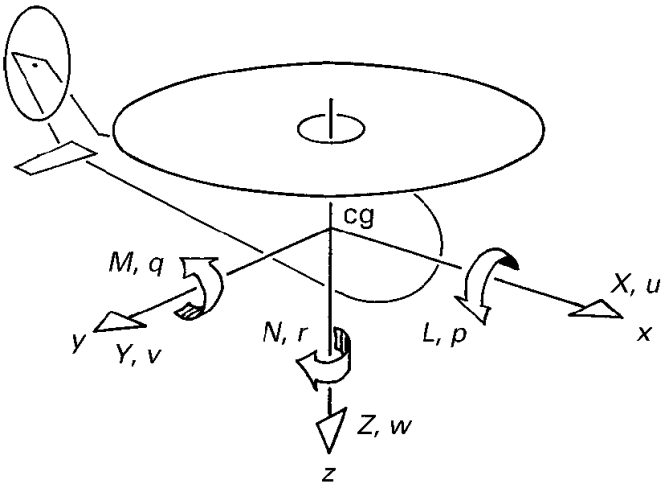

Fig.7 – The orthogonal axes system for helicopter flight dynamics

where:

X, *Y*, and *Z* are the linear forces in the respective axis;
u, *v*, and *w* are the linear velocities in the respective axis;
L, *M*, and *N* are the moments in the respective axis;
p, *q*, and *r* are the angular velocities (roll, pitch and yaw rate) about the respective axis.

1.3.1 *Coordinate Frames and Transformations*

Body fixed and *earth fixed* frames are needed to demonstrate the motion of the vehicle. The first assumption toward dynamic modeling of a helicopter is to consider it as a rigid body with six degrees of freedom [11].

In order to derive the equations of motion, two frames are required. The first one is the *earth fixed* frame. A typical convention of the *earth fixed* frame is the *North-East-Down*, which means *x* represents *North*, *y* represents *East* and *z* points to the center of the Earth (Fig.8).

The second frame is the *body fixed* reference frame. A typical convention of the *body fixed* frame is the *Aircraft-Body-Centered*, which means *x* points forward, *y* points at the right side and *z* points downwards (Fig.8).

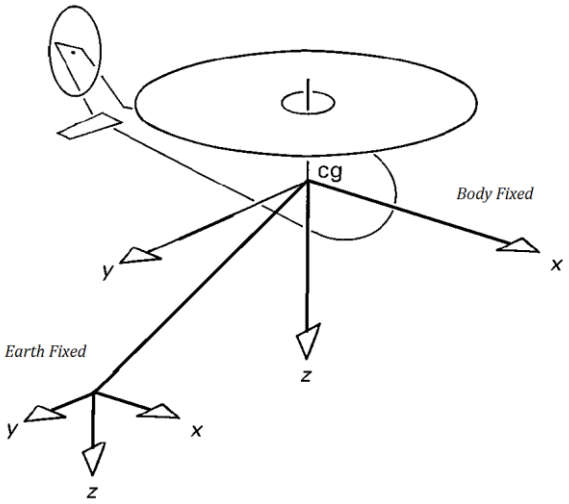

Fig.8 - Helicopter two main frames

To transform between body and earth frames, a rotation matrix *R* is used, i.e., the equations deduction that describe the orientation of the mobile reference in relation to fixed reference is achieved from the rotation matrix (1.4). This matrix is the product result of three rotation matrices, $R(\phi), R(\theta), R(\psi)$ (1.1-1.3) each of which represents the body frame rotation around each axis of the earth fixed frame [18].

$$R(\phi) = \begin{bmatrix} 1 & 0 & 0 \\ 0 & cos\,\phi & -sen\,\phi \\ 0 & sen\,\phi & cos\,\phi \end{bmatrix} \tag{1.1}$$

$$R(\theta) = \begin{bmatrix} cos\,\theta & 0 & sen\,\theta \\ 0 & 1 & 0 \\ -sen\,\theta & 0 & cos\,\theta \end{bmatrix} \tag{1.2}$$

$$R(\psi) = \begin{bmatrix} cos\,\psi & -sen\,\psi & 0 \\ sen\,\psi & cos\,\psi & 0 \\ 0 & 0 & 1 \end{bmatrix} \tag{1.3}$$

where ψ, θ, ϕ (*yaw, pitch* and *roll* respectively), are the *Euler* rotations defining the orientation of the fuselage axes with respect to earth [2].

$$R_{eb} = \begin{bmatrix} cos\theta cos\psi & sen\phi sen\theta cos\psi - cos\phi sen\psi & cos\phi sen\theta cos\psi + sen\phi sen\psi \\ cos\theta sen\psi & sen\phi sen\theta sen\psi + cos\phi cos\psi & cos\phi sen\theta sen\psi - sen\phi cos\psi \\ -sen\theta & sen\phi cos\theta & cos\phi cos\theta \end{bmatrix} \quad (1.4)$$

where R_{eb} is body frame to earth frame matrix, which is obtained multiplying the rotation matrices (1.1-1.3). We can obtain R_{be}, which is the earth frame to body frame matrix, by doing ${R_{be}}^{-1} = {R_{be}}^{T}$

$$R_{be} = \begin{bmatrix} cos\theta cos\psi & cos\theta sen\psi & -sen\theta \\ sen\phi sen\theta cos\psi - cos\phi sen\psi & sen\phi sen\theta sen\psi + cos\phi cos\psi & sen\phi cos\theta \\ cos\phi sen\theta cos\psi + sen\phi sen\psi & cos\phi sen\theta sen\psi - sen\phi cos\psi & cos\phi cos\theta \end{bmatrix} \quad (1.5)$$

1.3.2 *Equations of Motion*

The helicopter can make two types of movements: translational and rotational. It defines changes in position and rotation around the axis. Translational motion, which is the motion of the center of gravity, can be defined by *Newton's* second law and *Coriolis Effect* [1]. Linear accelerations along *x*, *y*, and *z* axes, along the body frame, are defined by [2]:

$$\dot{u} = vr - qw + \frac{F_x}{M_a} \quad (1.6)$$

$$\dot{v} = pw - ur + \frac{F_y}{M_a} \quad (1.7)$$

$$\dot{w} = uq - pv + \frac{F_z}{M_a} \quad (1.8)$$

where u, v, w are the translational velocity components along the fuselage [1], F_x, F_y, F_z are the forces acting in the fuselage and M_a is the helicopter mass [2].

On the other hand, angular accelerations around *x*, *y*, and *z* axes can be defined as [2]:

$$\dot{p} = qr\frac{I_{yy} - I_{zz}}{I_{xx}} + \frac{M_x}{I_{xx}} \quad (1.9)$$

$$\dot{q} = pr\frac{I_{zz} - I_{xx}}{I_{yy}} + \frac{M_y}{I_{yy}} \quad (1.10)$$

$$\dot{r} = pq\frac{I_{xx} - I_{yy}}{I_{zz}} + \frac{M_z}{I_{zz}} \quad (1.11)$$

where p, q, r are the angular velocity components on the fuselage, $I_{xx}, I_{yy,} I_{zz}$ are the moments of inertia of the helicopter [1] and M_x, M_y, M_z are the external aerodynamic moments about the respective axis [2].

Finally, we have rotational kinematic equations. The kinematic equations represent the motion of the helicopter with respect to earth fixed frame [2] and are represented by:

$$\dot{\phi} = p + tg\,\theta(q\,sen\phi + r cos\phi) \tag{1.12}$$

$$\dot{\theta} = q\,cos\,\phi - r\,sen\,\phi \tag{1.13}$$

$$\dot{\psi} = (q\,sen\,\phi + r\,cos\,\phi)\,sec\,\theta \tag{1.14}$$

1.3.3 *Force and Moments acting on a Helicopter*

In order to represent the motion of the helicopter, force and moment effects must be taken into account.

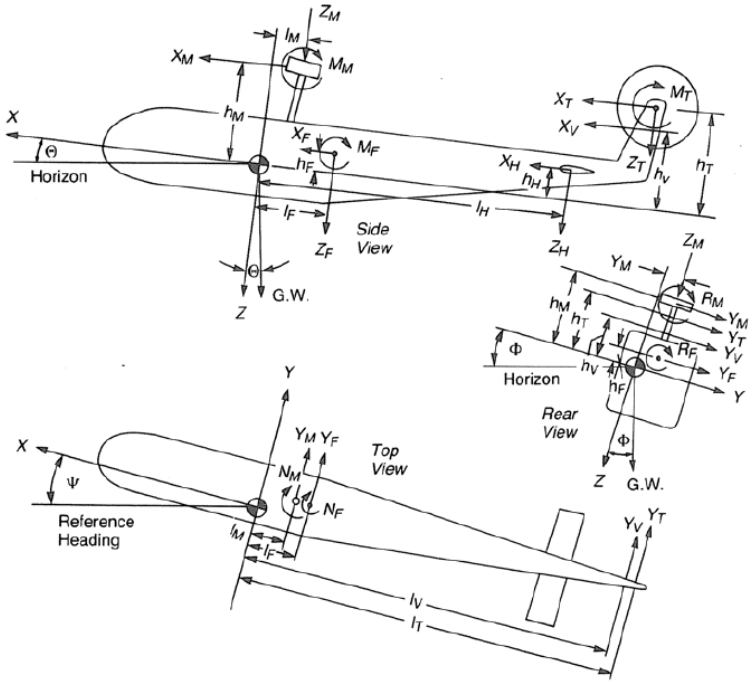

Fig.9 - Forces and moments acting on the helicopter

The set of forces and moments acting on the helicopter has been modeled as follows:

Main rotor forces and moments: For the main rotor thrust, it's assumed that the inflow is steady and uniform. As for the rotor moments, two contributions have been considered.

The first contribution comes from the blade attachment to the rotor head, where the restraint forces can be approximated using a linear torsional spring with a constant stiffness. The second contribution comes from the tilting of the thrust vector [25];

Fuselage forces: The fuselage creates lift and drag. Main rotor downwash effects are also included [25];

Tail rotor forces and moments: The only control input is the collective pitch coming from the pedals, directly influencing induced velocity and therefore thrust [25];

Empennage forces and moments: The horizontal and vertical stabilizers produce lift and drag. The empennage forces take into account the effect of the main and tail rotor wake. The corresponding moments are computed as the forces multiplied by their distance from the helicopter center of gravity [25].

As we stated before, a helicopter can be modeled by combining five subsystems. To define the force and moment effects originated from *main rotor*, *tail rotor*, *gravity* and *drag* on main rotor; mr, tr, g, and d subscripts are used respectively [2].

$$F_x = X = X_{mr} + X_{tr} + X_g \tag{1.15}$$

$$F_y = Y = Y_{mr} + Y_{tr} + Y_g \tag{1.16}$$

$$F_z = Z = Z_{mr} + Z_{tr} + Z_g \tag{1.17}$$

$$L = M_x = L_{mr} + L_{tr} + L_d \tag{1.18}$$

$$M = M_y = M_{mr} + M_{tr} + M_d \tag{1.19}$$

$$N = M_z = N_{mr} + N_{tr} + N_d \tag{1.20}$$

From [2], we obtain the following force equation matrix:

$$F_x = -T_{mr} \sin \beta_{1c} - \sin \theta * M_a g \tag{1.21}$$

$$F_y = T_{mr} * \sin \beta_{1s} + T_{tr} + \sin \phi * \cos \theta * M_a g \tag{1.22}$$

$$F_z = -T_{mr} * \cos \beta_{1s} * \cos \beta_{1c} + \cos \phi * \cos \theta * M_a g \tag{1.23}$$

where $T_{mr}, T_{tr}, \beta_{1c}, \beta_{1s}$, are the main rotor and tail rotor thrust, lateral and longitudinal flapping angle, respectively. The flapping variables are defined in Annex 2.

1.4 Generic Flight Control

The goal is to present a rather comprehensive and well justified analysis for designing controllers for helicopters guarantying stability. We know that a typical flight control system is composed of a mathematical algorithm that produces the appropriate command signals required to perform any flight. The control receives measurement signals from several sensors and triggers a suitable output for operating the helicopter [11].

The most reliable approach to designing a control algorithm and also examining the stability properties of the autonomous flight system is via modern control theory. According to this, the flight controller design is based on the helicopter's dynamic model that we have seen before.

Helicopters are highly nonlinear systems with significant dynamic coupling that needs to be considered during controller design and implementation. The dynamic coupling is attributed to two main reasons: The first one is the helicopter nonlinear equations of motion; the second one is the dynamic coupling between the generated aerodynamic forces and moments.

Helicopters are considered to be much more unstable than fixed-wing aircraft, and constant control action must be sustained at all times. As in most control applications, the helicopter model that is used for control design purposes is just an approximation of the actual nonlinear helicopter dynamics.

1.4.1 *General Flight Control*

So, in order to develop a general flight control system, we must successfully solve the following tasks [11]:

Derive the structure and the order of a parametric dynamic model that best describes the helicopter motion and *including only the necessary variables* that are required to represent the helicopter dynamics;

After the parametric helicopter model is derived, we must determine a nominal feedback control law such that the helicopter tracks a predefined reference trajectory. The design should guarantee that the control inputs remain bounded while the helicopter tracks the reference trajectory;

Given a specific helicopter, we must determine which is the best methodology to accurately extract the values of the parametric model that will be used to implement the controller.

1.4.2 *General Model of a Controlled System*

Consider the system in Figure 10 with *m* inputs and *r* outputs [26]. A *state-space model* for this system, relates the input and output of a system using (1.24).

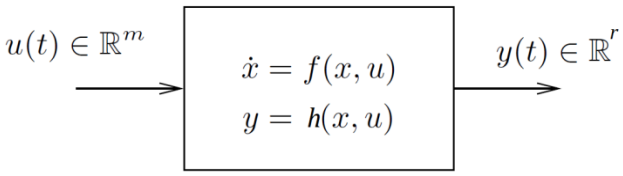

Fig.10 - System with *m* inputs and *r* outputs

The equations governing the behavior of these interactions, commonly take the form of nonlinear differential equations written in the form:

$$\begin{cases} \dot{x} = f(x,u) \\ y = h(x,u) \end{cases} \tag{1.24}$$

with initial conditions $x(0) = x_0$ and $x \in \mathbb{R}^n$ is the state variables column vector; $u \in \mathbb{R}^m$ is the control vector, f and h are nonlinear functions of the helicopter motion, control inputs and external disturbances [11] and $y \in \mathbb{R}^r$ is the observation vector.

1.4.3 Equilibrium State and Control

We mention that $x_e \in \mathbb{R}^n$ is an equilibrium state system with (1.24) if exists a control $u \in \mathbb{R}^m$

$$f(x_e, u_e) = 0 \tag{1.25}$$

In this case, x_e is the equilibrium state system when it suffers a input $u = u_e$, being u_e the equilibrium control system, and to find the system equilibrium conditions, we must solve (1.25).

1.4.4 Linearized Model

In general, most control designs are based on linearized helicopter dynamics using the widely adopted concept of stability derivatives. However, in recent years there is considerable research related to helicopter flight control based on nonlinear dynamic representations. The nonlinear controller designs are mostly valued for their theoretical contribution to the helicopter flight control problem.

Linearized helicopter models have a limited range of validity, which is limited to a flight operation in the vicinity of a certain operating point. On the other hand, nonlinear models provide a relative global description of the flight envelope. It is important that the mathematical model is accurate, yet, manageable enough for the design of a controller [11]. The purpose of linearization and its application is to obtain their corresponding linear model because it is easier to use tools for linear calculus than nonlinear [7].

Around the state and control equilibrium system, which are the solutions of (1.25), the model of (1.24) must be linearized and can be written:

$$\begin{cases} \dot{\tilde{x}} = A\tilde{x} + B\tilde{u} \\ y = C\tilde{x} + D\tilde{u} \end{cases} \tag{1.26}$$

where $\tilde{x} = x - x_e$; $\tilde{u} = u - u_e$; $A \in \mathbb{R}^{nxn}, B \in \mathbb{R}^{nxm}, C \in \mathbb{R}^{rxn}, D \in \mathbb{R}^{rxm}$ and they are the state matrix, the control matrix, the exit matrix and feed forward matrix respectively.

1.4.5 Controllability, Observability, Stability

Controllability, observability and *stability* are among the fundamental concepts in modern mathematical control theory. They are qualitative properties of control systems are of particular importance in control theory. Study of controllability and observability was started in the beginning of the 60's, when the theory of controllability and observability based on a description in the form of state space for both time-invariant and time-varying linear control systems was worked out. The concept of stability is also important, because almost every workable control system is designed to be stable. If a control system is not stable, it's usually of no use in practice. Many dynamical systems are such that the control does not affect the complete state of the dynamical system but only a part of it. On the other hand, in real industrial processes, it's very often possible to observe only a certain part of the complete state of the dynamical system.

Therefore, it's very important to determine whether or not controllability and observation of the complete state of the dynamical system are possible. Roughly speaking, controllability, means that is possible to steer a dynamical system from an arbitrary initial state to an arbitrary final state using the set of admissible controls. On the other hand, observability means that is possible to recover the initial state of the dynamical system from knowledge of the input and output.

There are important relationships between stability, controllability and observability of linear control systems. Controllability and observability are also connected with the theory of minimal realization of linear time-invariant control systems. It should be pointed out that a formal duality exists between the concepts of controllability and observability [27].

1.4.5.1 Controllability

C*ontrollability* concept refers to the ability of a controller to arbitrarily alter the functionality of the system plant.

The system (1.24) is said to be c*ontrollable* when given any initial state $x_i \in \mathbb{R}^n$, any final state $x_f \in \mathbb{R}^n$, and any finite time T, one can find an input signal $u(t)$ that takes the state of (1.24) from x_i to x_f in the interval of time $0 \leq t \leq T$.

To determine if a system is controllable, we can compute the *controllability matrix*, which is defined by

$$\Delta = [B \quad AB \quad A^2B \quad \dots \quad A^{n-1}B] \tag{1.27}$$

The system is controllable if and only if this matrix has rank equal to the size n of the state vector [lqr_2].

1.4.5.2 Observability

Observability is a measure for how well internal states of a system can be inferred by knowledge of its external outputs.

The system (1.24) is said to be *observable* when we can determine the initial condition $x(0)$ by simply looking at the input and output signals $u(t)$ and $y(t)$ on a certain time interval $0 \leq t \leq T$.

To determine if a system is observable, we can compute the *observability matrix*, which is defined by

$$\Theta = \begin{bmatrix} C \\ CA \\ CA^2 \\ \vdots \\ CA^{n-1} \end{bmatrix} \tag{1.28}$$

The system is observable if and only if this matrix has rank equal to the size n of the state vector [26].

1.4.5.3 Stability

The stability of a system is determined by its response to inputs or disturbances. Intuitively, a stable system is the one that will remain at rest unless excited by an external source and will return to rest if all excitations are removed. A system is stable if its impulse response approaches zero as time approaches infinity [20].

1.4.6 Linear Quadratic Regulator Controller Design (LQR)

The theory of optimal control is concerned with operating a dynamic system at minimum cost. The case where the system dynamics are described by a set of linear differential equations and the cost is described by a quadratic functional is called the LQ problem. One of the main results in the theory is that the solution is provided by the *linear-quadratic regulator (LQR)*, a feedback controller whose equations are given in the next page [19].

LQR is an optimal controller because provide the smallest possible error to its input, i.e., one or more of the outputs of the controlled system, combined with minimizing the control output. Compared to *LQR*, a *PID* (Proportional Integral Derivative**)** controller simply creates a stable system, without explicitly optimizing anything. *LQR* is also straightforward to use for multivariable systems; the design procedure is essentially the same as for single-input-single-output (*SISO*) systems [23] .

LQR is a control scheme that provides the best possible performance with respect to some given measure of performance. The *LQR* design problem is to design a state feedback controller *K* (1.32) such that the objective function *J* (1.31) is minimized. In this method a feedback gain matrix is designed which minimizes the objective function in order to achieve some compromise between the use of control effort, the magnitude, and the speed of response that will guarantee a stable system [21].

In a *LQR* project it's necessary that the parameters don't vary during the time and are based in quadratic performance criteria. In this case, we force the helicopter to return to the equilibrium when disturbed. Let's consider the linear system

$$\dot{x} = Ax + Bu \tag{1.29}$$

with $x \in \mathbb{R}^n,\ u \in \mathbb{R}^m,\ A \in \mathbb{R}^{nxn},\ B \in \mathbb{R}^{nxm}$

We are interested in parameterize the control vector of the LQR in a linear vector function

$$u(t) = -Kx(t) \tag{1.30}$$

where $K \in \mathbb{R}^{m \times n}$, in order to minimize the performance index

$$J(u) = \int_0^\infty (x^T Q x + u^T u)\, dt \tag{1.31}$$

where Q is an $l \times l$ symmetric positive-definite matrix and R an $m \times m$ symmetric positive-definite matrix. The second term on the right side account for the expenditure of the energy on the control efforts. The matrix Q and R determine the relative importance of the error and the expenditure of this energy.

The system control law that minimizes (1.31) as the form of (1.30), where *K* is the system gain matrix and it's represented as

$$K = R^{-1} B^T P \tag{1.32}$$

in which P must satisfy the *Algebraic Riccati Equation (ARE*) equation:

$$A^T P + PA - PBR^{-1}B^T P + Q = 0 \tag{1.33}$$

The *LQR* design selects the weight matrix Q and R such that the performances of the closed loop system can satisfy the desired requirements mentioned earlier. The selection of Q and R is weakly connected to the performance specifications, and a certain amount of trial and error is required with an interactive computer simulation before a satisfactory design results [24].

1.4.6.1 Bryson's Rule

A first choice for the matrices Q and R is given by the *Bryson's Rule* [7] whose diagonal is given by

$$Q_{ii} = \frac{1}{maximum\ acceptable\ value\ of\ x_i^2}, \text{with } i \in \{1,2,..,l\} \tag{1.34}$$

$$R_{jj} = \frac{1}{maximum\ acceptable\ value\ of\ u_j^2}, \text{with } j \in \{1,2,..,m\} \tag{1.35}$$

In essence, Bryson's rule scales the variables that appear in $J(u)$ so that the maximum acceptable value for each term is one. This is especially important when the units used for the different components of x and u make the values for these variables numerically very different from each other [lqr_2].

Sometimes the results are not satisfactory and we may have to readjust Q and R. The next method permits a rigorous calculus of Q and R obtaining an optimal system response.

1.4.6.2 *Pole Assignment Controller Design*

A full state feedback controller based on the pole assignment method can improve the system characteristics such that the closed loop system performance will satisfy the requirement criteria. In the *Riccati* equation (1.33), weight matrices Q and *R* are needed. These matrices, and mainly matrix Q, are calculated rigorously in order to make the control more efficient. Pole assignment method allows this computation allowing the calculation of matrix Q basing on eigenvalues imposed on the system by the designer [27].

Here, eigenvalues of the system (1.29) are calculated from the closed loop feedback matrix, $\hat{A}$, when matrix *K* is calculated by (1.32) with matrices Q and *R* determined by *Bryson's Rule*.

$$\hat{\mathrm{A}} = A - BK \tag{1.36}$$

To calculate the matrix Q using the pole assignment method we need the matrix *H* called *Hamiltonian* matrix. It is given by and its eigenvalues, $\lambda_i(H)$, are divided into two groups having the form presented in [1.53].

$$H(q) = \begin{bmatrix} A^T & -BR^{-1}B^T \\ -Q & -A^T \end{bmatrix} \tag{1.37}$$

Group I: λ_1,…, λ_n with $Re(\lambda_i) < 0, i = 1, \dots, n$ (1.38)

Group II: λ_{n+1},…, λ_{2n} with $Re(\lambda_k) > 0, k = n+1, \dots, 2n$

The pole allocation method aims to determine Q so that eigenvalues of *Group I* of the *Hamiltonian* matrix *H* match with the eigenvalues previously specifies by the designer of the controller so that the helicopter has certain flight qualities. Then the equation (1.39) must be fulfilled.

$$\lambda(H)_{group\ I} = \lambda_{specified} \tag{1.39}$$

The matrix Q is constituted

$$Q = \begin{bmatrix} q_1^2 & 0 & 0 & 0 \\ 0 & q_2^2 & 0 & 0 \\ 0 & 0 & \ddots & 0 \\ 0 & 0 & 0 & q_n^2 \end{bmatrix} \tag{1.40}$$

The elements $q_i's$ of the matrix Q are computed by forcing

$$\forall\, i\,, \det\big(\lambda_i I - H(q)\big) = 0 \tag{1.41}$$

Thus, the problem to find the matrix Q becomes a problem of optimization where we have to calculate $q_i's$ values that satisfies

$$f_i(q) = \det\big(\lambda_i I - H(q)\big) = 0 \tag{1.42}$$

So, at this point, what we have to do to find Q is minimize the function J indicated in (1.43)

$$J(q) = \sum_{i=1}^{n} (f_i(q))^2 \tag{1.43}$$

Relatively to matrix R, we can see by cost function (1.31) that its weight is the form $u^T R u$, where we can conclude that when the elements of matrix R are higher, lower is the cost to stabilize the system, i.e, the magnitude of the control variables is lower. Therefore, there is flexibility in choosing the elements of matrix R, where they can be have any values since they are larger than zero, $r_i's > 0$. Thus, matrix R can be simply computed by the ***Bryson's Rule*** as shown in (1.35).

1.5 Objectives

This work has as main objective the control, when a disturbance occurs, of a specific helicopter during flight, hover and autorotation phases, but also to find among the various controllers in the market, which is desirable for the mission.

Being itself, an unstable platform, using controller will obviously indispensable. It was projected then two controllers, robust *LQR* and a normal *LQR*, so we can find the difference between them and compare which one will be best suited for the phases under study, for a linearized and normalized model, and which controller is faster and more accurate to stabilize the model without compromising performance.

The *LQR*, being the most used controller due to its characteristics, was used to stabilized the system and an robust approach was also submitted to this work. The robust approach, which we will see later, was adapted to this rotary wing platform and implemented. They were compared to see which one was faster and smoother to stabilized the model in a particular reference.

In each approach we are also going to use the Bryson and Pole Allocation methods to compare and obtain expected results.

Chapter 2

Problem Modeling

Has we stated before, our work will focus in the control of the platform during leveled forward flight, hover and autorotation. In the forward and hover flight, the state matrix A and control matrix B, for the different velocities are given in Annex 3. These matrices were obtained using *HeliSIM*. *HeliSIM* is a program that creates high-fidelity rotary wing flight dynamic simulation and has two input files: one describing the aircraft configuration data (geometry, mass properties, aerodynamic and structural characteristics, control system parameters); the other the flight condition parameters (airspeed, climb/descent rate, sideslip and turn rate) and atmospheric conditions [1]. In the autorotation case, some of the stability and control derivatives have to be calculated and some variables we must take into account. But first, let's see the general form of trim and stability analysis.

2.1 Trim Analysis

To extract the linear models, the non-linear model must be *trimmed* first. The helicopter, flying forward in straight trimmed flight, is assumed to consist of a main and tail rotor with a fuselage experiencing only a drag force. The rotor is assumed to be teetering in flap, with no moments transmitted through the hub to the fuselage, and the center of mass lies on the shaft, below the rotor. Assuming the fuselage pitch and roll attitudes are close to zero, the following elementary model of trim can be constructed

$$T \approx W \tag{2.1}$$

This condition actually holds true up to moderate forward speeds for most helicopters and can be considered for hover and autorotation. Since the thrust remains constant in *trimmed straight flight*, the pitch angle follows the drag and varies as the square of forward speed. In this simple model, the absence of any aerodynamic pitching moment from the fuselage or tail requires that the hub moment is zero, or that the disc has zero longitudinal flapping [1], [10].

2.1.1 *General Trim Problem*

The most general trim condition resembles a spin mode illustrated in Fig.12. The spin axis is always directed vertically in the trim, thus ensuring that the rates of change of the Euler angles θ and ϕ are both zero, and hence the gravitational force components are constant.

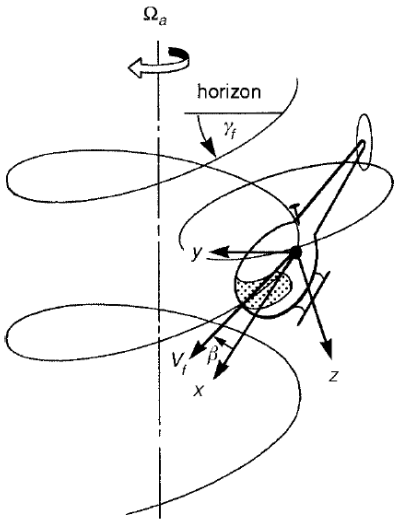

Fig.11 – The general trim condition of a helicopter

The helicopter can be climbing or descending and flying out of lateral balance with sideslip. The general condition requires that the rate of change of magnitude of the velocity vector is identically zero. Considering [1], the trim forms can be reduced to:

$$-(W_e Q_e - V_e R_e) + \frac{X_e}{M_a} - g sen\Theta_e = 0 \tag{2.2}$$

$$-(U_e R_e - W_e P_e) + \frac{Y_e}{M_a} - g cos\Theta_e sen\Phi_e = 0 \tag{2.3}$$

$$-(V_e P_e - U_e Q_e) + \frac{Z_e}{M_a} - g cos\Theta_e cos\Phi_e = 0 \tag{2.4}$$

$$(I_{yy} - I_{zz}) Q_e R_e + I_{xz} P_e Q_e + L_e = 0 \tag{2.5}$$

$$(I_{zz} - I_{xx}) R_e P_e + I_{xz}(R_e^2 - P_e^2) + M_e = 0 \tag{2.6}$$

$$(I_{xx} - I_{yy}) P_e Q_e + I_{xz} Q_e R_e + N_e = 0 \tag{2.7}$$

For the case where the turn rate is zero, the aerodynamic loads, X_e, Y_e, Z_e and the applied moments L_e, M_e and N_e are zero. P_e, Q_e, R_e are the angular velocities in trim. For a non-zero turn rate, the non-zero inertial forces and moments are included in the trim balance. For our first-order approximation, we assume that the applied forces and moments are functions of the translational velocities (u, w, v), the angular velocities (p, q, r) and the rotor controls $(\theta_0, \theta_{1s}, \theta_{1c}, \theta_{0T})$.

The Euler angles are given by the relationship between the body axis angular rates and the rate of change of Euler angle Ψ, the turn rate about the vertical axis, i.e.,

$$P_e = -\dot{\Psi}_e sen\Theta_e = -\Omega_{ae} sen\Theta_e \tag{2.8}$$

$$Q_e = \dot{\Psi}_e sen\Phi_e cos\Theta_e = \Omega_{ae} sen\Phi_e cos\Theta_e \tag{2.9}$$

$$R_e = \dot{\Psi}_e cos\Phi_e cos\Theta_e = \Omega_{ae} cos\Phi_e cos\Theta_e \tag{2.10}$$

We shall concern with the classic case where the four prescribed trim states are defined as in Fig.11: V_{fe} (flight speed) , γ_{fe} (flight path angle), $\dot{\Psi}_e = \Omega_{ae}$ (turn rate), β_e (sideslip).

The question that arises is: what happens if the helicopter trim is disturbed? The answer regarding the effects of small perturbations can be found through analysis of the linearized equations using the concepts of the stability and control derivatives.

2.2 Stability Analysis

In the stability case, we consider only the linear analysis. Classical six DoF is considered and its theory is that higher order rotor and inflow dynamics are much faster than fuselage motions and have time to reach their steady state well within the typical time constants of the whole aircraft response modes. The stability and control matrices appear in the linearized equation (1.29) To do that, we have to find first our state matrix A and control matrix B. The tables of stability and control derivatives are presented in Annex 3 [1].

2.2.1 Description of Stability and Control Derivatives

There are 36 stability derivatives and 24 control derivatives in the standard six DoF set. We shall discuss a limited number of the more important derivatives and their variation with configuration and flight condition parameters. Each derivative is made up of a contribution from the different aircraft components – the main rotor, fuselage, etc. In view of the dominant nature of the rotor in helicopter flight dynamics, we shall give particular, but certainly not exclusive, attention to main rotor derivatives in the following discussion [1]. The three most significant rotor disc variables are the rotor thrust *T* and the two multi-blade coordinate disc tilts β_{1c} and β_{1s}. Considering the simple approximation that the rotor thrust is normal to the disc, for small flapping angles, the rotor *X* and *Y* forces take the form

$$X_R = T\beta_{1c} \tag{2.11}$$

$$Y_R = -T\beta_{1s} \tag{2.12}$$

2.2.1.1 *Translational Velocity Derivatives*

Velocity perturbations give rise to rotor flapping, changes in rotor lift and drag and the incidence and sideslip angles of the flow around the fuselage and empennage. Although flapping appears to be a strongly nonlinear function of forward velocity, the longitudinal cyclic required to trim, is actually fairly linear up to moderate forward speeds. This gives evidence that the moment required to trim the flapping at various speeds is fairly constant and hence the primary longitudinal flapping derivative with forward speed is also relatively constant [1]. The translational derivatives are shown in Annex 4.

2.2.1.2 *Angular Velocity Derivatives*

Our discussion on derivatives with respect to roll, pitch and yaw rate covers three distinct groups – the force derivatives, the roll/pitch moment derivatives due to roll and pitch and the roll/yaw derivatives due to yaw and pitch. Derivatives in the first group largely share their positions in the system matrix with the trim inertial velocity components. In some cases the inertial velocities are so dominant that the aerodynamic effects are negligible (e.g., Z_q , Y_r). In other cases the aerodynamic effects are important to primary response characteristics. Two such examples are X_q and Y_p. We can find these derivatives in Annex 4.

2.2.1.3 *Control Derivatives*

Of the 24 control derivatives, we have selected the 11 most significant to discuss in detail and have arranged these into four groups: collective force, collective moment, cyclic moment and tail rotor collective force and moment. They are represented in Annex 4.

2.2.2 Linearized Model

We consider the helicopter equations of motion described in nonlinear form (1.29) and have obtained the following motion states:

$$x = \{u, w, q, \theta, v, p, \phi, r, \psi\} \tag{2.13}$$

where u, v, w are translational velocities; p, q, r are angular velocities; θ, ϕ, ψ are the Euler angles.

The controls are

$$u = \{\theta_0, \theta_{1s}, \theta_{1c}, \theta_{0T}\} \tag{2.14}$$

where $\theta_0, \theta_{1s}, \theta_{1c}, \theta_{0T}$ is *main rotor collective*, *longitudinal cyclic*, *lateral cyclic* and tail rotor *collective pitch*, respectively. Now we consider the state matrix A and control matrix B from (1.29).

Matrix A is constituted in four parts: longitudinal dynamic A_{long}, lateral dynamic A_{lat}, longitudinal/lateral coupling $A_{long/lat}$, and lateral/longitudinal coupling $A_{lat/long}$. Matrix A can be obtained in Annex [2].

$$A = \begin{bmatrix} A_{long} & A_{long/lat} \\ A_{lat/long} & A_{lat} \end{bmatrix} \tag{2.15}$$

General forms of these four sub-matrices are provided

$$A_{long} = \begin{bmatrix} X_u & X_w + Q_e & X_q + W_e & -g\cos\Theta_e \\ Z_u + Q_e & Z_w & Z_q + U_e & -g\cos\Phi_e sen\Theta_e \\ M_u & M_w & M_q & 0 \\ 0 & 0 & \cos\Theta_e & 0 \end{bmatrix} \tag{2.16}$$

$$A_{long/lat} = \begin{bmatrix} X_v + R_e & X_p & 0 & X_r + V_e \\ Z_v - P_e & Z_p - V_e & -g sen\Phi_e \cos\Theta_e & Z_r \\ M_v & M_p - 2P_e I_{xz} I_{yy} - R_e (I_{xx} I_{zz}) I_{yy} & 0 & M_r - 2R_e I_{xz} I_{yy} - P_e (I_{xx} I_{zz}) I_{yy} \\ 0 & 0 & -\Omega_a \cos\Theta_e & -sen\Theta_e \end{bmatrix} \tag{2.17}$$

$$A_{lat/long} = \begin{bmatrix} Y_u - R_e & Y_w + P_e & Y_q & g sen\Phi_e sen\Theta_e \\ L'_u & L'_w & L'_q + k_1 P_e - k_2 R_e & 0 \\ 0 & 0 & sen\Phi_e tg\Theta_e & -\Omega_a sec\Theta_e \\ N'_v & N'_p - k_3 Q_e & N'_q + k_1 R_e P_e - k_3 P_e & 0 \end{bmatrix} \tag{2.18}$$

$$A_{lat} = \begin{bmatrix} Y_u & Y_p + W_e & g\cos\Phi_e \cos\Theta_e & Y_r + U_e \\ L'_v & L'_p - k_1 Q_e & 0 & N'_r - k_2 Q_e \\ 0 & 1 & 0 & \cos\Phi_e tg\Theta_e \\ N'_v & N'_p - k_3 Q_e & 0 & N'_r - k_1 Q_e \end{bmatrix} \tag{2.19}$$

All the elements in the above matrices can be obtained through numerical perturbation. However, there are gravitational and inertial terms in the matrix that can be accurately obtained through an analytical study of the equations of motion [11].

Finally, the control matrix *B* is provided by:

$$B = \begin{bmatrix} X_{\theta_0} & X_{\theta_{1s}} & X_{\theta_{1c}} & X_{\theta_{0T}} \\ Z_{\theta_0} & Z_{\theta_{1s}} & Z_{\theta_{1c}} & Z_{\theta_{0T}} \\ M_{\theta_0} & M_{\theta_{1s}} & M_{\theta_{1c}} & M_{\theta_{0T}} \\ 0 & 0 & 0 & 0 \\ Y_{\theta_0} & Y_{\theta_{1s}} & Y_{\theta_{1c}} & Y_{\theta_{0T}} \\ L'_{\theta_0} & L'_{\theta_{1s}} & L'_{\theta_{1c}} & L'_{\theta_{0T}} \\ 0 & 0 & 0 & 0 \\ N'_{\theta_0} & N'_{\theta_{1s}} & N'_{\theta_{1c}} & N'_{\theta_{0T}} \end{bmatrix} \tag{2.20}$$

The stability analysis for the helicopter starts with trim to establish steady state condition, to obtain linearized model with respect to the established trim condition, and centers on static and dynamic stability studies. Static stability provides clues on the system's initial response, while dynamic stability looks at the system behavior in the long term.

The importance of stability analysis provides us with a clue to the system characteristics and is also the basis of flight control system design [25].

2.3 Autorotation

What if the engine suddenly fails? The answer is: the helicopter enters in autorotation. Autorotation is the state of flight where the main rotor system is being turned by the action of relative wind rather than engine power. It is the means by which a helicopter can be landed safely in the event of an engine failure. In this case, you are using altitude as potential energy and converting it to kinetic energy during the descent and touchdown [5].

All helicopters must have this capability in order to be certified. Autorotation is permitted mechanically because of a freewheeling unit, a type of clutch, which allows the main rotor to continue turning even if the engine is not running. In normal powered flight, air is drawn into the main rotor system from above and exhausted downward. During autorotation, airflow enters the rotor disc from below as the helicopter descends.

The autorotation is also studied, but there are some variables to take into account. One of them is, considering the Blade Element Theory (BET) shown in Fig.11, since the optimal descent is purely vertical [3], we assume $\phi = 0$, i.e., $\theta = \alpha$. The rest of the studied variables are calculated in Annex 2.

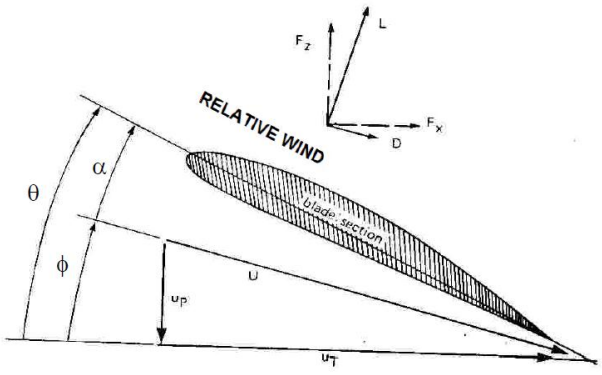

Fig.12 – Blade Element Theory

To the work at hand, the platform as having a rigid structure has about 36 differential equations, which makes the problem really non-linear and very difficult to solve. The following simplifications are implemented in order to make the autorotation problem easier:

1. The helicopter structure is considered to be absolutely rigid;
2. Longitudinal and lateral motions are uncoupled so they can be treated independently;
3. One DoF (throttle) is eliminated and the rotor speed is set as constant;
4. The blades are assumed as uniform and the lag bending, elastic twist, and axial deflections are disregarded (rotor blade coning β_0 and flapping motion β_{1c} and β_{1s});
5. The blades do not bend or twist elastically;
6. The blades have homogeneous mass distribution;
7. Climb angle and sideslip angle are set as zero;
8. Induced wake flux and ground effect are ignored.

Chapter 3

Helicopter Robust Control Modeling

We have seen earlier the normal *LQR* approach, now we are going to see a proposed robust method based in the *LQR* approach.

3.1 Robust Control

Modern control techniques have allowed engineers to optimize the control systems they build for cost and performance. However, optimal control algorithms are not always tolerant to changes in the control system or environment [4].

Robust control is a method to measure the performance changes of a control system with changing system parameters. Application of this technique is important to building dependable embedded systems. The goal is to allow exploration of the design space for alternatives that are insensitive to changes in the system and can maintain their stability and performance. One desirable outcome is for systems that exhibit graceful degradation in the presence of changes or partial system faults.

Based on classical automatic control theory, which we've seen before, R.T. Yanushevsky considered an approach of robust control systems with uncertain parameters which is based on the optimal control problem with a specified performance [4], [13].

3.1.1 *Statement of the Problem*

Let's consider a linear controllable plant described by the equation (1.29). It's assumed first that only elements of the state matrix A are not known exactly, i.e.

$$A_1 \leq A \leq A_2 \tag{3.1}$$

where $A_1 = |a_{1ij}|$ and $A_2 = |a_{2ij}|$ characterize the upper and lower bounds of A, respectively.

The robust control problem consists of finding controller equations that make the closed-loop system asymptotically stable for all state matrices of the form of (3.1). The procedure of analytical controller design for systems (1.29) is based on minimization of the equation (1.31).

Unlike the standard procedure of the analytical controller design, in the case under consideration we lack the proper information to calculate the matrix *P*. It is known that minimization of the functional

$$J_1(u) = \int_0^\infty e^{2\gamma}(x^T Q x + u^T R u)\, dt \tag{3.2}$$

subject to the boundary conditions described by (1.29) is equivalent to minimization of (1.31) subject to the system

$$\dot{x} = A_0 x + Bu \tag{3.3}$$

and we have that

$$A_0 = A + \gamma I \tag{3.4}$$

where I is the identity matrix; the eigenvalues of the matrix A_0 are shifted by γ in comparison to the eigenvalues of the matrix A.

A special optimal control problem for (1.29) with fixed constant parameters is considered. Some information regarding choosing γ in (3.2) can be obtained from the estimate of the upper bound of the eigenvalues of the state family matrices (3.1).

We will call γ the upper bound of the eigenvalues of the matrix A of (1.29) if the half-plane $Re\ s \geq \gamma$ contains no eigenvalues (3.1) of A. A simple estimate of γ follows from the expression

$$\gamma = min\left[max \sum_{j=1}^{n} |a_{ij}|, max \sum_{i=1}^{n} |a_{ij}|\right] \tag{3.5}$$

Then, we can say that given a controllable system (1.29) with the elements of A satisfying (3.1), the optimal control law (1.32) makes (1.29) and (1.32) asymptotically stable for all matrices satisfying (3.1).

The proposed method is based on the consideration of special optimal control problem for the system with specified constant parameters. The estimate of the upper bound of the eigenvalues of the state matrices family, can be used to determine the exponential factor used in the performance index. The given procedure allows us to build robust linear systems as well as a wide class of nonlinear systems.

3.1.2 *Conclusion*

After we applied the proposed method [4] to the helicopter control, rapidly we saw that, by adding (3.5), the outcome graphics didn't satisfied what we were looking for, which was a faster and smoother platform control. Instead of that, we've obtained great amplitude of values. To overcome this problem, we verified that γ values were to great and this approach only worked for a specific interval. So, instead of finding the minimum value of the matrix sum of columns and rows, we did the opposite, i.e., we found the maximum value of the matrix sum of columns and rows. We considered (3.6) without compromising the stability.

$$\gamma = max\left[min \sum_{j=1}^{n} |a_{ij}|, min \sum_{i=1}^{n} |a_{ij}|\right] \tag{3.6}$$

The results shown on Chapter 4 are the proof that this alteration works and we can get a faster stabilization without compromising the performance of the system.

Chapter 4

Validation

In the different forward flight velocities and hover, we've obtained the state and control matrices from [1] and they are represented in Annex 5. For the autorotation, the state matrix and control matrix was calculated and is represented in Annex 3. In this validation process, we are going to observe the difference between the normal *LQR* and robust *LQR* response. The results are presented to autorotation, hover and forward flight at 20 knots. The results for the rest of the velocities are presented in Annex 5.

4.1 *LQR* Simulation – Westland Lynx in hover flight (V = 0)

Longitudinal Simulation

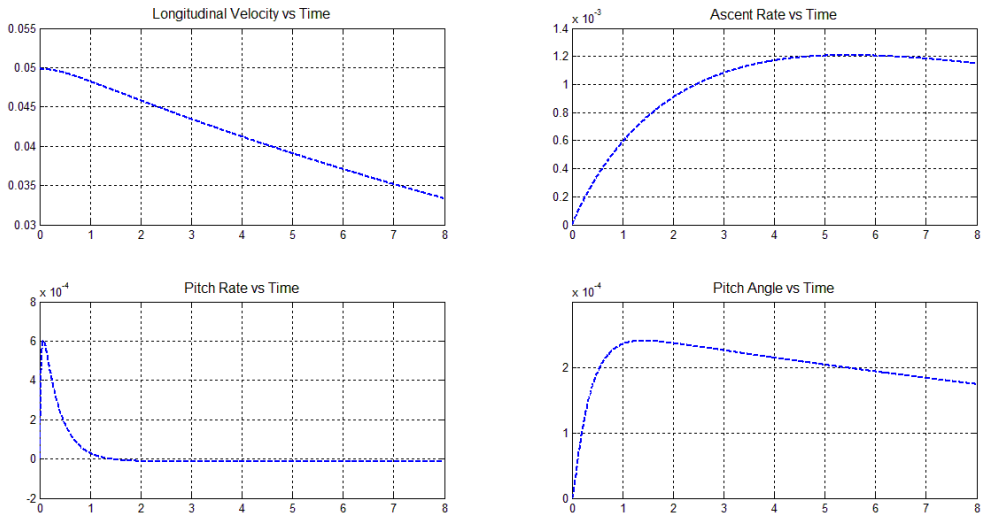

Fig.13 – *LQR* (with Bryson's Rule) Longitudinal Response

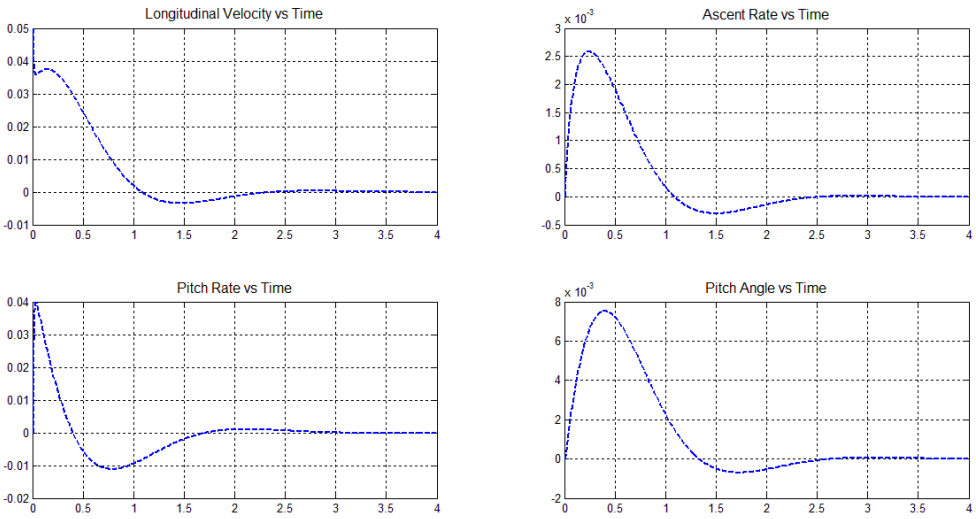

Fig.14 – *LQR* (with Pole Assignment) Longitudinal Response

We can easily see that with the *LQR* with Bryson's rule, the longitudinal velocity, ascent rate and pitch angle, when disturbed, their tendency to stabilize is slower than with the pole allocation method. With the first method, they all tend to stabilize further than 8 seconds (Fig13). That doesn't happen with the second method that stabilizes from 2.5 seconds (Fig.14). The pitch rate in the first method will tend to equilibrium more smoothly than in the second method. None the less, we guarantee a good and faster control of the system when disturbed.

Let us consider now the robust case:

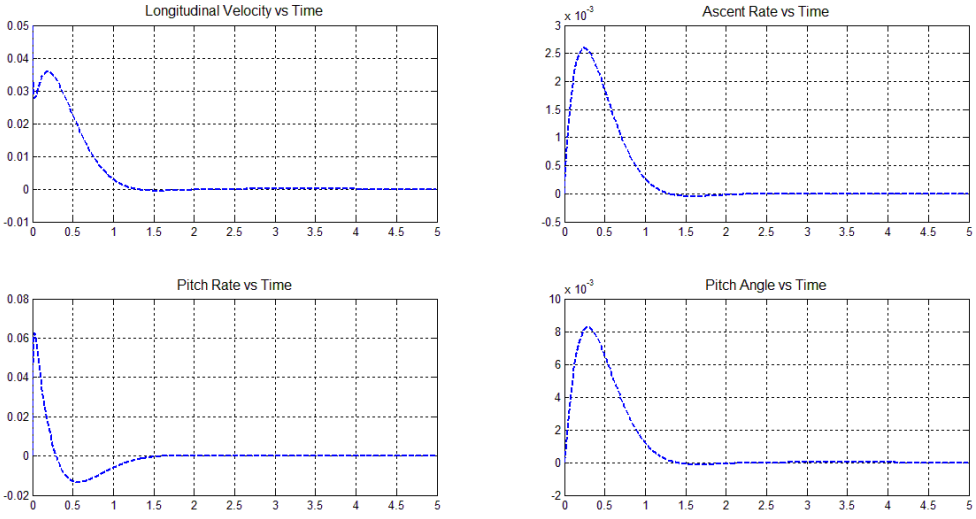

Fig.15 - Robust *LQR* (with Bryson's Rule) Longitudinal Response

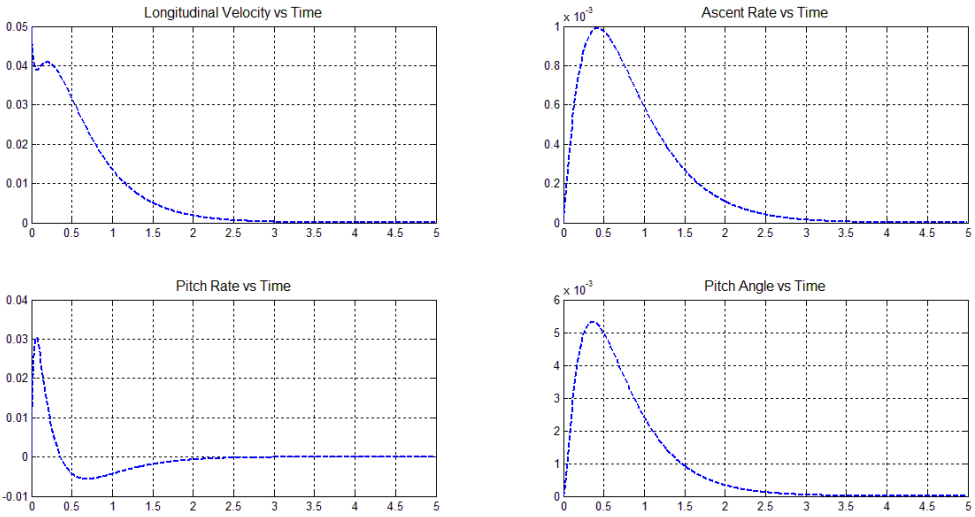

Fig.16 – Robust *LQR* (with Pole Assignment) Longitudinal Response

In the first method, we can see that the system rapidly tends to zero in the first 2,5 seconds after the disturbance (Fig.15), the longitudinal velocity, ascent rate and pitch angle, respectively. The pitch rate tries to stabilize faster, but encounters as well at 2,5 seconds the equilibrium. The second method shows us the same time for stabilization, but as we can see, it is smoother and also faster, taking only about 3 seconds to find it's equilibrium position.

Lateral Simulation

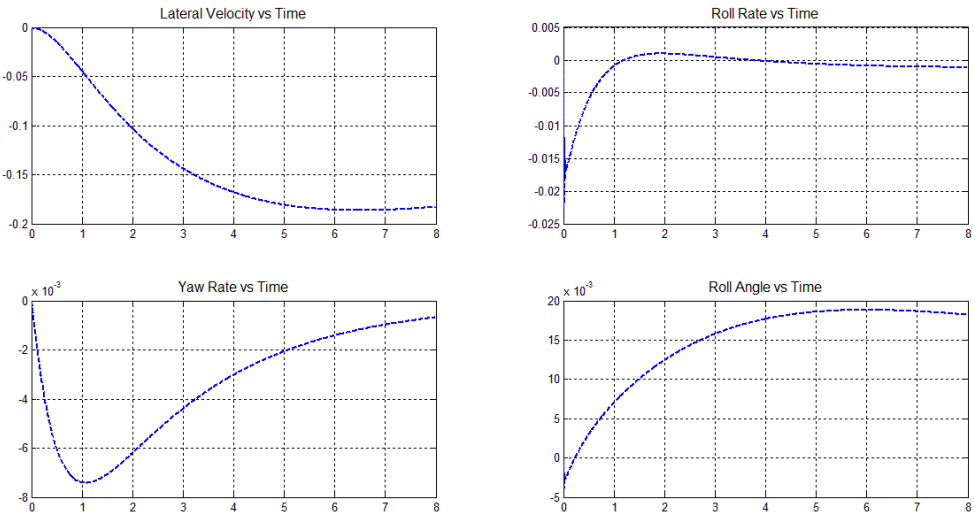

Fig.17 - *LQR* (with Bryson's Rule) Lateral Response

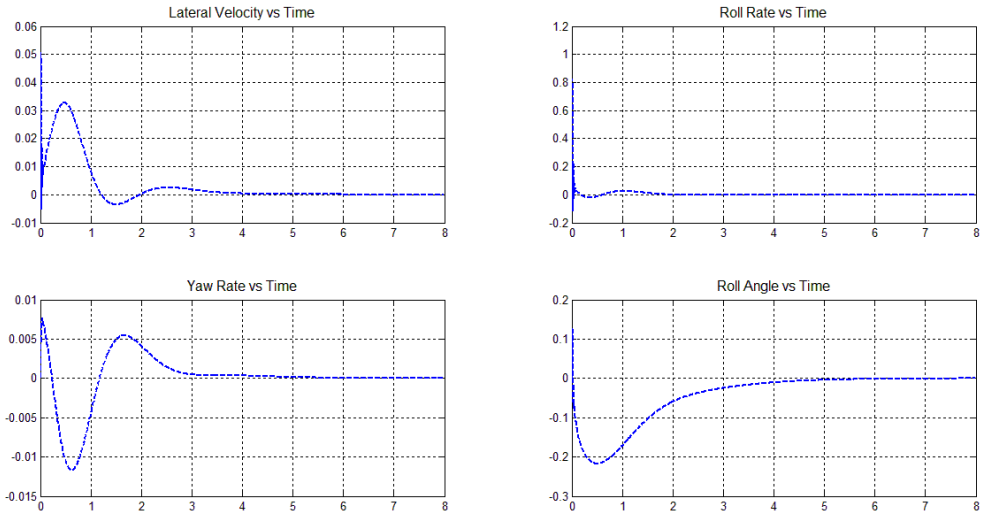

Fig.18 - *LQR* (with Pole Assignment) Lateral Response

For the lateral case, we can see that also the pole allocation method results better, making the stabilization of the aircraft more suitable and faster. The controller in Fig.17 is smoother than in Fig.18 but only stabilizes later. In Fig.18 the roll rate is practically zero from the beginning and in the other cases, it returns to the equilibrium roughly 4 seconds after the disturbance. In Fig.19 and Fig.20, the robust controller is faster to return to its original position.

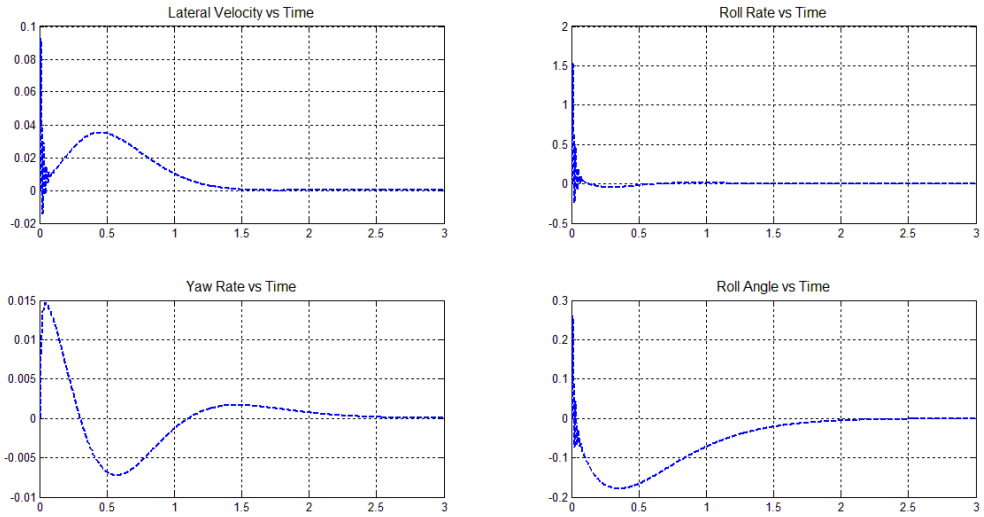

Fig.19 – Robust *LQR* (with Bryson's Rule) Lateral Response

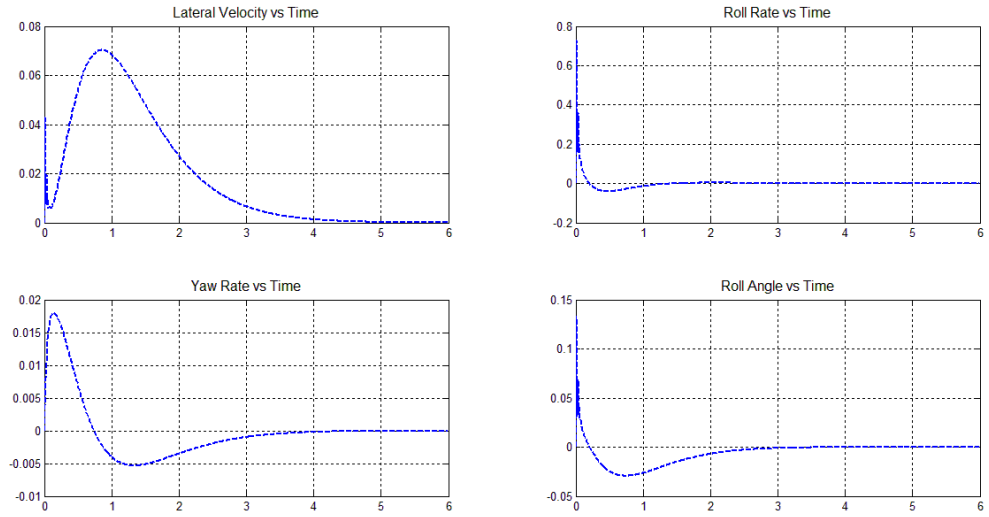

Fig.20 – Robust *LQR* (with Pole Assignment) Lateral Response

4.2 *LQR* Simulation – Westland Lynx in forward flight (V = 20)

Longitudinal Simulation

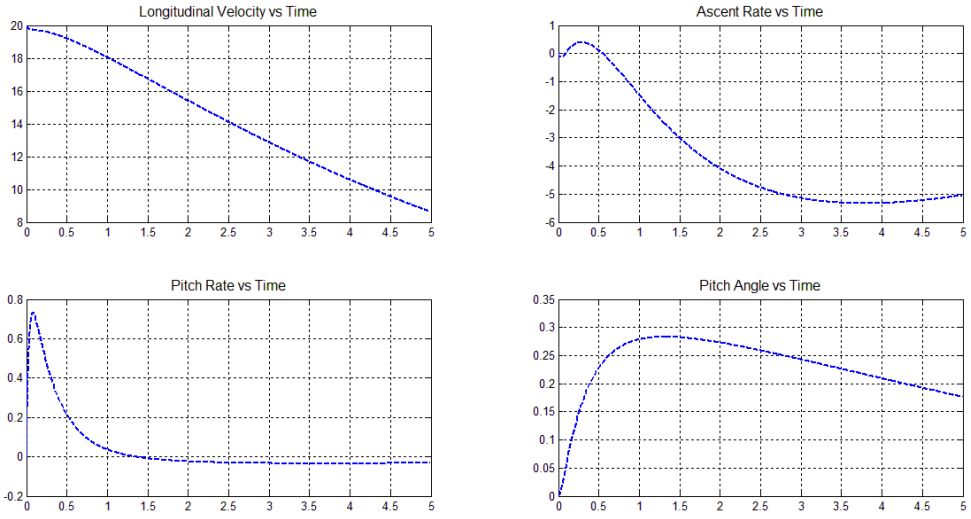

Fig.21 – *LQR* (with Bryson's Rule) Longitudinal Response

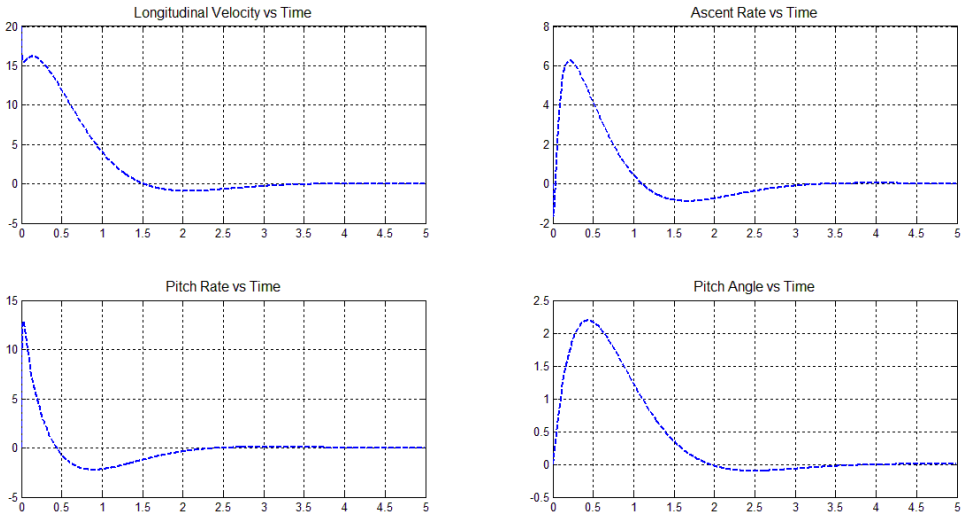

Fig.22 – *LQR* (with Pole Assignment) Longitudinal Response

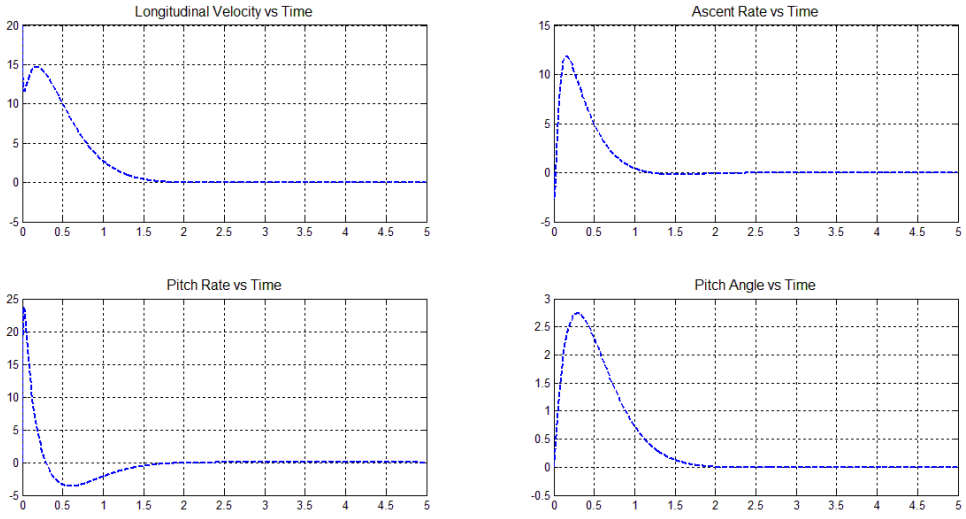

Fig.23 – Robust *LQR* (with Bryson's Rule) Longitudinal Response

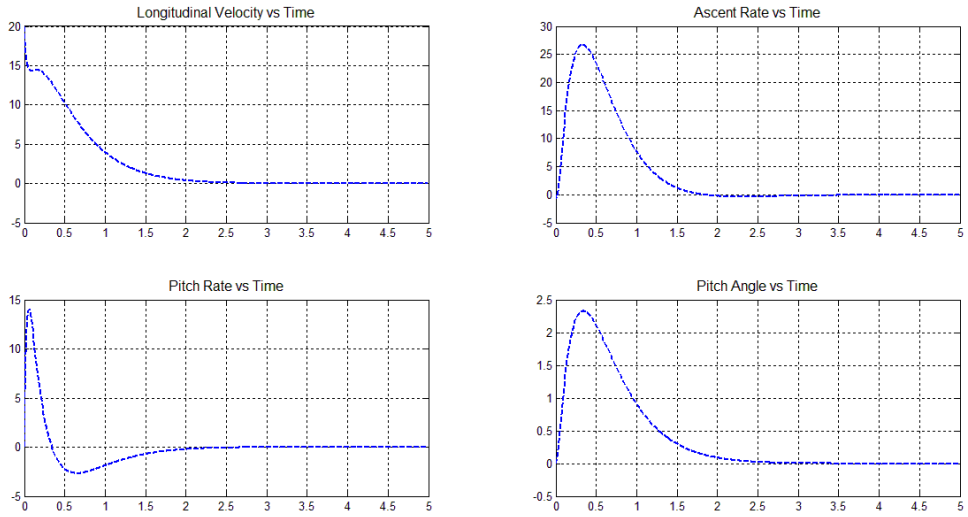

Fig.24 – Robust *LQR* (with Pole Assignment) Longitudinal Response

Lateral Simulation

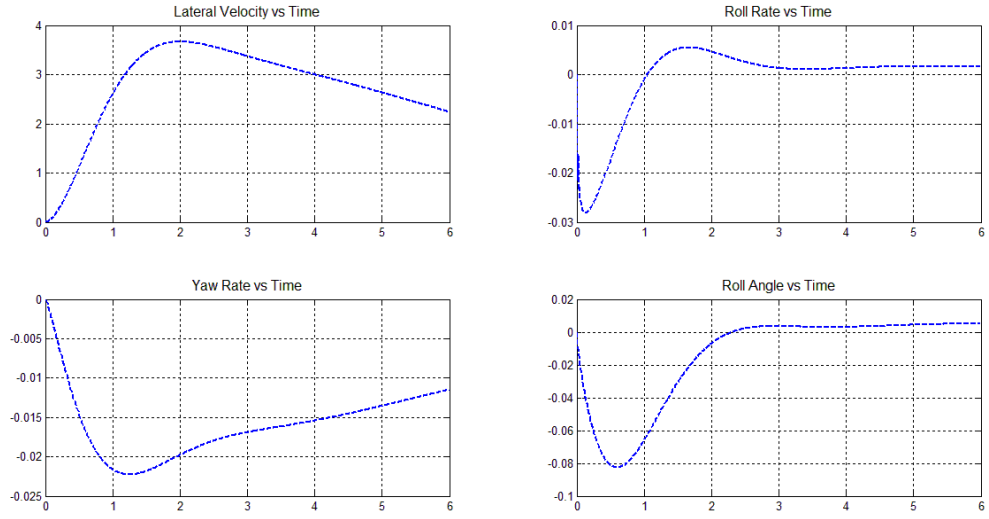

Fig.25 - *LQR* (with Bryson's Rule) Lateral Response

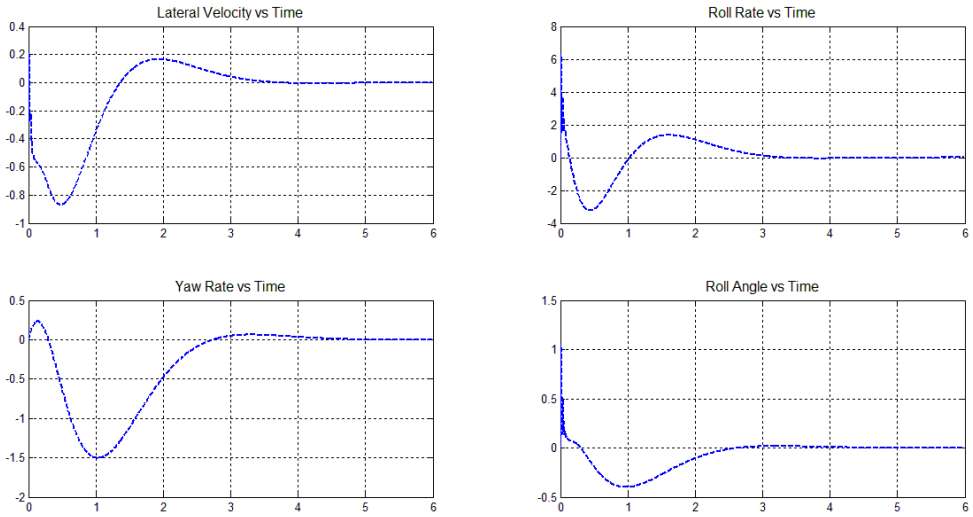

Fig.26 - *LQR* (with Pole Assignment) Lateral Response

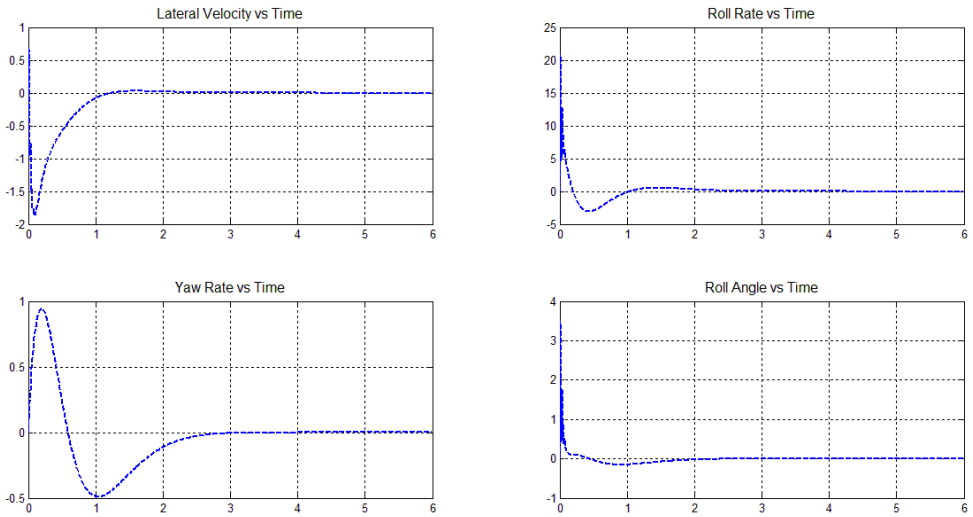

Fig.27 – Robust *LQR* (with Bryson's Rule) Lateral Response

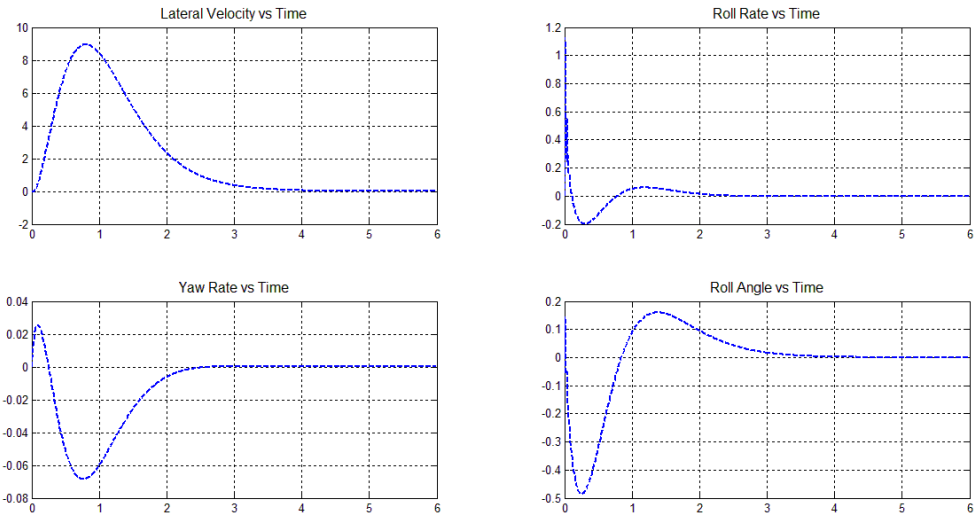

Fig.28 - Robust *LQR* (with Pole Assignment) Lateral Response

4.3 *LQR* Simulation – Westland Lynx in autorotation

Longitudinal Simulation

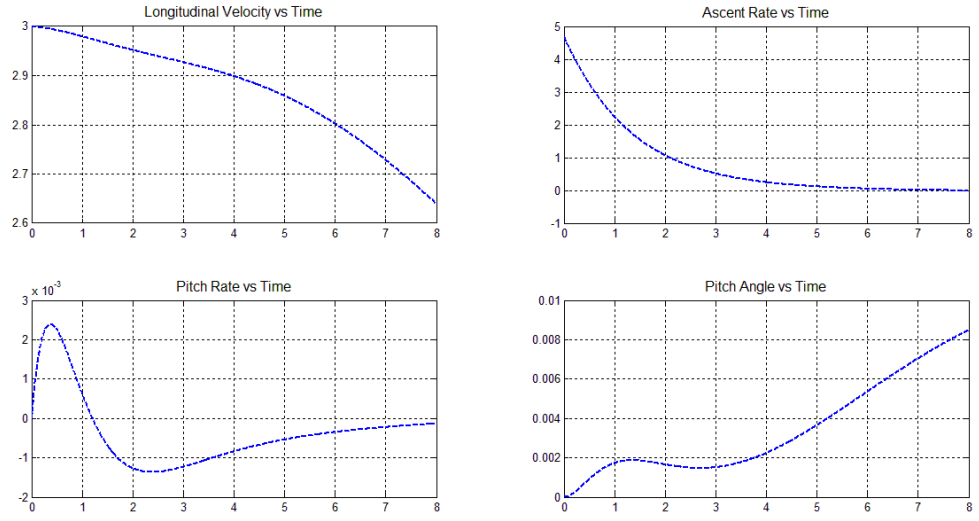

Fig.29 – *LQR* (with Bryson's Rule) Longitudinal Response

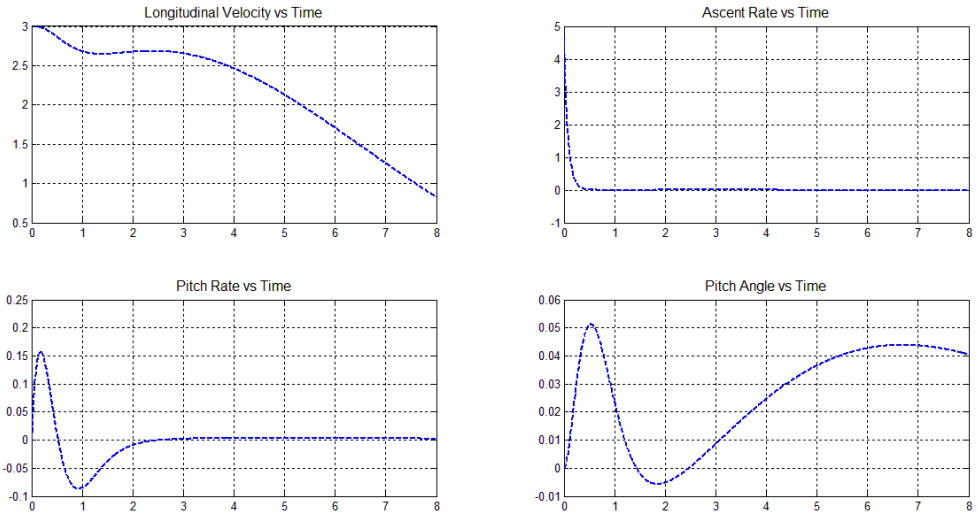

Fig.30 – *LQR* (with Pole Assignment) Longitudinal Response

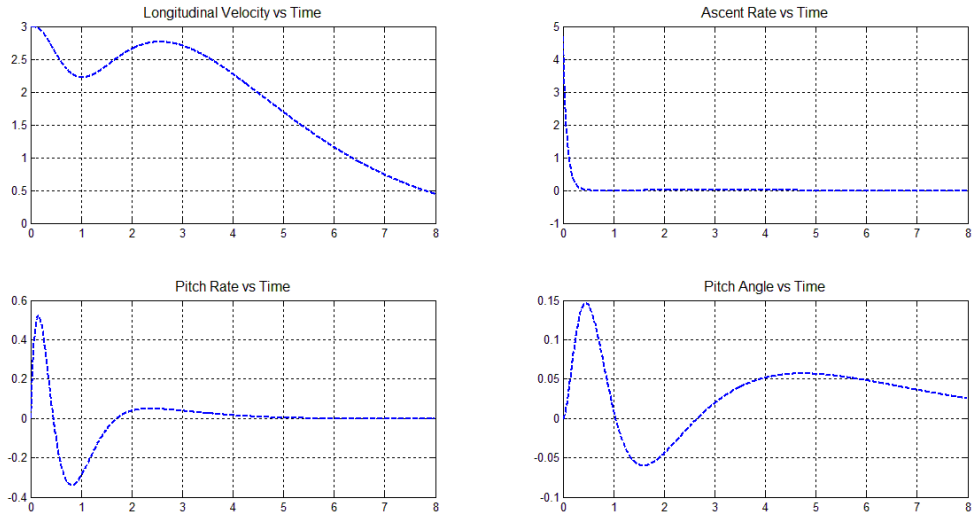

Fig.31 – Robust *LQR* (with Bryson's Rule) Longitudinal Response

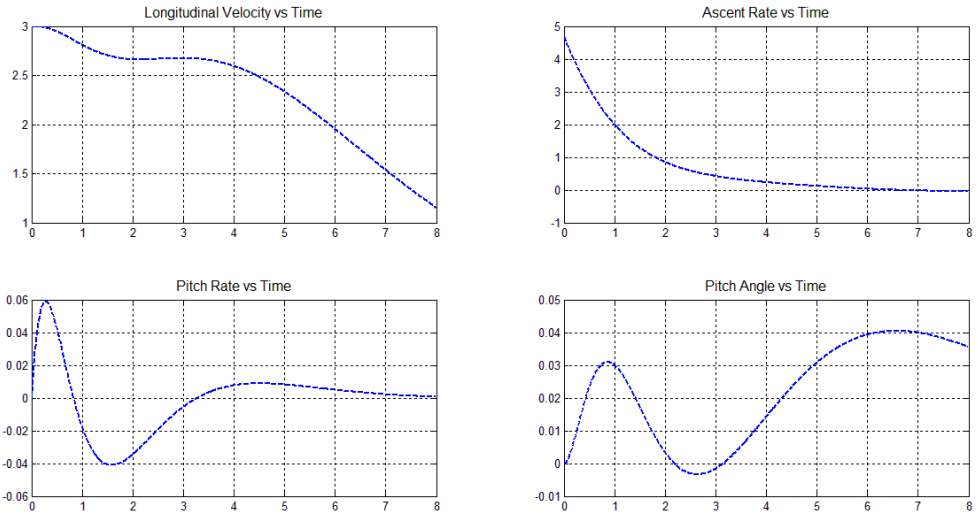

Fig.32 – Robust *LQR* (with Pole Assignment) Longitudinal Response

Lateral Simulation

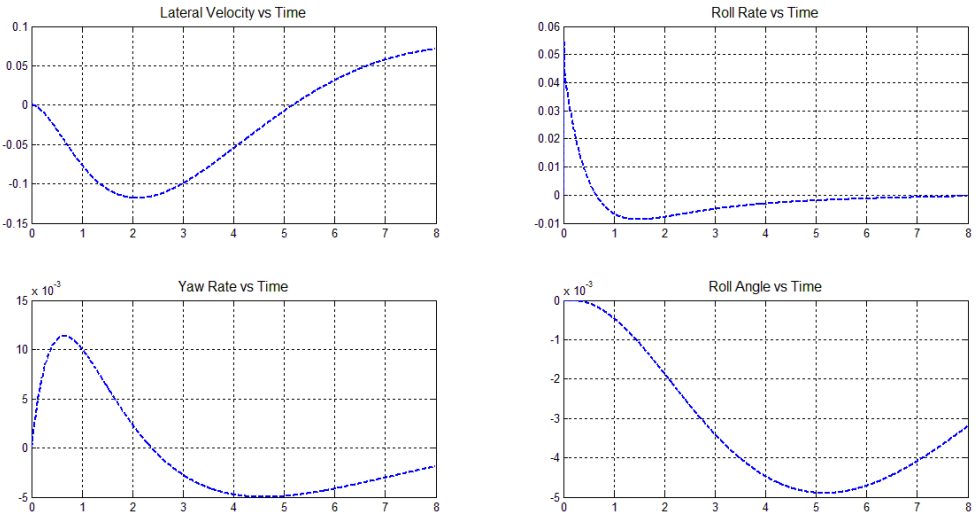

Fig.33 – *LQR* (with Bryson's Rule) Lateral Response

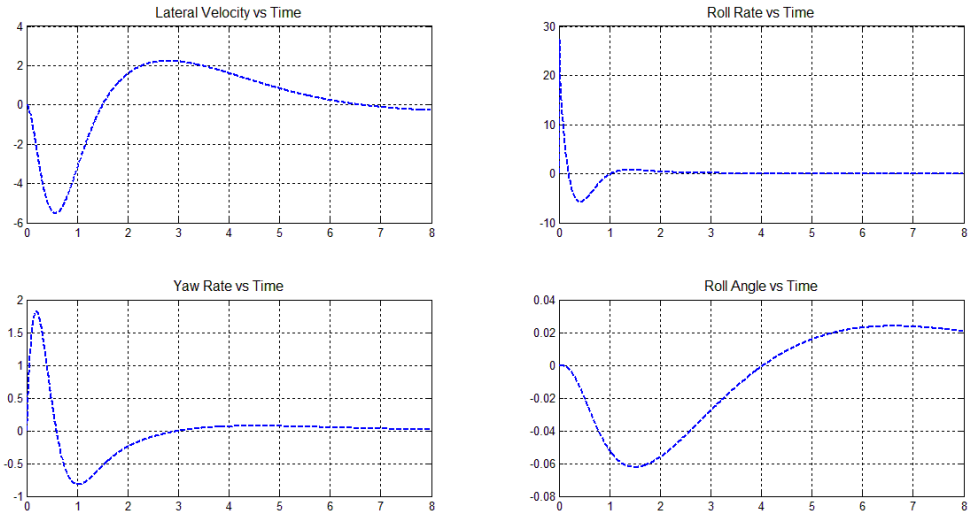

Fig.34 – *LQR* (with Pole Assignment) Lateral Response

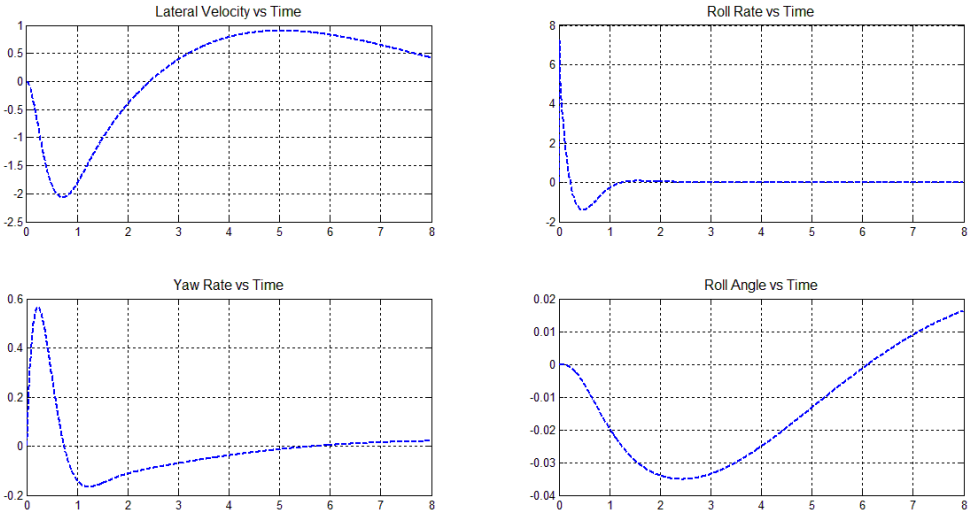

Fig.35 – Robust *LQR* (with Bryson's Rule) Lateral Response

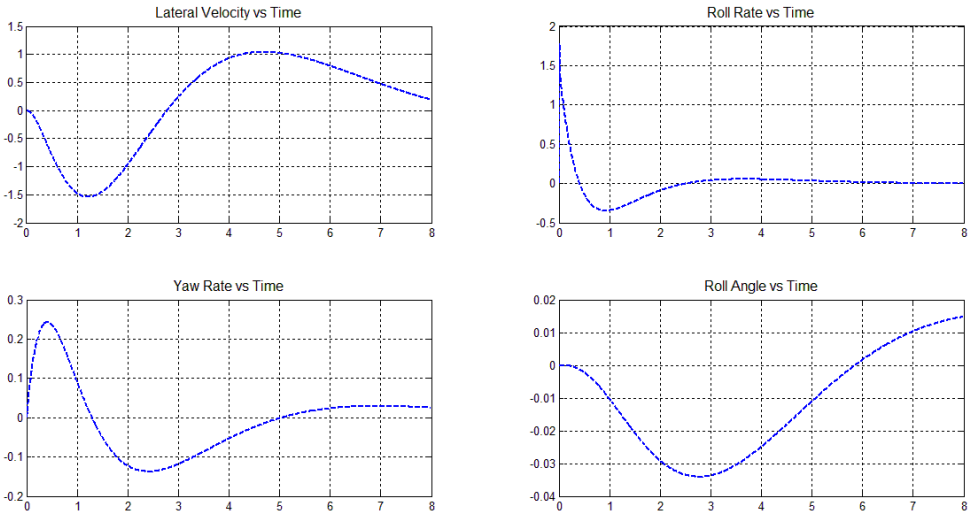

Fig.36 – Robust *LQR* (with Pole Assignment) Lateral Response

The autorotation control is a very difficult task for the pilot without the use of a controller. We have considered for the program the parameters [3] to obtain the previous graphics results. For the longitudinal case, the helicopter starts its descent at 3 knots and land, in all cases, 8 seconds later and the descent rate is very controlled during the process. Of course the pitch rate is very small because the helicopter is in vertical descent so it as to be controlled not to crash the aircraft. The pitch angle is also very small because the controller don't need a great angle to control the machine. This is for the *LQR* with Bryson's rule. We will ignore the results of the *LQR* with pole assignment and robust *LQR* with Bryson's rule because the descent rate is so fast, that in a real autorotation this would not be considered a safe landing. For the last robust *LQR*, it has the same results for the velocity and descent rate that the first *LQR*, but the pitch rate and pitch angle are different because we have to control the descent with the cyclic, i.e., we have to reduce velocity by altering the blades incidence angle.

For the lateral simulation, it was supposed the graphics appear all at zero because we do not consider the four parameters. None the less, in each case the controller tend to the reference point, which means if there is a lateral disturbance, the controller can always stabilize the system.

Chapter 5

Conclusion and Future Work

5.1 Conclusion

Robust state feedback controller and *LQR* feedback controller for linear time in variant systems with uncertain parameters have been presented in this thesis. The helicopter is an extremely unstable aircraft due to constant vibration. This instabilities makes the development of a reliable control imperative, to make the helicopter effectiveness during the mission. In the helicopter simulation, the results focus specially in the attitude, heading and direction, and they were very satisfying, but none the less we have to discuss the outputs.

The *LQR* controller is suitable for our work due to its accuracy and reliability. Also, the sensitivity of the system can be controlled when variations occur, load and input voltage is considerably low, the system easily adapts itself to these variations.

With the *LQR* we've obtained a desirable stabilization and we have proved that a robustly stabilizing state feedback can be calculated by solving an auxiliary *LQR* problem. This controller was implemented by considering the Yanushevsky robust control approach but with a little difference as we saw before.

One of the considerations is that, being in this case a military helicopter, when an exterior factor actuates in the machine and the flight is disturbed, he must stabilize rapidly. The other considered case is a civil or medicalized helicopter, we must consider the comfort of the passengers and therefore, when disturbed, it must stabilize smoothly.

We have also to take into account, that we are simulating with values that were obtained with *HeliSIM,* who gives a great amount of data. With *HeliSIM* we can conceive and deploy a complete aerodynamic model for the real-time simulation of any rotary wing aircraft, specify subsystems behavior, including flight management systems, autopilot, flight controls and enter aerodynamics and environmental parameters into the model to perform the simulation.

Starting in autorotation, we had only considered optimal conditions as we've said already before. We had to disregard some of the stability and control derivatives, because some were hard to find and probably only can be found utilizing *HeliSIM* and other, due to autorotation conditions, are not considered. With autorotation, the helicopter is in emergency so it must land safer as fast as he can but without compromising men and machine. So the robust control is, as well, the most suitable controller for this situation.

For the stationary case, the machine is exposed to all kinds of disturbances (wind gusts, vibration from the blades to the fuselage, etc.) and have to be perfectly still. For example, in a SAR or anti-submarine mission, the *AFCS* and the pilot, have to keep the platform stand still, because

the sonar can give erroneous readings or the balance of the winch can further hurt the victim. In this case also we consider that the most suitable controller will be the robust *LQR*.

Finally, for the various velocities, the helicopter flies in straight flight. When disrupted from the flight, the robust controller immediately actuates, and we can observe that in each case, the robust controller with pole assignment is the one who tends to the imposed reference more quickly.

5.2 Future Work

In this work, we covered a small amount of work that can be made in this area. In the future, we can use and compare other control methods and observe which one is more accurate for the problem. In the autorotation case, for example, to see better the system's behavior, since we have disregarded other parameters also important such as aerodynamics, moment forces, structural analysis, etc. We can also considered optimal conditions in our system but perhaps, and because helicopters can operate in difficult conditions, we could study the model for the worst case scenario possible.

As we stated before, rotary wing platform as many advantages and a more detailed and precise study must be made in this area. More studies about trim and stability must be take into account because it will always be the most important part of helicopter study.

Finally, the development of a *RC* scale helicopter can be also be interesting. To implement these, and more controller, depending on the mission, and see how it responds.

Bibliography

[1] Padfield, G. D., *Helicopter Flight Dynamics: The Theory and Application of Flying Qualities and Simulation Modeling*, AIAA Educational Series, 1995.

[2] Semuel, F., "LQR-Based Trajectory Control Of Full Envelope: Autonomous Helicopter", *Proceedings of the World Congress on Engineering* (WCE 2009), Vol I, July 1 - 3, London, ISBN: 978-988-17012-5-1, 2009.

[3] Lee, A. Y., Bryson, A. E. Jr., William S. H., "Optimal Landing of a Helicopter in Autorotation", *Journal of Guidance, Control and Dynamics*, Vol. 11, No.1,1988, pp. 7-12.

[4] Yanushevsky, R. T., "Approach to Robust Control Systems Design"*, Journal of Guidance, Control and Dynamics*, Vol.14, No. 1, 1990, pp. 218-219.

[5] WWW < http://www.helis.com/howflies/autorotation.php>, Consulted in June de 2012.

[6] WWW<http://quizlet.com/12877497/helicopter-stability-control-section-8-derivatives-flash-cards/> Consulted in July 2012.

[7] Bousson, K., *Apontamentos da Cadeira de Mecânica de Voo 2*, Departamento de Ciências Aeroespaciais, Universidade da Beira Interior, Covilhã, 2010.

[8] Franklin, G. F., Powell, J. D., Emami-Naeini, A. *Feedback Control of Dynamic Systems*, Prentice Hall, Upper Saddle River, NJ, 4th edition, 2002.

[9] McGowen, S. S., *Helicopters: An Illustrated History of their Impact*, California: ABC-CLIO, ISBN 1-85109-468-7, 2005.

[10] Ren, B. et al., *Modeling, Control and Coordination of Helicopter Systems*, Springer New York, Dordrecht, Heidelberg, London, ISBN 978-1-4614-1562-6, 2012.

[11] Raptis, I. A., Valavanis, K. P., *Intelligent Systems, Control and Automation: Science and Engeneering. Linear and Nonlinear Control of Small-Scale Unmanned Helicopters*, Springer Dordrecht, vol. 45, Heidelberg, London, New York, ISBN 978-94-007-0022-2, 2011.

[12] Carico, D., *Helicopter Controllabillity*, MSc. Thesis, Naval Postgraduate School, Monterey, California, 1989.

[13] WWW<http://www.ece.cmu.edu/~koopman/des_s99/control_theory/> Consulted in May 2012.

[14] WWW<http://ma3naido.blogspot.pt/2009/11/introduction-to-flight-controls.html> Consulted in September 2012.

[15] U.S. Department of Transportation, *Helicopter Flying Handbook*, Federal Aviation Administration, Flight Standards Service, 2012, pp. 20-21.

[16] Klamka, J., *System Characteristics: Stability, controllability, observability*, Institute of Automatic Control, Technical University, Gliwice, Poland, 2000.

[17] WWW http://pt.wikipedia.org/wiki/Esquadra_751 Consulted in May 2012

[18] Bramwell, A. R. S., Done, G., Balmford, D., *Bramwell's Helicopter Dynamics*, Butterworth-Heinemann, 2001, Second Edition, pp. 21-23.

[19] WWW <http://en.wikipedia.org/wiki/Linear-quadratic_regulator> Consulted in September 2012.

[20] DiStefano, J.J., Stubberud, A.R.,Williams, I.J., *Feedback and Control Systems*, Schaum's Outline Series, McGraw-Hill Book Company, 1994.

[23] WWW <http://www.control.com/thread/966880428> Consulted in August 2012.

[24] WWW <http://etd.lib.fsu.edu/theses/available/etd-11242003174221/unrestricted/ liqunthesisxing.pdf > Consulted in September 2012.

[25] Çaliskan, S.; "Development of forward flight trim and longitudinal dynamic stability codes and their application to a UH-60 helicopter", February 2009, MSc. Thesis, Graduate School of Natural and Applied Sciences of Middle East Technical University, pp.27-28.

[26] Hespanha, J.P., *Undergraduate Lecture Notes on LQG/LQR controller design*, Lecture notes, University of Santa Barbara, 2007.

[27] Luo, J., "Determination of Weighting Matrices of a Linear Quadratic Regulator", *Journal of Guidance, Control and Dynamics*, Vol. 18, No. 6, 1996, pp. 1462-1463.

ANNEXES

Annex 1

Helicopter configuration parameters

The Westland Lynx Mk7 is a twin engine, utility/battlefield helicopter currently in service in the British Army Air Corps. The aircraft has been used extensively in a research programme to calibrate agility standards of future helicopter types. The four-bladed hingeless rotor is capable of producing large control moments and hence angular accelerations. It also embodies many features with significant innovation for its age – hingeless rotor with cambered aerofoil sections, titanium monoblock rotor head and conformal gears [1]. A three-view drawing of the aircraft is shown. The physical characteristics of the aircraft used to construct the *Helisim* simulation model are provided in the Configuration Data table.

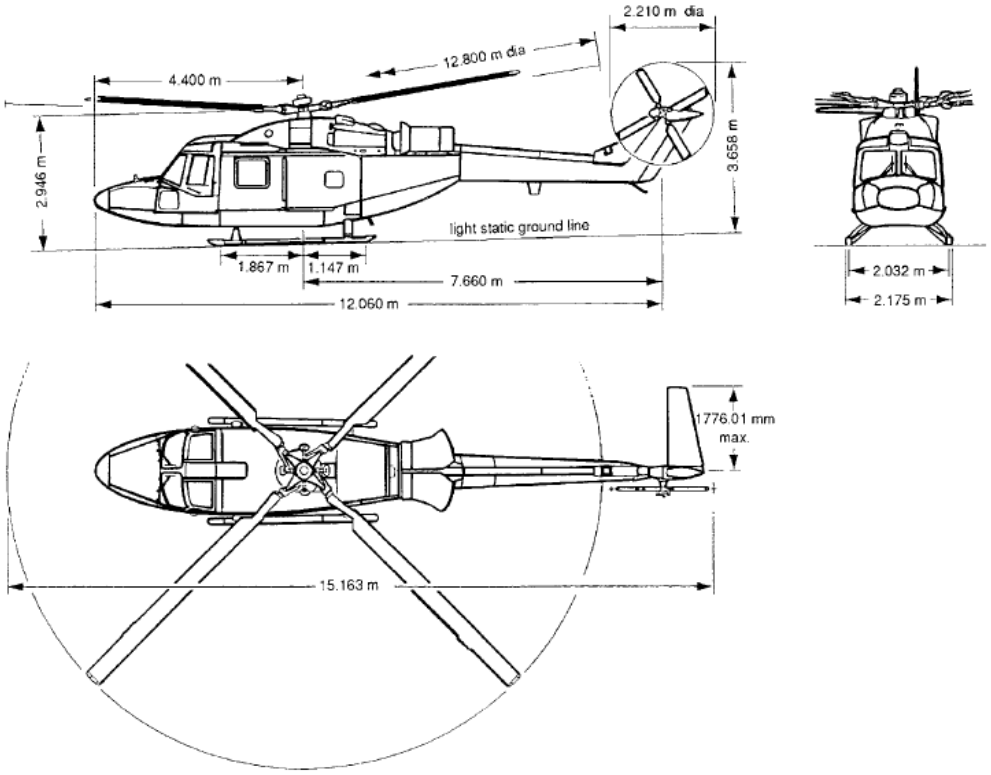

Configuration data – Lynx

a_0	6.0/rad	I_{zz}	12 208.8 kg m^2	x_{cg}	−0.0198
a_{0T}	6.0/rad	K_β	166 352 N m/rad	δ_0	0.009
α_{tp0}	−0.0175 rad	l_{fn}	7.48 m	δ_2	37.983
β_{fn0}	−0.0524 rad	l_{tp}	7.66 m	δ_3	−45°
c	0.391 m	l_T	7.66 m	δ_{T0}	0.008
g_T	5.8	M_a	4313.7 kg	δ_{T2}	5.334
h_R	1.274 m	N_b	4		
h_T	1.146 m	R	6.4 m	γ	7.12
I_β	678.14 kg m^2	R_T	1.106 m	γ_s	0.0698 rad
I_{xx}	2767.1 kg m^2	S_{fn}	1.107 m^2	λ_β^2	1.193
I_{xz}	2034.8 kg m^2	S_{tp}	1.197 m^2	θ_{tw}	−0.14 rad
I_{yy}	13 904.5 kg m^2	s_T	0.208	Ω_{idle}	35.63 rad/s

Annex 2

Since we have that optimal autorotation descent from hover is purely vertical, we can consider certain parameters:

- $v = 0$ (lateral velocity);
- $\phi = 0$ (roll angle);
- $p = 0$ (roll ratio);
- $\beta = 0$ (sideslip angle)

From here, we can use the general flight dynamics equations [7] we have:

$$u = V \cos\beta \cos\alpha$$

$$v = Vsin\beta$$

$$w = Vcos\beta sin\alpha$$

and

$$V = \sqrt{u^2 + v^2 + w^2}$$

For autorotation [3], we have:

$$V = \sqrt{u^2 + w^2}$$

The angle of attack and sideslip are defined by:

$$\alpha = arctg\frac{w}{u}$$

$$\beta = arcsin\frac{v}{V}$$

Since we consider the sideslip angle $\beta = 0$, in all flight phases and we obtain:

$$u = V \cos\alpha$$

$$v = 0$$

$$w = Vsin\alpha$$

Annex 3

System matrix *A* in the general form

$A =$

$$\begin{bmatrix} X_u & X_w - Q_e & X_q - W_e & -g\cos\Theta_e & X_v + R_e & X_p & 0 & X_r + V_e \\ Z_u + Q_e & Z_w & Z_q + U_e & -g\cos\Phi_e sen\Theta_e & Z_v - P_e & Z_p - V_e & -gsen\Phi_e\cos\Theta_e & Z_r \\ M_u & M_w & M_q & 0 & M_v & M_p - 2P_e I_{xz}/I_{yy} - R_e(I_{xx} - I_{zz})/I_{yy} & 0 & M_r + 2R_e I_{xz}/I_{yy} - P_e(I_{xx} - I_{zz})/I_{yy} \\ 0 & 0 & \cos\Phi_e & 0 & 0 & 0 & -\Omega_a\cos\Theta_e & -sen\Phi_e \\ Y_u - R_e & Y_w + P_e & Y_q & -gsen\Phi_e sen\Theta_e & Y_v & Y_p + W_e & g\cos\Phi_e\cos\Theta_e & Y_r - U_e \\ L'_u & L'_w & L'_q + k_1 P_e - k_2 R_e & 0 & L'_v & L'_p + k_1 Q_e & 0 & L'_r - k_2 Q_e \\ 0 & 0 & sen\Phi_e tg\Theta_e & \Omega_a sec\Theta_e & 0 & 1 & 0 & \cos\Phi_e tg\Theta_e \\ N'_u & N'_w & N'_q - k_1 R_e - k_3 P_e & 0 & N'_v & N'_p + K_3 Q_e & 0 & N'_r - k_1 Q_e \end{bmatrix}$$

Control matrix *B* in the general form

$$B = \begin{bmatrix} X_{\theta_0} & X_{\theta_{1s}} & X_{\theta_{1c}} & X_{\theta_{0T}} \\ Z_{\theta_0} & Z_{\theta_{1s}} & Z_{\theta_{1c}} & Z_{\theta_{0T}} \\ M_{\theta_0} & M_{\theta_{1s}} & M_{\theta_{1c}} & M_{\theta_{0T}} \\ 0 & 0 & 0 & 0 \\ Y_{\theta_0} & Y_{\theta_{1s}} & Y_{\theta_{1c}} & Y_{\theta_{0T}} \\ L'_{\theta_0} & L'_{\theta_{1s}} & L'_{\theta_{1c}} & L'_{\theta_{0T}} \\ 0 & 0 & 0 & 0 \\ N'_{\theta_0} & N'_{\theta_{1s}} & N'_{\theta_{1c}} & N'_{\theta_{0T}} \end{bmatrix}$$

Annex 4

This description focuses on contributing sources, physical interpretation, and typical signs of these derivatives [1], [6], [12].

X_u (drag damping): is main contribution from fuselage parasite drag and main rotor *H-force*. By definition, the sign of X_u is negative, corresponding the increase of drag with the increase of speed. The effect is to require more forward tilt as speed increases.

$$\frac{X_u}{M_a} \cong -\frac{\rho u S}{M_a}$$

X_w (drag due to vertical velocity): At hover and autorotation, X_w is zero. Is not very significant to either static or dynamic stability characteristics.

Z_w (heave damping): For the helicopter at low speed, it is an important vertical control response parameter. It plays an important part in hover and forward flight.

$$Z_w = -\frac{\rho a_0 \mu (\Omega R) A_b}{2M_a}\left(\frac{4}{8\mu + a_0 s}\right)$$

Z_u (lift due to forward speed): At hover and autorotation, Z_u is zero. This derivative is not especially significant, except possibly at high speed where it may affect dynamic divergence.

M_u (speed stability): At hover, the rotor flaps back in response to a head wind disturbance. As the resultant nose-up moment is in the direction opposing the disturbance, the rotary-wing vehicle is statically stable with M_u being positive. But an excessive value of M_u may lead to unstable phugoid response and is sensitive to gust. In forward flight, the rotor has a similar contribution
while the horizontal stabilizer may have a significant effect to M_u.

M_w (angle of attack stability): At hover and autorotation, the value of M_w is considered zero. In forward flight, a positive increase of angle of attack leads to backward tilting of the rotor, creating a nose-up moment to further increase the angle of attack. Thus, the contribution from the rotor to M_w is destabilizing with its corresponding value taking positive sign. A horizontal stabilizer

contributes a stabilizing effect, which is the main reason to justify its existence in a pure helicopter configuration.

$$M_w = -\frac{3}{2}\frac{g}{R}I_\beta$$

M_q (pitch damping): For a rotor with counter clockwise rotation, a positive change in the pitch rate results in a negative roll due to gyroscopic moment. This in turn causes a flap-down for the blade over the nose and a flap-up for the blade over the tail. The resultant nose-down moment opposes the original pitch rate variation, thus the damping effect.

$$M_q \approx -\frac{N_b S_\beta I_\beta \Omega}{I_{yy}}\left(1 + S_\beta \frac{\gamma}{16}\right)$$

L_v (dihedral effect): L_v is the lateral counterpart of M_u. For a right sideslip, the rotor responds with a left roll. A positive dihedral effect thus takes a negative value. The contributions from both tail rotor and vertical tail depend on their relative location above or below C.G. When above C.G., the effect is stabilizing and *vice versa*. Similar to M_u, an excessively large value of L_v may not be preferable. In some helicopter configurations, the vertical tail is placed underneath the tail boom in order to have a moderate value of L_v.

L_p (roll damping): L_p is the lateral counterpart of M_q. The contribution of the main rotor to the damping in roll is an important characteristic for lateral-directional stability.

$$L_p \approx -\frac{N_b S_\beta I_\beta \Omega}{I_{xx}}\left(1 + S_\beta \frac{\gamma}{16}\right)$$

N_v (weathercock stability): In autorotation N_v is zero. The main contributions to N_v are from the tail rotor and vertical tail. Both are stabilizing with N_v taking a positive value.

N_r (yaw damping): Both tail rotor and vertical tail will produce contributions to the yaw damping. In hover, the main contribution to the yaw damping is from the tail rotor.

$$N_r \approx -l_t \frac{M_a}{I_{zz}} Y_r$$

M_p and L_q (cross − coupling due to roll/pitch rates): M_p takes a positive value while L_q is negative.

$$M_p \approx -\frac{N_b S_\beta I_\beta \Omega}{I_{yy}} \left(S_\beta - \frac{\gamma}{16}\right)$$

$$L_q \approx \frac{N_b S_\beta I_\beta \Omega}{I_{xx}} \left(S_\beta - \frac{\gamma}{16}\right)$$

Y_v (sideforce due to sideslip): The sideforce due to sideslip or sideward velocity will act to resist or damp sideward motion.

Y_r (sideforce due to yaw rate): The primary contribution to side force due to yaw rate will be from the tail rotor for conventional helicopters. The vertical tail fin will also affect the side force due to yaw rate.

Y_p (sideforce due to roll rate): Both main and tail rotors will contribute to the side force due to roll rate.

$Y_{\theta 1s}$ (sideforce due to lateral control): The side force due to lateral control results from tilting the rotor tip path plane to the side.

$Y_{\theta 0T}$ (side force due to directional control): The side force due to directional control will be a function of tail rotor thrust resulting from a rudder pedal control input.

$N_{\theta 0T}$ (yaw control moment): The directional control (yaw control) is the tail rotor effectiveness or yawing moment resulting from rudder pedal inputs.

$L_{\theta 1s}$ (lateral control) The lateral control derivative is primarily a function of the rate of change of rotor tip path tilt with lateral cyclic input.

N_p (yaw due to roll rate): The yaw due to roll rate derivative depends primarily on the height of the tail rotor with some contribution from the vertical stabilizer.

$Z_{\theta 0}$ (heave control sensitivity) : The heave control sensitivity, in hover, is

$$Z_{\theta 0} \approx -\frac{8}{3}\frac{a_0 A_b \rho (\Omega R)^2 \lambda_0}{(16\lambda_0 + a_0 s)M_a}$$

and in forward flight

$$Z_{\theta 0} \approx -\frac{4}{3}\frac{a_0 A_b \rho (\Omega R)^2 \mu}{(8\mu + a_0 s)M_a}(1 + 1.5\mu)$$

$Z_{\theta 1s}$: In hover, $Z_{\theta 1s} = 0$ but in forward flight is

$$Z_{\theta 1s} \approx -\frac{2a_0 A_b \rho (\Omega R)^2 \mu^2}{(8\mu + a_0 s)M_a}$$

$L_{\theta 1c}$ (rolling moment):

$$L_{\theta 1c} \approx -\frac{N_b S_\beta \gamma I_\beta \Omega^2}{16 I_{xx}}$$

$X_{\theta 0T}, Z_{\theta 0T}, M_{\theta 0T}$ (tail rotor collective pitch angle): Are considered zero.

$X_{\theta 0}, X_{\theta 1s}, X_{\theta 1c}, M_{\theta 1s}, Z_{\theta 1c}, X_{\theta 1c}$: Derivatives values considered zero.

Annex 5

State and Control matrices and results of the different velocities

Autorotation

$$A = \begin{bmatrix} -0.004214 & 0.0000 & 0.0000 & -9.8100 & -0.0220 & 0.0000 & 0.0000 & 0.0000 \\ 0.0000 & -0.45212 & 0.0000 & -4.2857 & 0.0000 & 0.0000 & 0.0000 & 0.0000 \\ 0.0000 & 0.0000 & -1.69947 & 0.0000 & 0.0000 & 0.347589 & 0.0000 & 0.0000 \\ 0.0000 & 0.0000 & 0.9981 & 0.0000 & 0.0000 & 0.0000 & 0.0000 & -0.4432 \\ 0.0000 & 0.0000 & -0.1297 & 0.0000 & -0.1250 & 0.0000 & -8.8243 & 0.0000 \\ 0.3397 & 0.0000 & -1.7657 & 0.0000 & -0.0550 & -8.53972 & 0.0000 & 0.0000 \\ 0.0000 & 0.0000 & 0.0039 & 0.0000 & 0.0000 & 1.0000 & 0.0000 & -0.4857 \\ 0.0000 & 0.0000 & 0.0000 & 0.0000 & 0.0137 & 0.0000 & 0.0000 & 0.0000 \end{bmatrix}$$

$$B = \begin{bmatrix} 0.0000 & 0.0000 & 0.0000 & 0.0000 \\ -93.9179 & -0.006832 & 0.0000 & 0.0000 \\ 0.0000 & 0.0000 & 0.0000 & 0.0000 \\ 0.0000 & 0.0000 & 0.0000 & 0.0000 \\ 0.0000 & 0.0000 & 0.0000 & 0.0000 \\ 0.0000 & 0.0000 & -123.203 & 0.0000 \\ 0.0000 & 0.0000 & 0.0000 & 0.0000 \\ 0.0000 & 0.0000 & 0.0000 & 0.0000 \end{bmatrix}$$

Hover [V = 0]

$$A = \begin{bmatrix} -0.0199 & 0.0215 & 0.6674 & -9.7837 & -0.0205 & -0.1600 & 0.0000 & 0.0000 \\ 0.0237 & -0.3108 & 0.0134 & -0.7215 & -0.0028 & -0.0054 & 0.5208 & 0.0000 \\ 0.0468 & 0.0055 & -1.8954 & 0.0000 & 0.0588 & 0.4562 & 0.0000 & 0.0000 \\ 0.0000 & 0.0000 & 0.9985 & 0.0000 & 0.0000 & 0.0000 & 0.0000 & 0.0532 \\ 0.0207 & 0.0002 & -0.1609 & 0.0380 & -0.0351 & -0.6840 & 9.7697 & 0.0995 \\ 0.3397 & 0.0236 & -2.6449 & 0.0000 & -0.2715 & -10.9759 & 0.0000 & -0.0203 \\ 0.0000 & 0.0000 & -0.0039 & 0.0000 & 0.0000 & 1.0000 & 0.0000 & 0.0737 \\ 0.0609 & 0.0089 & -0.4766 & 0.0000 & -0.0137 & -1.9367 & 0.0000 & -0.2743 \end{bmatrix}$$

$$B = \begin{bmatrix} 6.9417 & -9.2860 & 2.0164 & 0.0000 \\ -93.9179 & -0.0020 & -0.0003 & 0.0000 \\ 0.9554 & 26.4011 & -5.7326 & 0.0000 \\ 0.0000 & 0.0000 & 0.0000 & 0.0000 \\ -0.3563 & -2.0164 & -9.2862 & 3.6770 \\ 7.0476 & -33.2120 & -152.9537 & -0.7358 \\ 0.0000 & 0.0000 & 0.0000 & 0.0000 \\ 17.3054 & -5.9909 & -27.5911 & -9.9111 \end{bmatrix}$$

Forward Flight [V = 20]

$$A = \begin{bmatrix} -0.0082 & 0.0254 & -0.0685 & -9.7868 & -0.0158 & -0.1480 & 0.0000 & 0.00000 \\ -0.1723 & -0.4346 & 10.4965 & -0.6792 & -0.0150 & -0.1044 & 0.45450 & 0.0000 \\ 0.0417 & 0.0157 & -2.0012 & 0.0000 & 0.0482 & 0.4441 & 0.00000 & 0.0000 \\ 0.0000 & 0.0000 & 0.9989 & 0.0000 & 0.0000 & 0.0000 & 0.00000 & 0.0464 \\ 0.0173 & 0.0161 & -0.1435 & 0.0311 & -0.0604 & 0.0308 & 9.77607 & -10.1108 \\ 0.1531 & 0.2739 & -2.4044 & 0.0000 & -0.2439 & -10.9208 & 00.0000 & -0.0793 \\ 0.0000 & 0.0000 & -0.0032 & 0.0000 & 0.0000 & 1.0000 & 0.00000 & 0.0694 \\ 0.0037 & 0.0455 & -0.3753 & 0.0000 & 0.0025 & -1.9201 & 0.00000 & -0.4404 \end{bmatrix}$$

$$B = \begin{bmatrix} 5.6326 & -8.9083 & 2.0273 & 0.0000 \\ -89.9908 & -6.0809 & 0.0010 & 0.0000 \\ 3.8558 & 26.6794 & -5.7663 & 0.0000 \\ 0.0000 & 0.0000 & 0.0000 & 0.0000 \\ 0.1249 & -2.0098 & -9.3275 & 3.4515 \\ 13.2029 & -32.8252 & -153.5913 & -0.6907 \\ 0.0000 & 0.0000 & 0.0000 & 0.0000 \\ 16.5240 & -5.9080 & -27.5007 & -9.3029 \end{bmatrix}$$

Forward Flight [V = 40]

$$A = \begin{bmatrix} -0.0146 & 0.0347 & -0.5681 & -9.7934 & -0.0083 & -0.1321 & 0.0000 & 0.0000 \\ -0.1186 & -0.6156 & 20.6855 & -0.5779 & -0.0180 & -0.2022 & 0.3519 & 0.0000 \\ 0.0319 & 0.0212 & -2.1033 & 0.0000 & 0.0277 & 0.4210 & 0.0000 & 0.0000 \\ 0.0000 & 0.0000 & 0.9994 & 0.0000 & 0.0000 & 0.0000 & 0.0000 & 0.0359 \\ 0.0070 & 0.0184 & -0.1303 & 0.0205 & -0.0915 & 0.5342 & 9.7869 & -20.3077 \\ -0.0255 & 0.3040 & -2.1361 & 0.0000 & -0.1949 & -10.7839 & 0.0000 & -0.1441 \\ 0.0000 & 0.0000 & -0.0021 & 0.0000 & 0.0000 & 1.0000 & 0.0000 & 0.0590 \\ -0.0325 & 0.0314 & -0.2522 & 0.0000 & 0.0316 & -1.8857 & 0.0000 & -0.68597 \end{bmatrix}$$

$$B = \begin{bmatrix} 4.8686 & -8.5123 & 2.0305 & 0.0000 \\ -95.5241 & -12.7586 & 0.0003 & 0.0000 \\ 7.2883 & 27.0667 & -5.7827 & 0.0000 \\ 0.0000 & 0.0000 & 0.0000 & 0.0000 \\ 1.1239 & -1.8435 & -9.3132 & 3.3289 \\ 27.3295 & -30.1532 & -153.4552 & -0.6662 \\ 0.0000 & 0.0000 & 0.0000 & 0.0000 \\ 15.9423 & -5.8252 & -27.2699 & -8.9726 \end{bmatrix}$$

Longitudinal Simulation

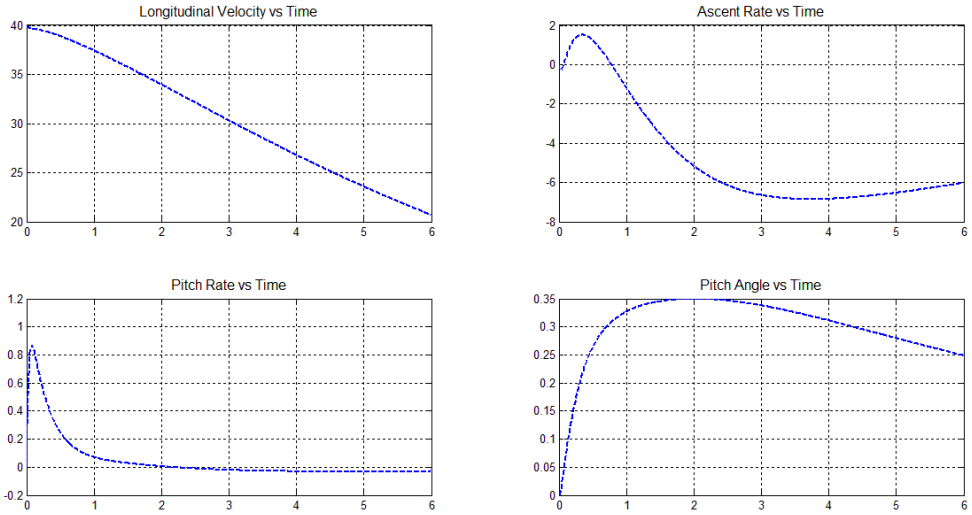

Fig.37 – *LQR* (with Bryson's Rule) Longitudinal Response

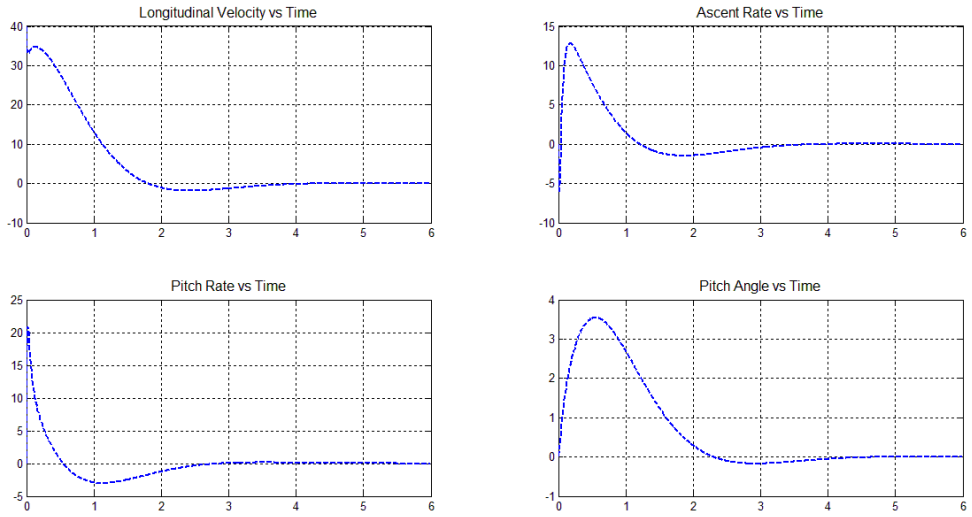

Fig.38 – *LQR* (with Pole Assignment) Longitudinal Response

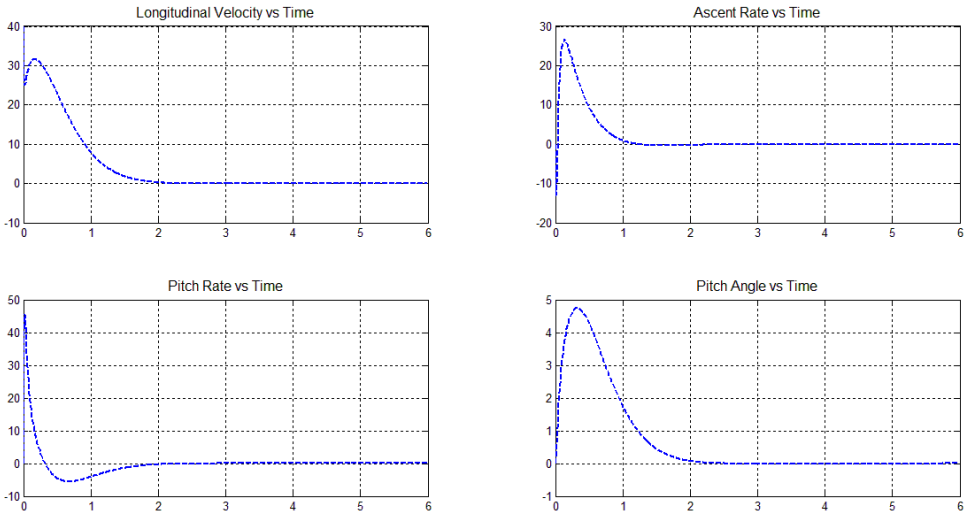

Fig.39 – Robust *LQR* (with Bryson's Rule) Longitudinal Response

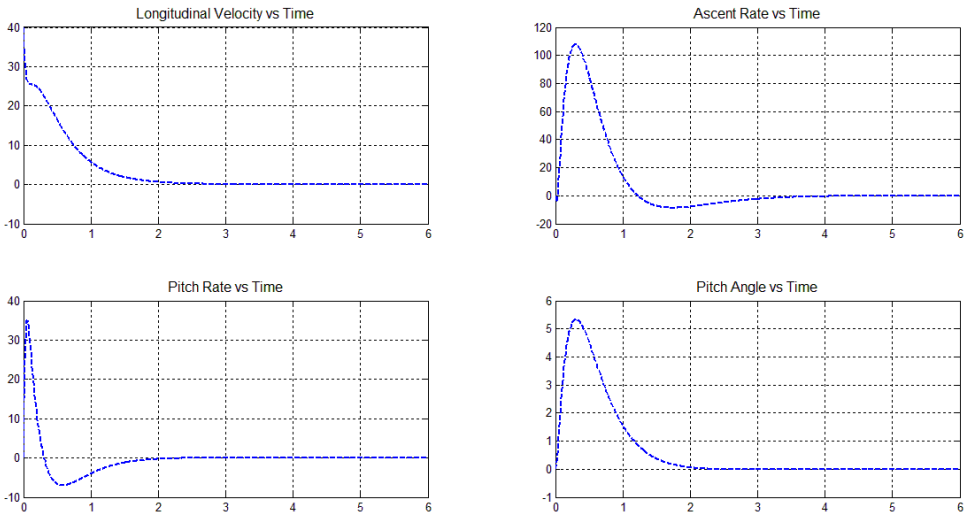

Fig.40 – Robust *LQR* (with Pole Assignment) Longitudinal Response

Lateral Simulation

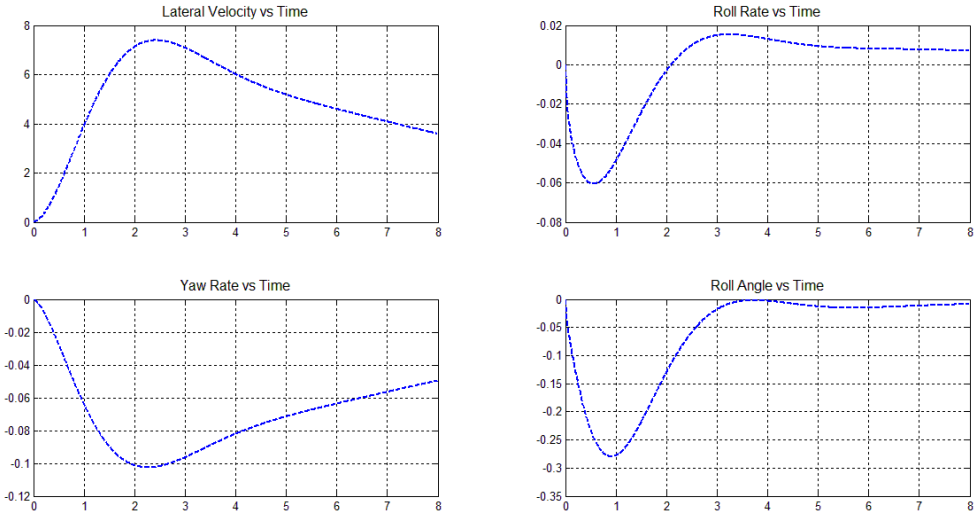

Fig.41 – *LQR* (with Bryson's Rule) Lateral Response

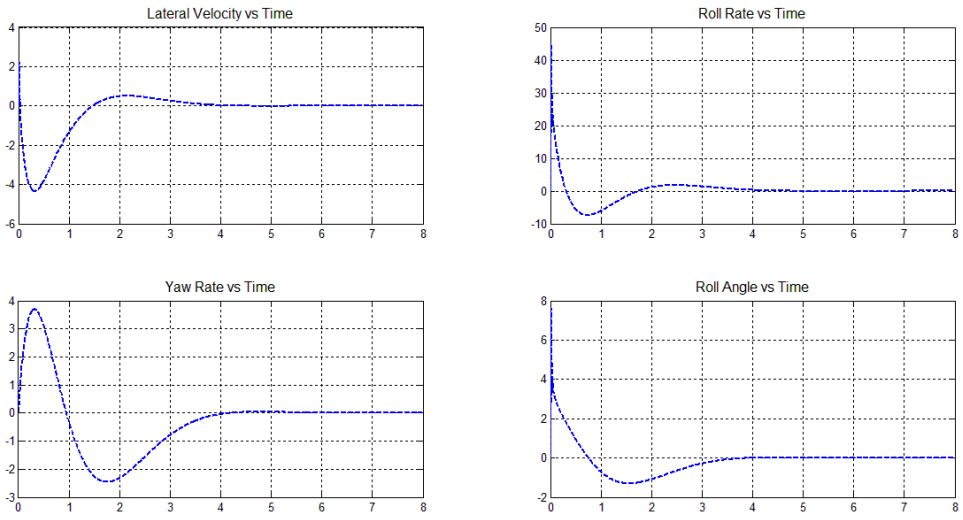

Fig.42 – *LQR* (with Pole Assignment) Lateral Response

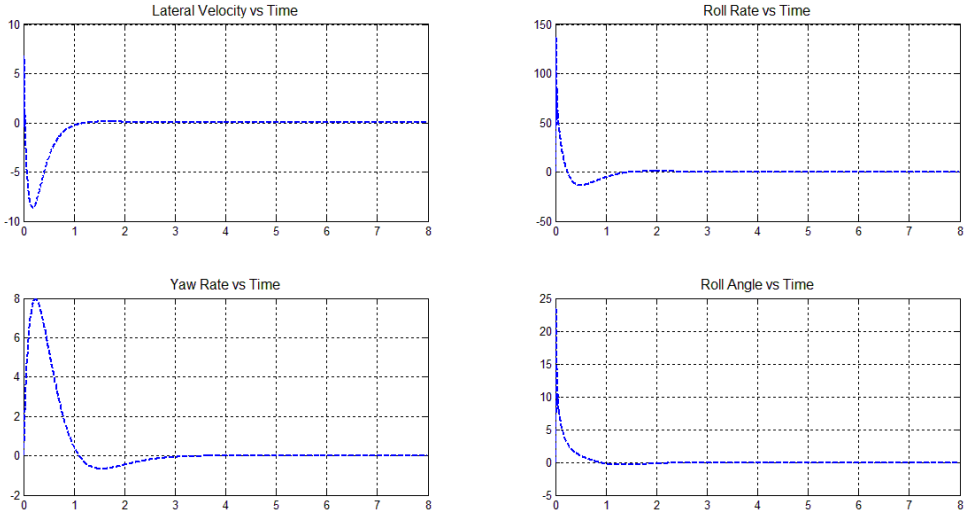

Fig.43 – Robust *LQR* (with Bryson's Rule) Lateral Response

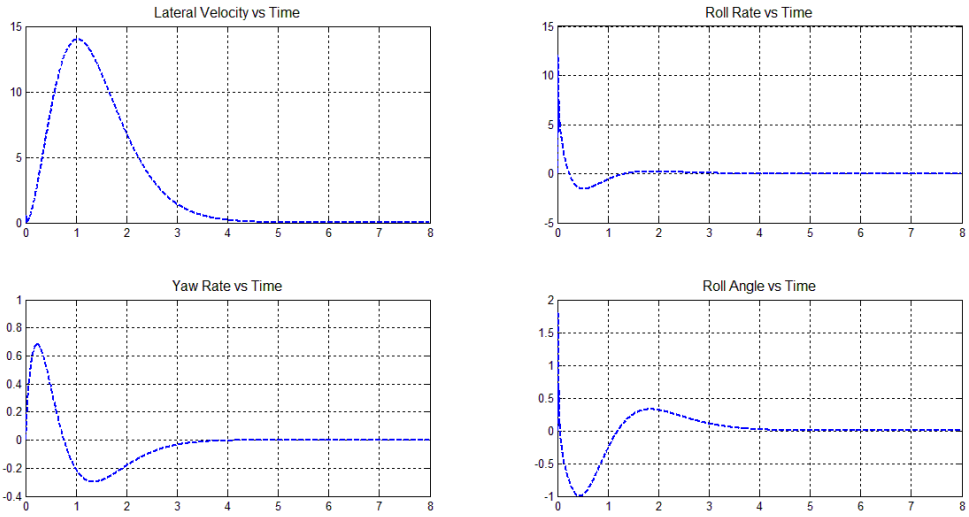

Fig.44 – Robust *LQR* (with Pole Assignment) Lateral Response

Forward Flight [V = 60]

$$A = \begin{bmatrix} -0.0243 & 0.0392 & -0.6705 & -9.8014 & -0.0041 & -0.1190 & 0.0000 & 0.0000 \\ -0.0467 & -0.7285 & 30.8640 & -0.4200 & -0.0186 & -0.3216 & 0.3117 & 0.0000 \\ 0.0280 & 0.0248 & -2.2156 & 0.0000 & 0.0159 & 0.4108 & 0.0000 & 0.0000 \\ 0.0000 & 0.0000 & 0.9995 & 0.0000 & 0.0000 & 0.0000 & 0.0000 & 0.0318 \\ 0.0035 & 0.0159 & -0.1293 & 0.0133 & -0.1228 & 0.6465 & 9.7964 & -30.5334 \\ -0.0437 & 0.2611 & -2.0532 & 0.0000 & -0.1713 & -10.6565 & 0.0000 & -0.2069 \\ 0.0000 & 0.0000 & -0.0014 & 0.0000 & 0.0000 & 1.0000 & 0.0000 & 0.0429 \\ -0.0273 & 0.0109 & -0.1661 & 0.0000 & 0.0529 & -1.8568 & 0.0000 & -0.9039 \end{bmatrix}$$

$$B = \begin{bmatrix} 4.6289 & -8.0560 & 2.0386 & 0.0000 \\ -107.3896 & -21.2288 & 0.0000 & 0.0000 \\ 10.7004 & 27.6889 & -5.8115 & 0.0000 \\ 0.0000 & 0.0000 & 0.0000 & 0.0000 \\ 1.4472 & -1.6712 & -9.3018 & 3.7509 \\ 31.4636 & -27.4424 & -153.3177 & -0.7505 \\ 0.0000 & 0.0000 & 0.0000 & 0.0000 \\ 14.5826 & -5.9178 & -27.0369 & -10.1087 \end{bmatrix}$$

Longitudinal Simulation

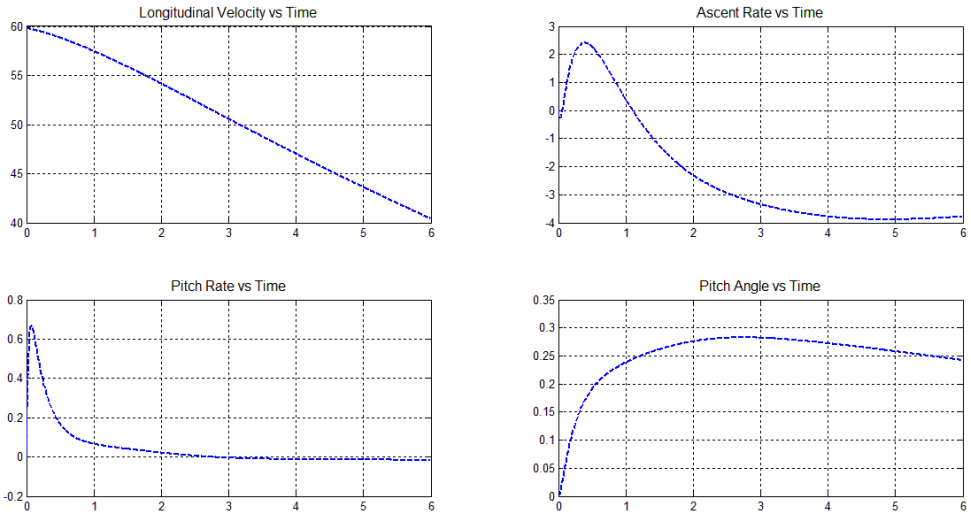

Fig.45 – *LQR* (with Bryson's Rule) Longitudinal Response

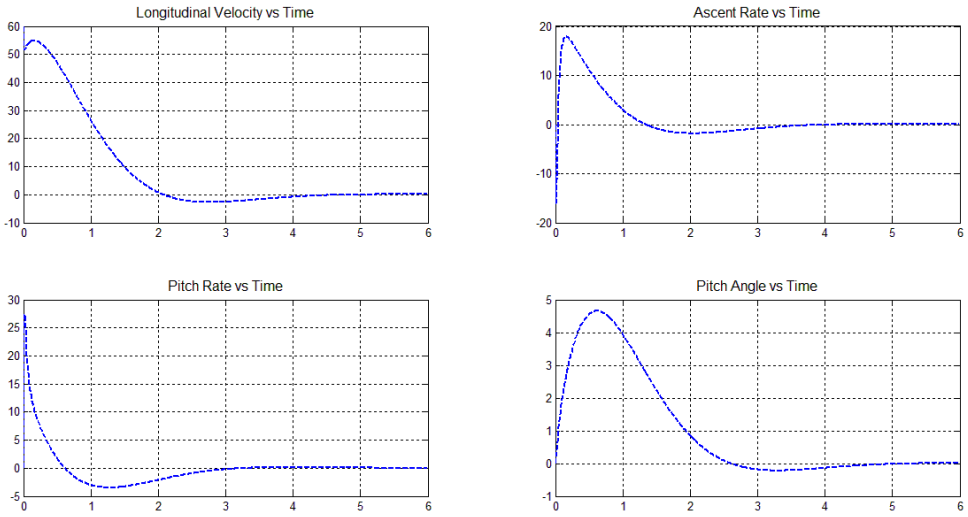

Fig.46 – *LQR* (with Pole Assignment) Longitudinal Response

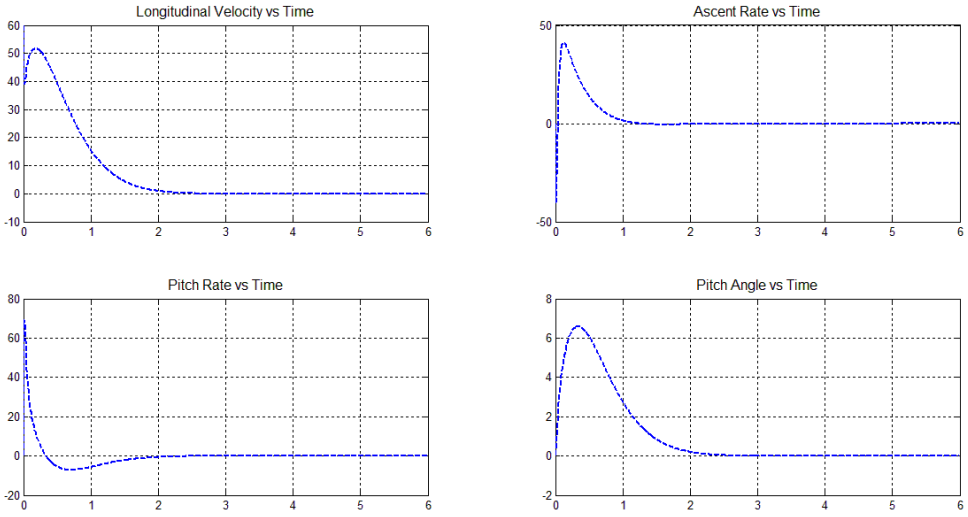

Fig.47 – Robust *LQR* (with Bryson's Rule) Longitudinal Response

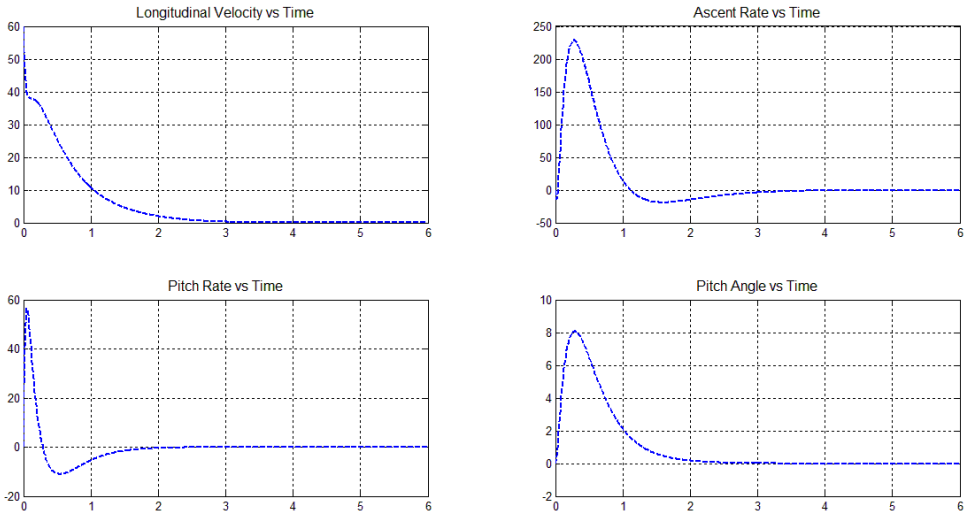

Fig.48 – Robust *LQR* (with Pole Assignment) Longitudinal Response

Lateral Simulation

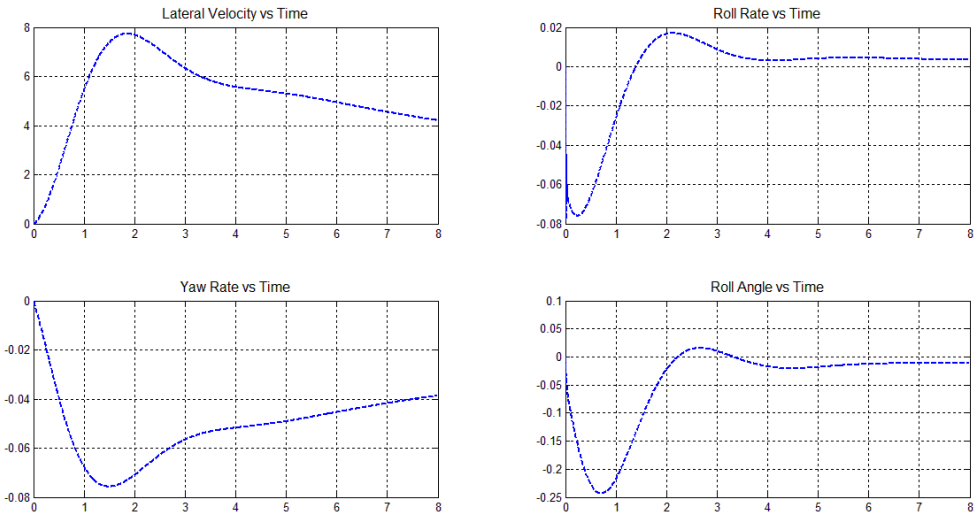

Fig.49– *LQR* (with Bryson's Rule) Lateral Response

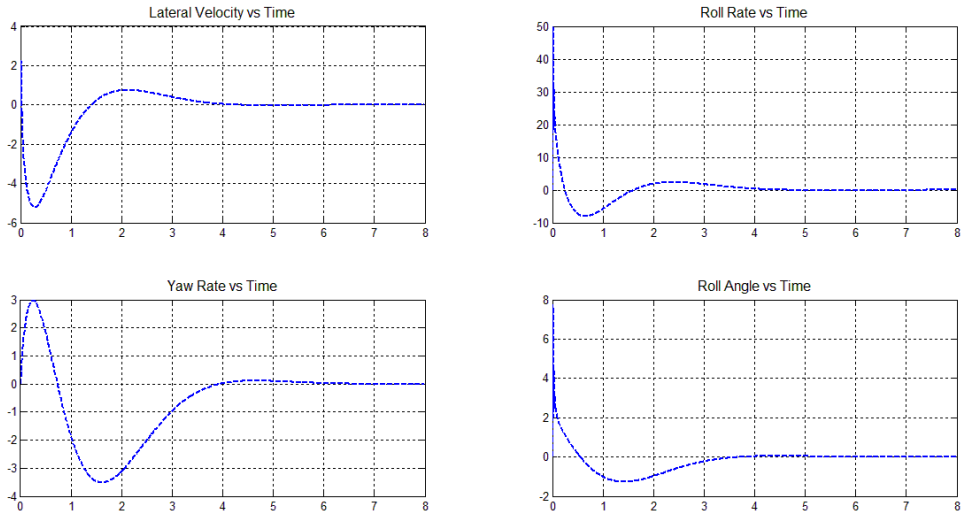

Fig.50 – *LQR* (with Pole Assignment) Lateral Response

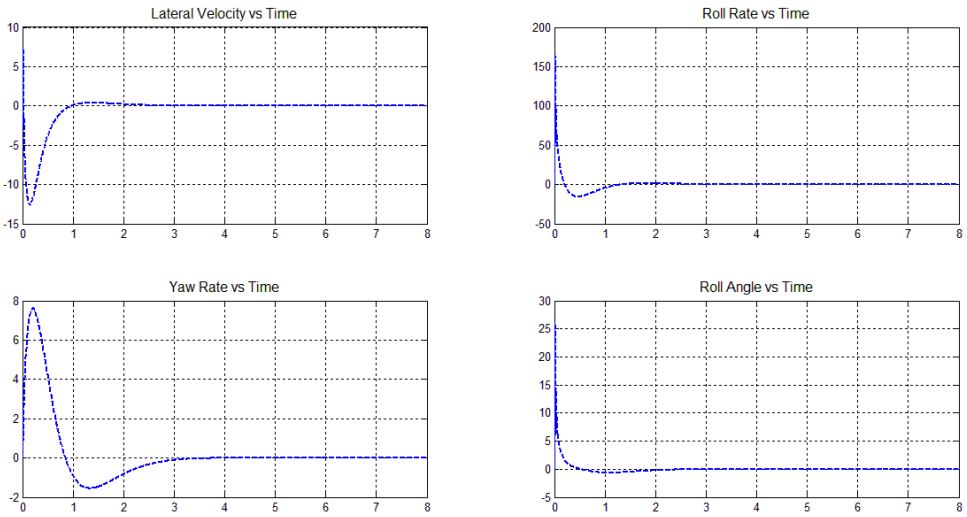

Fig.51 – Robust *LQR* (with Bryson's Rule) Longitudinal Response

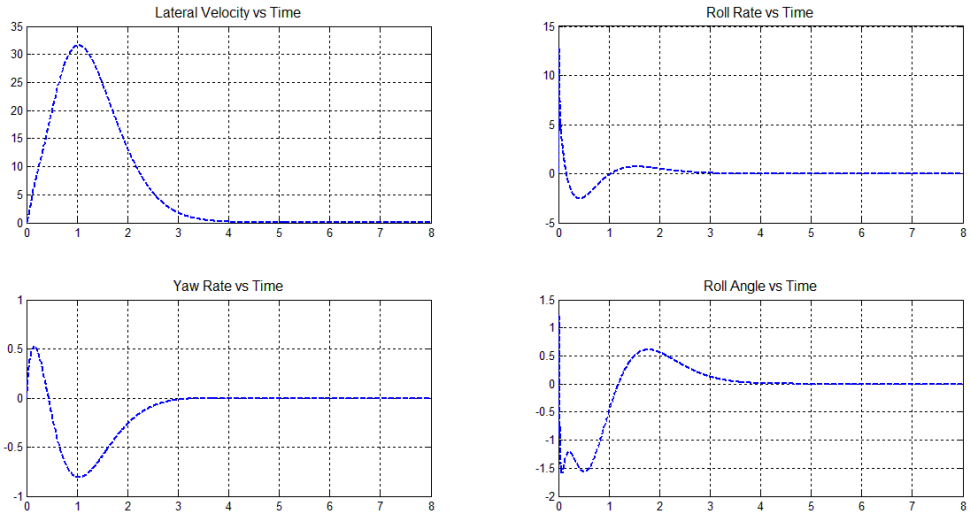

Fig.52 – Robust *LQR* (with Pole Assignment) Lateral Response

Forward Flight [V = 80]

$$A = \begin{bmatrix} -0.0322 & 0.0403 & -0.2262 & -9.8081 & -0.0021 & -0.1086 & 0.0000 & 0.0000 \\ -0.0010 & -0.8018 & 41.0936 & -0.2113 & -0.0194 & -0.4512 & 0.3223 & 0.0000 \\ 0.0271 & 0.0288 & -2.3350 & 0.0000 & 0.0104 & 0.4102 & 0.0000 & 0.0000 \\ 0.0000 & 0.0000 & 0.9995 & 0.0000 & 0.0000 & 0.0000 & 0.0000 & 0.0329 \\ 0.0032 & 0.0143 & -0.1287 & 0.0069 & -0.1535 & 0.2134 & 9.8028 & -40.7844 \\ -0.0371 & 0.2344 & -1.9959 & 0.0000 & -0.1659 & -10.5388 & 0.0000 & -0.2668 \\ 0.0000 & 0.0000 & -0.0007 & 0.0000 & 0.0000 & 1.0000 & 0.0000 & 0.0215 \\ -0.0227 & 0.0025 & -0.0877 & 0.0000 & 0.0662 & -1.8331 & 0.0000 & -1.0840 \end{bmatrix}$$

$$B = \begin{bmatrix} 4.3447 & -7.6327 & 2.0578 & 0.0000 \\ -117.7857 & -30.3913 & 0.0000 & 0.0000 \\ 14.0778 & 28.5401 & -5.8552 & 0.0000 \\ 0.0000 & 0.0000 & 0.0000 & 0.0000 \\ 1.4988 & -1.5282 & -9.3201 & 4.1854 \\ 32.0714 & -25.0312 & -153.2298 & -0.8376 \\ 0.0000 & 0.0000 & 0.0000 & 0.0000 \\ 13.9462 & -5.9565 & -26.8073 & -11.2811 \end{bmatrix}$$

Longitudinal Simulation

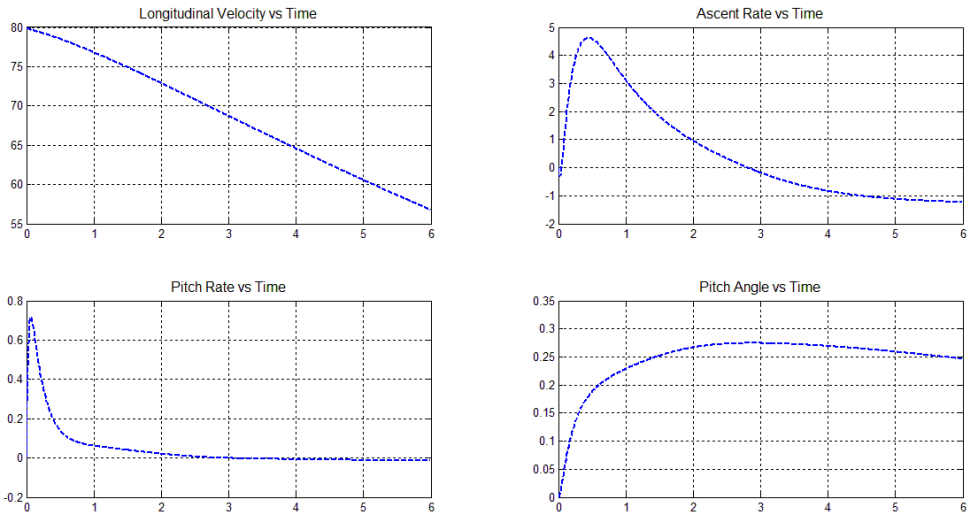

Fig.53 – *LQR* (with Bryson's Rule) Longitudinal Response

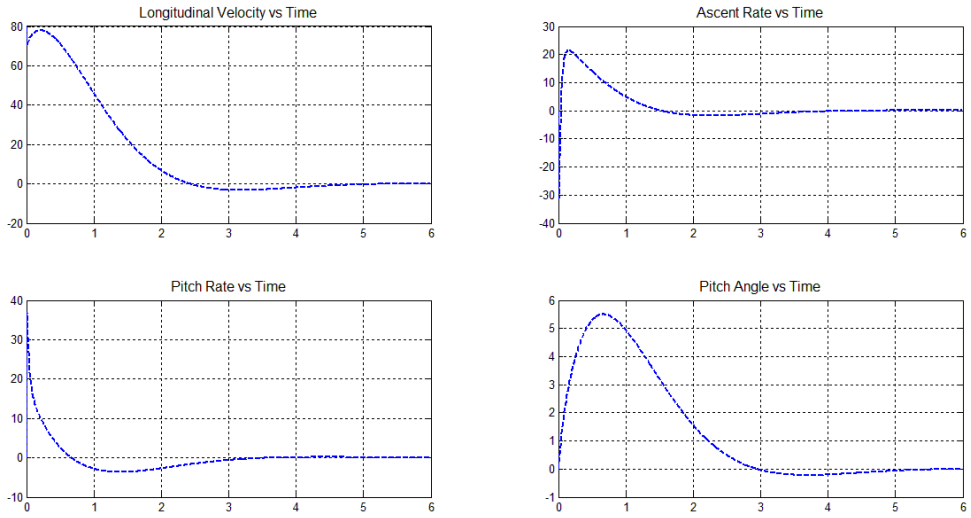

Fig.54 – *LQR* (with Pole Assignment) Longitudinal Response

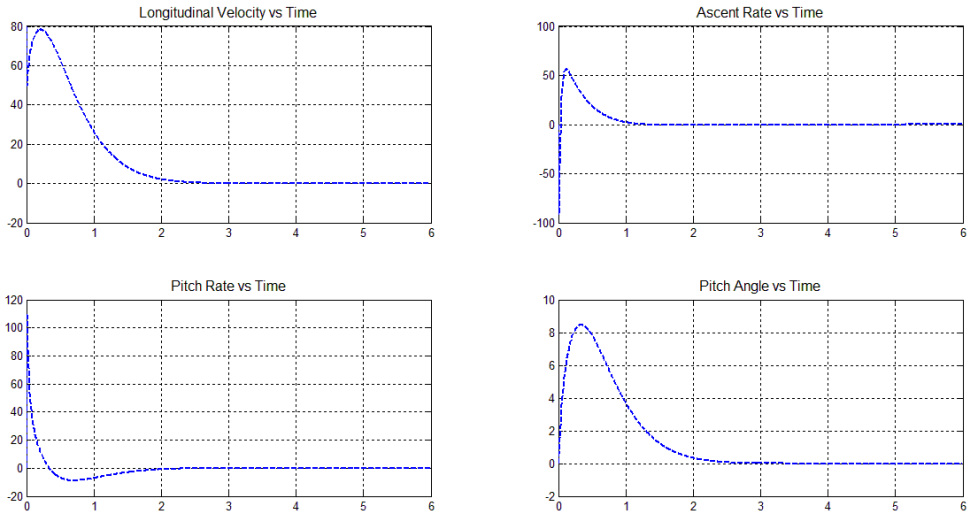

Fig.55 – Robust *LQR* (with Bryson's Rule) Longitudinal Response

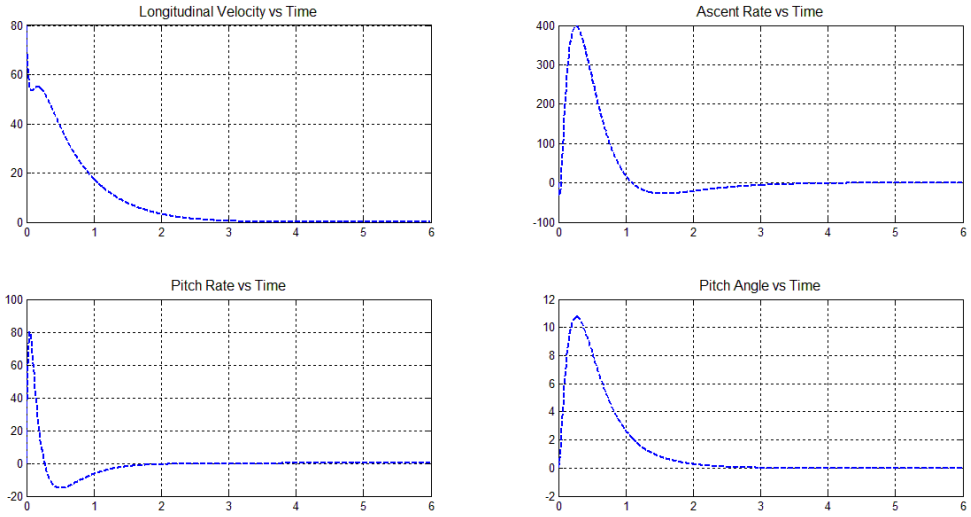

Fig.56 – Robust *LQR* (with Pole Assignment) Longitudinal Response

Lateral Simulation

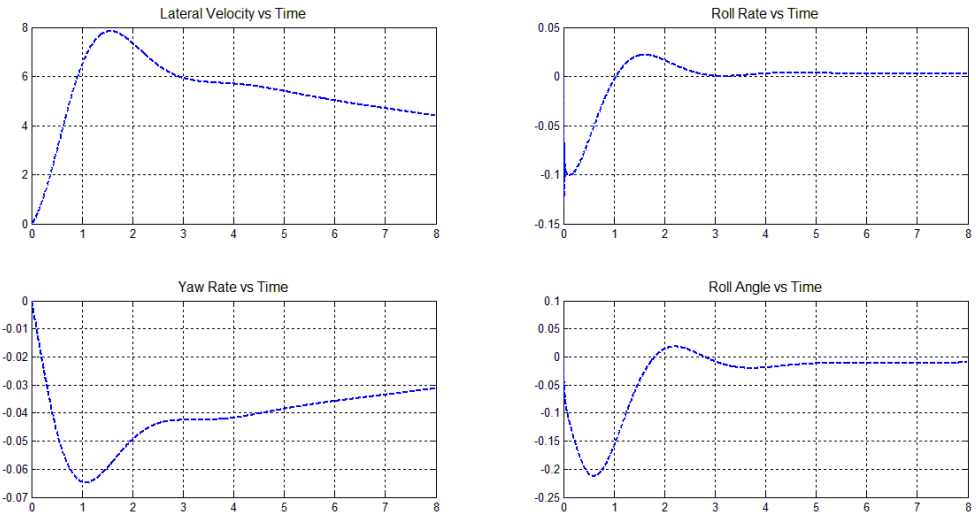

Fig.57 – *LQR* (with Bryson's Rule) Lateral Response

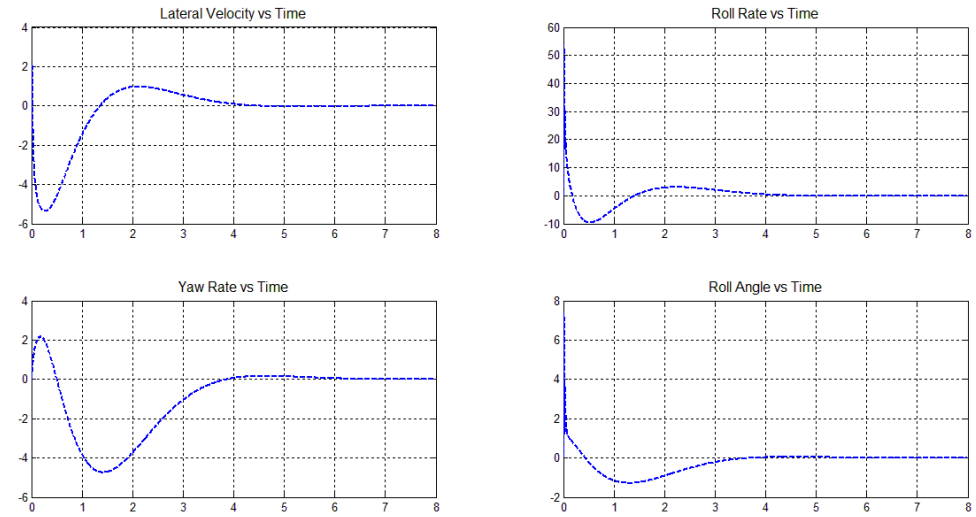

Fig.58 – *LQR* (with Pole Assignment) Lateral Response

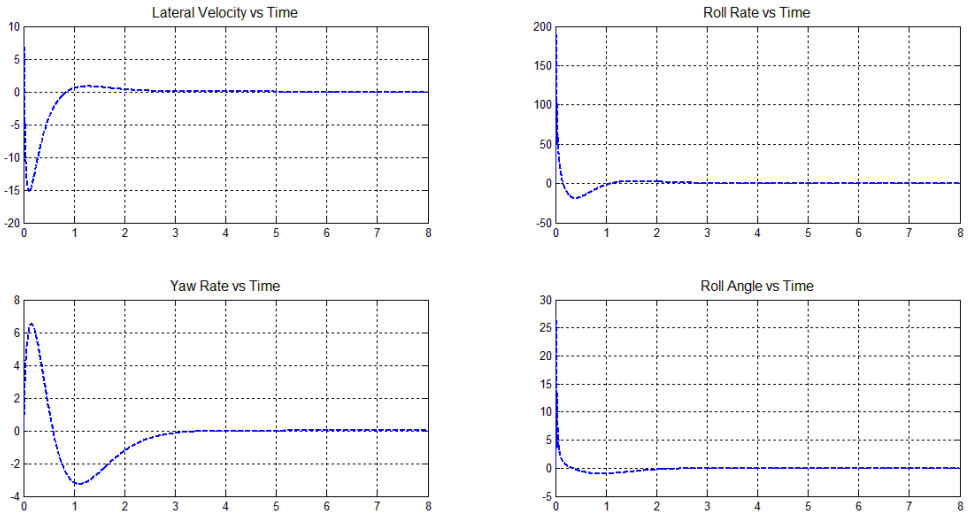

Fig.59 – Robust *LQR* (with Bryson's Rule) Lateral Response

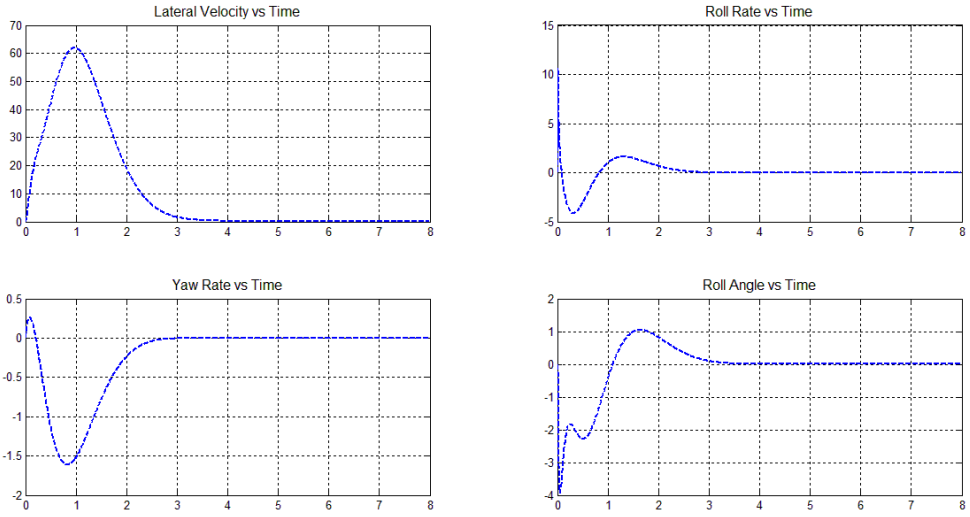

Fig.60 – Robust *LQR* (with Pole Assignment) Lateral Response

Forward Flight [V = 100]

$$A = \begin{bmatrix} -0.0393 & 0.0398 & 0.8831 & -9.8103 & -0.0010 & -0.0997 & 0.0000 & 0.0000 \\ 0.0104 & -0.8564 & 51.3352 & 0.0397 & -0.0210 & -0.5854 & 0.3744 & 0.0000 \\ 0.0279 & 0.0334 & -2.4604 & 0.0000 & 0.0075 & 0.4148 & 0.0000 & 0.0000 \\ 0.0000 & 0.0000 & 0.9993 & 0.0000 & 0.0000 & 0.0000 & 0.0000 & 0.0382 \\ 0.0037 & 0.0134 & -0.1282 & -0.0015 & -0.1838 & -0.8825 & 9.8032 & -51.0333 \\ -0.0327 & 0.2252 & -1.9302 & 0.0000 & -0.1713 & -10.4201 & 0.0000 & -0.3253 \\ 0.0000 & 0.0000 & 0.0002 & 0.0000 & 0.0000 & 1.0000 & 0.0000 & -0.0040 \\ -0.0219 & 0.0056 & -0.0044 & 0.0000 & 0.0751 & -1.8067 & 0.0000 & -1.2436 \end{bmatrix}$$

$$B = \begin{bmatrix} 4.0394 & -7.2845 & 2.0955 & 0.0000 \\ -126.8300 & -39.8088 & 0.0000 & 0.0000 \\ 17.4865 & 29.6369 & -5.9169 & 0.0000 \\ 0.0000 & 0.0000 & 0.0000 & 0.0000 \\ 1.5127 & -1.4002 & -9.4000 & 4.5569 \\ 32.9346 & -22.4516 & -153.2494 & -0.9119 \\ 0.0000 & 0.0000 & 0.0000 & 0.0000 \\ 14.7283 & -5.6161 & -26.5849 & -12.2824 \end{bmatrix}$$

Longitudinal Simulation

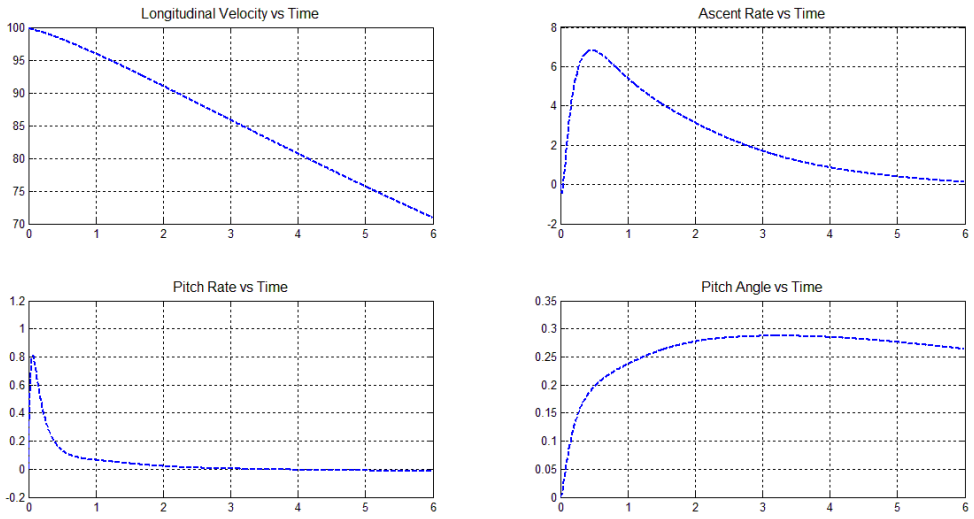

Fig.61 – *LQR* (with Bryson's Rule) Longitudinal Response

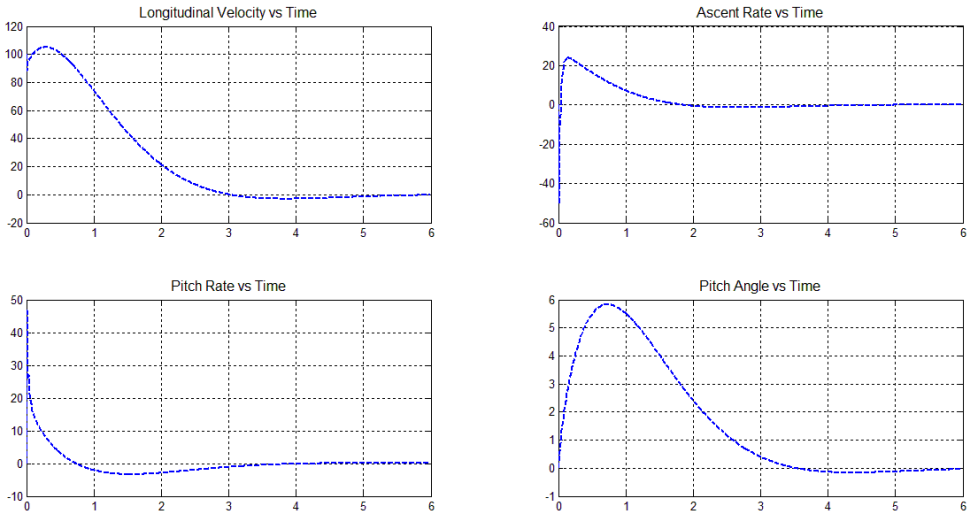

Fig.62 – *LQR* (with Pole Assignment) Longitudinal Response

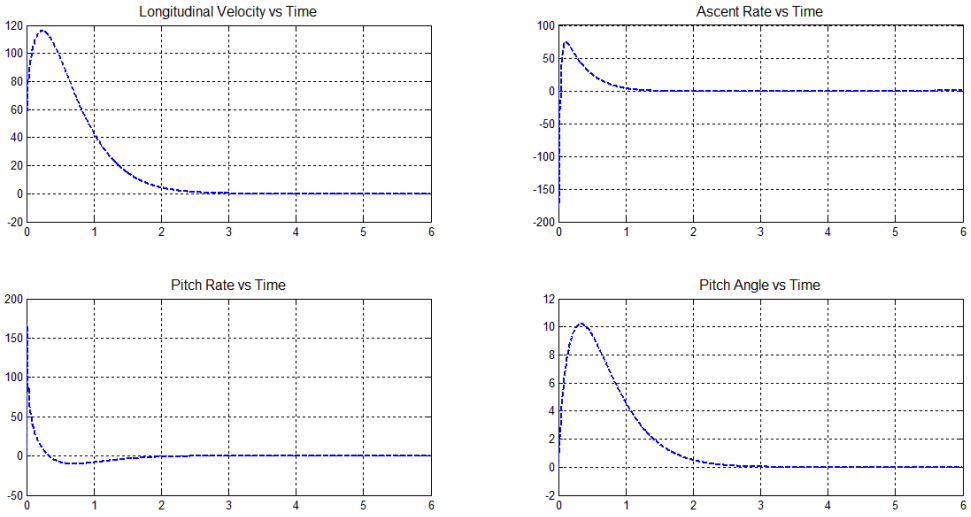

Fig.63 – Robust *LQR* (with Bryson's Rule) Longitudinal Response

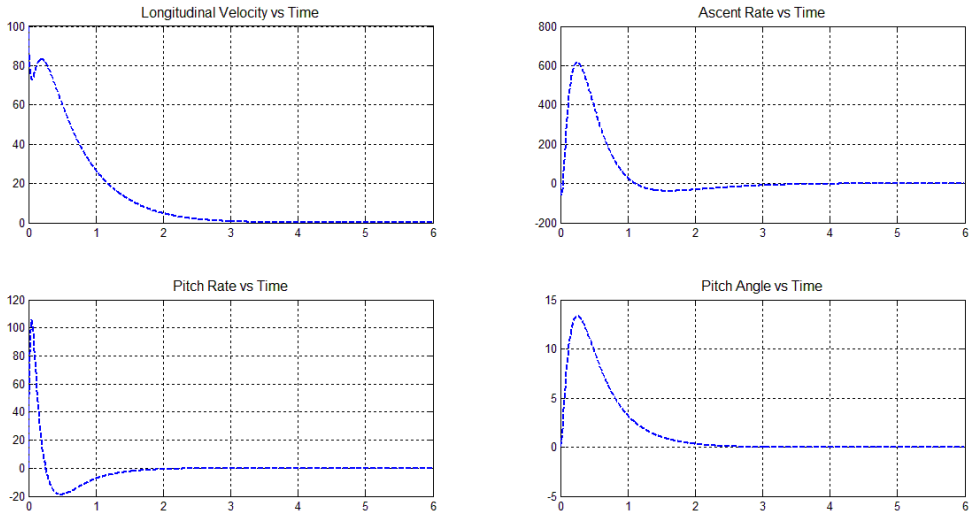

Fig.64 – Robust *LQR* (with Pole Assignment) Longitudinal Response

Lateral Simulation

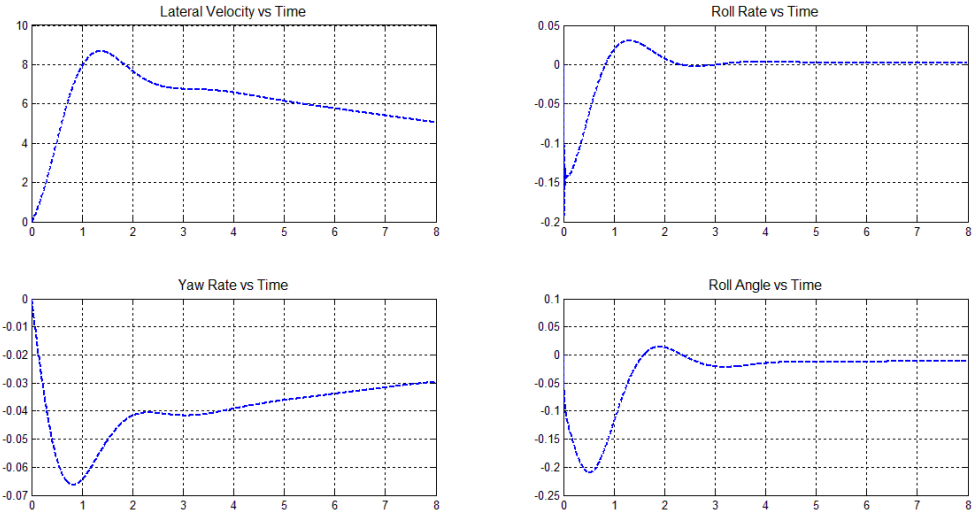

Fig.65 – *LQR* (with Bryson's Rule) Lateral Response

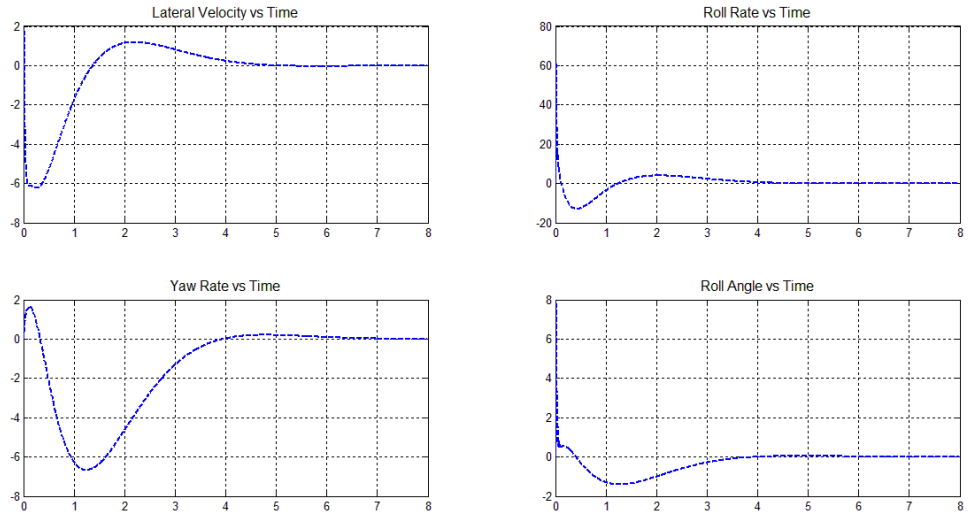

Fig.66 – *LQR* (with Pole Assignment) Lateral Response

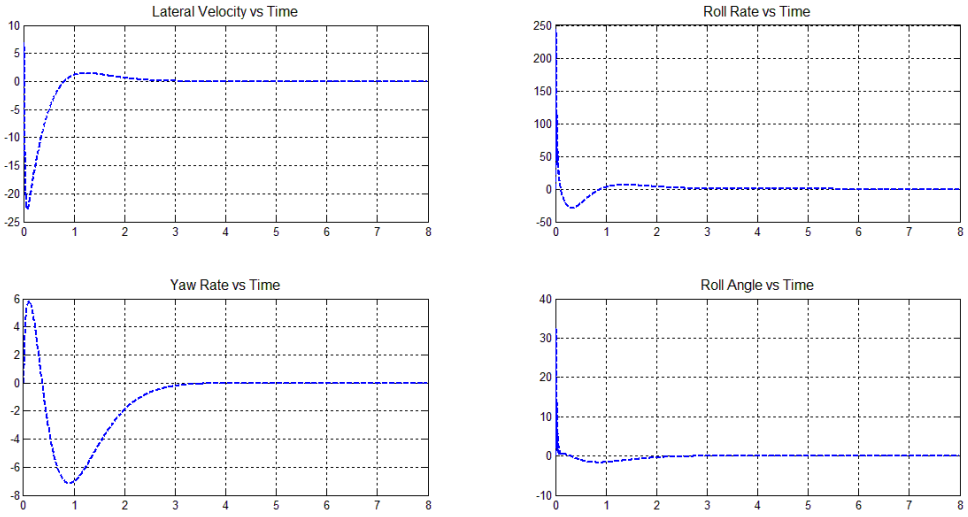

Fig.67 – Robust *LQR* (with Bryson's Rule) Lateral Response

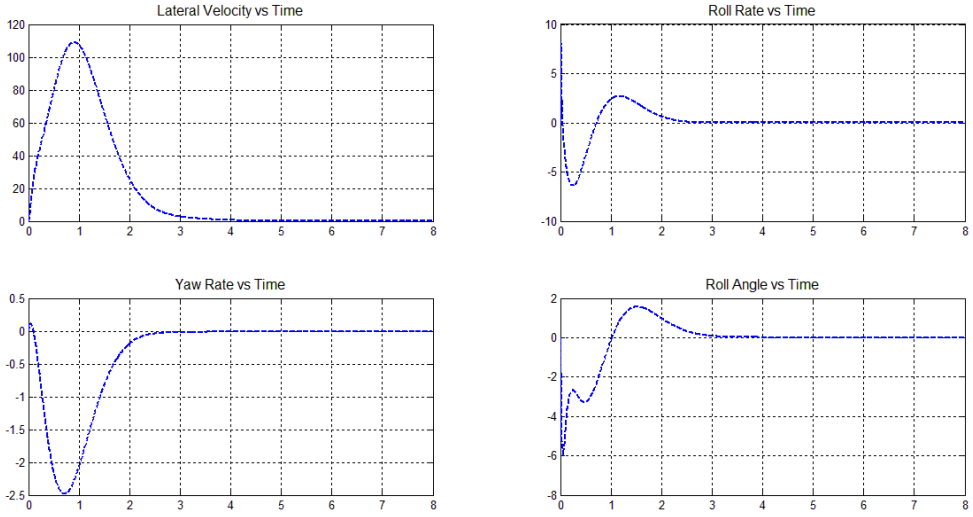

Fig.68 – Robust *LQR* (with Pole Assignment) Lateral Response

Forward Flight [V = 120]

$$A = \begin{bmatrix} -0.0460 & 0.0385 & 2.7192 & -9.8052 & -0.0001 & -0.0916 & 0.0000 & 0.0000 \\ 0.0221 & -0.9008 & 61.5464 & 0.3205 & -0.0236 & -0.7219 & 0.4681 & 0.0000 \\ 0.0299 & 0.0380 & -2.5919 & 0.0000 & 0.0058 & 0.4225 & 0.0000 & 0.0000 \\ 0.0000 & 0.0000 & 0.9989 & 0.0000 & 0.0000 & 0.0000 & 0.0000 & 0.0477 \\ 0.0043 & 0.0129 & -0.1283 & -0.0152 & -0.2142 & -2.7024 & 9.7940 & -61.2455 \\ -0.0320 & 0.2281 & -1.8534 & 0.0000 & -0.1847 & -10.2992 & 0.0000 & -0.3827 \\ 0.0000 & 0.0000 & 0.0016 & 0.0000 & 0.0000 & 1.0000 & 0.0000 & -0.0327 \\ -0.0237 & 0.0187 & 0.0877 & 0.0000 & 0.0811 & -1.7721 & 0.0000 & -1.3896 \end{bmatrix}$$

$$B = \begin{bmatrix} 3.8024 & -7.0223 & 2.1602 & 0.0000 \\ -135.2500 & -49.3051 & 0.0001 & 0.0000 \\ 20.9344 & 30.9867 & -6.0002 & 0.0000 \\ 0.0000 & 0.0000 & 0.0000 & 0.0000 \\ 1.5360 & -1.2845 & -9.5747 & 4.8851 \\ 34.9038 & -19.4471 & -153.4332 & -0.9776 \\ 0.0000 & 0.0000 & 0.0000 & 0.0000 \\ 17.1838 & -4.6280 & -26.3702 & -13.1671 \end{bmatrix}$$

Longitudinal Simulation

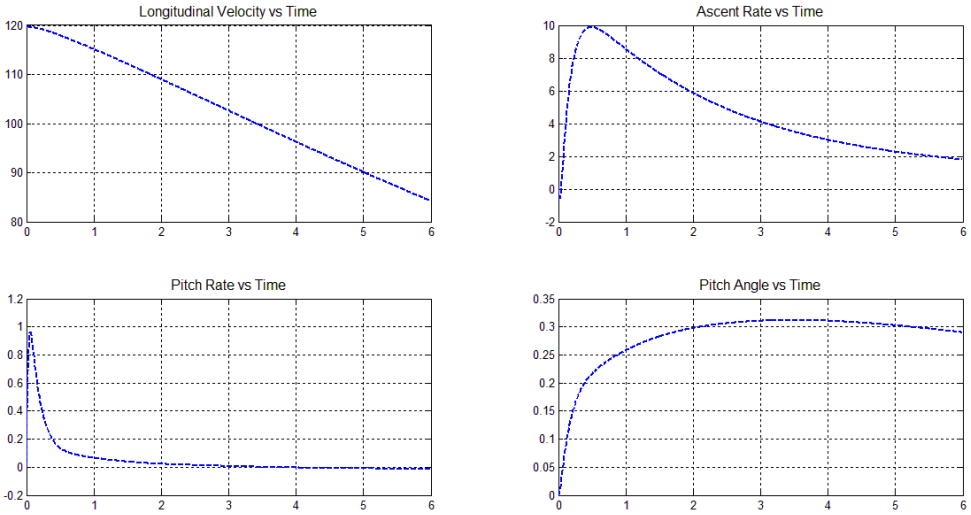

Fig.69 – *LQR* (with Bryson's Rule) Longitudinal Response

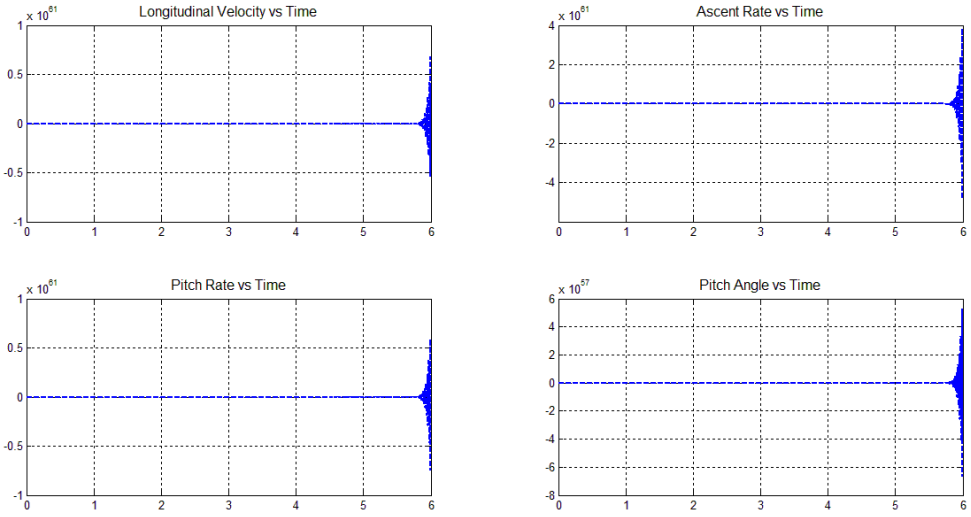

Fig.70 – *LQR* (with Pole Assignment) Longitudinal Response

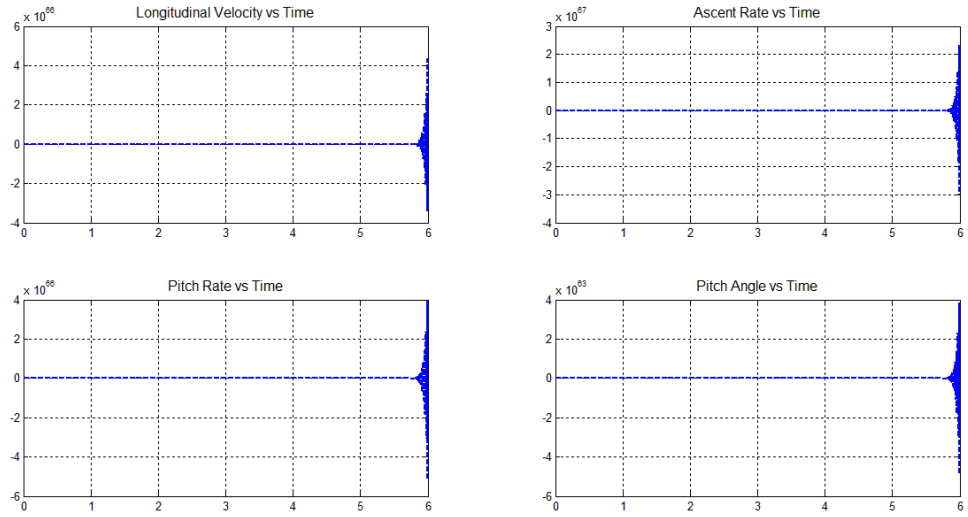

Fig.71 – Robust *LQR* (with Bryson's Rule) Longitudinal Response

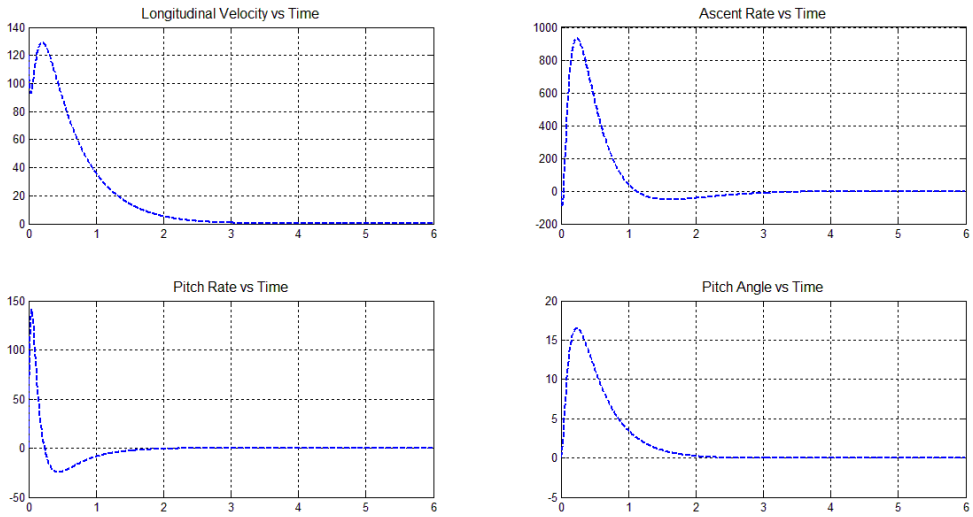

Fig.72 – Robust *LQR* (with Pole Assignment) Longitudinal Response

Lateral Simulation

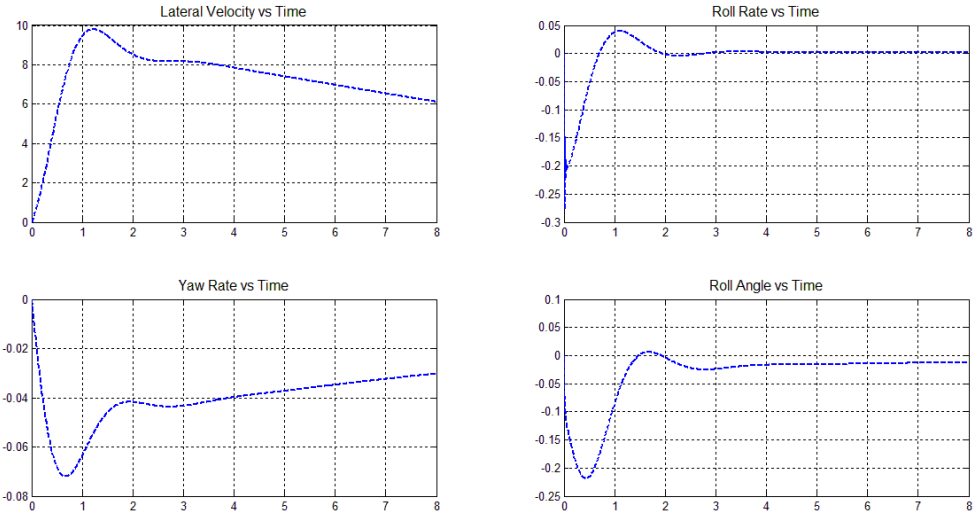

Fig.73 – *LQR* (with Bryson's Rule) Lateral Response

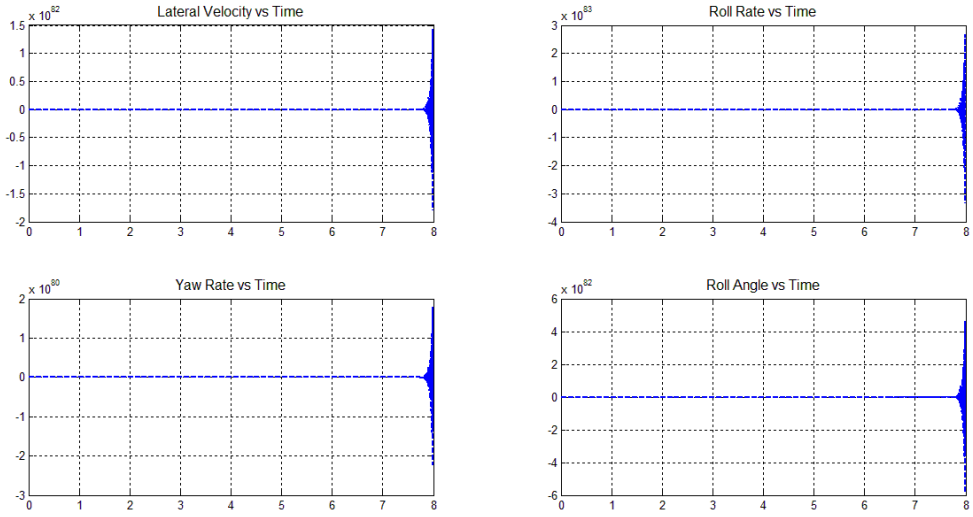

Fig.74 – *LQR* (with Pole Assignment) Lateral Response

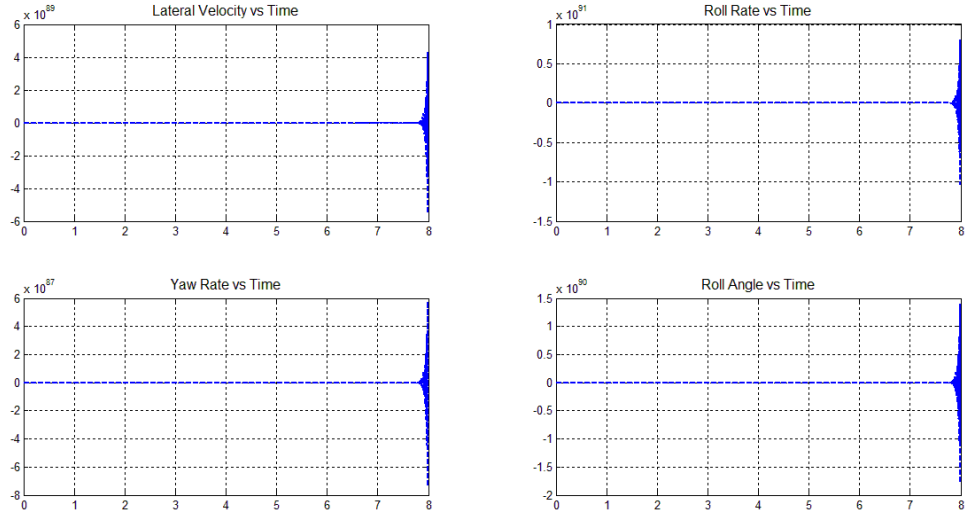

Fig.75 – Robust *LQR* (with Bryson's Rule) Lateral Response

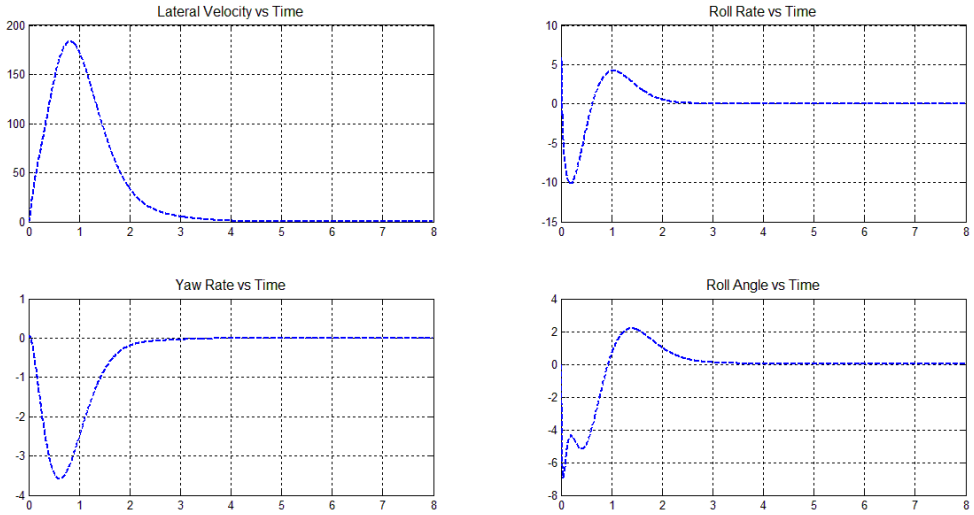

Fig.76 – Robust *LQR* (with Pole Assignment) Lateral Response

Forward Flight [V = 140]

$$A = \begin{bmatrix} -0.0525 & 0.0370 & 5.2710 & -9.7910 & 0.0000 & -0.0838 & 0.0000 & 0.0000 \\ 0.0286 & -0.9392 & 71.6880 & 0.6160 & -0.0272 & -0.8596 & 0.6083 & 0.0000 \\ 0.0328 & 0.0426 & -2.7297 & 0.0000 & 0.0047 & 0.4327 & 0.0000 & 0.0000 \\ 0.0000 & 0.0000 & 0.9981 & 0.0000 & 0.0000 & 0.0000 & 0.0000 & 0.0621 \\ 0.0052 & 0.0127 & -0.1297 & -0.0383 & -0.2446 & -5.2343 & 9.7720 & -71.3836 \\ -0.0338 & 0.2396 & -1.7657 & 0.0000 & -0.2050 & -10.1775 & 0.0000 & -0.4394 \\ 0.0000 & 0.0000 & 0.0039 & 0.0000 & 0.0000 & 1.0000 & 0.0000 & -0.0629 \\ -0.0269 & 0.0406 & 0.1928 & 0.0000 & 0.0851 & -1.7264 & 0.0000 & -1.5264 \end{bmatrix}$$

$$B = \begin{bmatrix} 3.6956 & -6.8427 & 2.2599 & 0.0000 \\ -143.5034 & -58.7853 & 0.0001 & 0.0000 \\ 24.4192 & 32.5904 & -6.1083 & 0.0000 \\ 0.0000 & 0.0000 & 0.0000 & 0.0000 \\ 1.5764 & -1.1831 & -9.8730 & 5.1875 \\ 38.1461 & -15.8917 & -153.8247 & -1.0381 \\ 0.0000 & 0.0000 & 0.0000 & 0.0000 \\ 21.4497 & -2.7783 & -26.1582 & -13.9821 \end{bmatrix}$$

Longitudinal Simulation

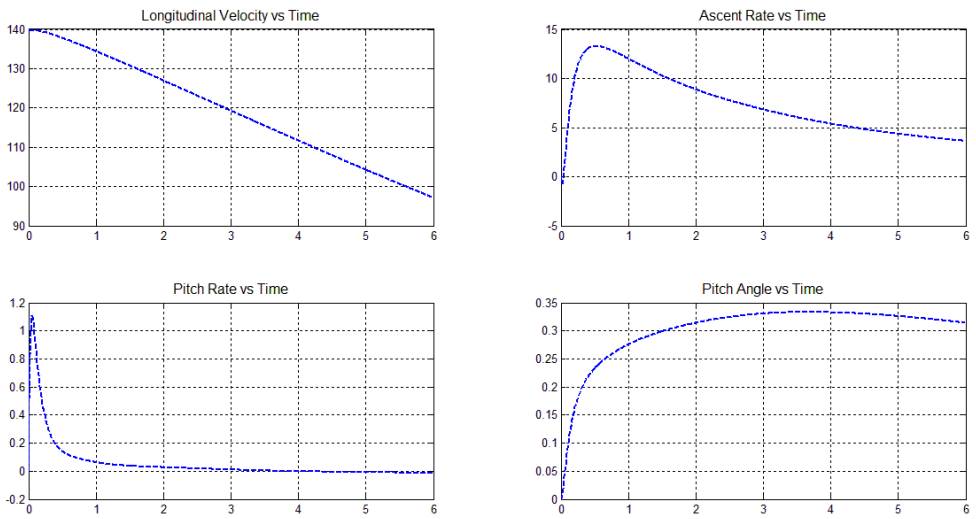

Fig.77 – *LQR* (with Bryson's Rule) Longitudinal Response

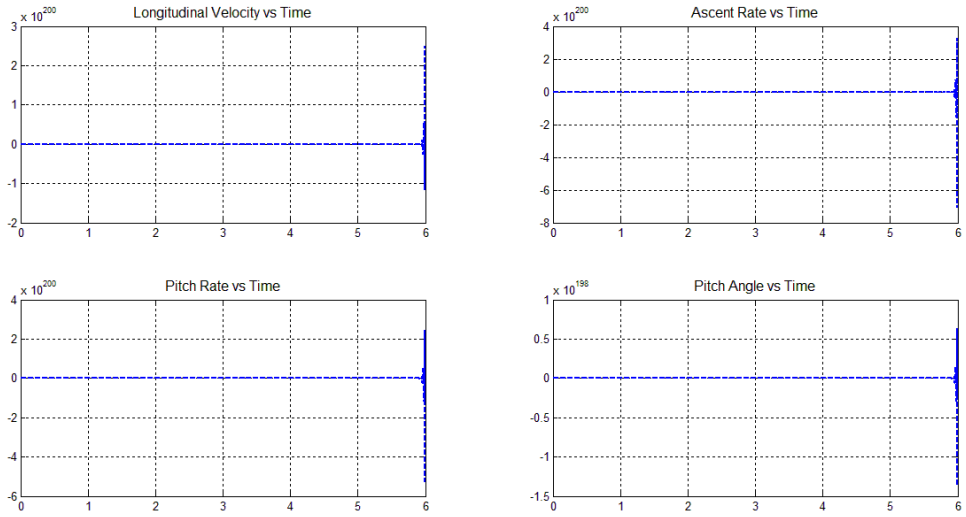

Fig.78 – *LQR* (with Pole Assignment) Longitudinal Response

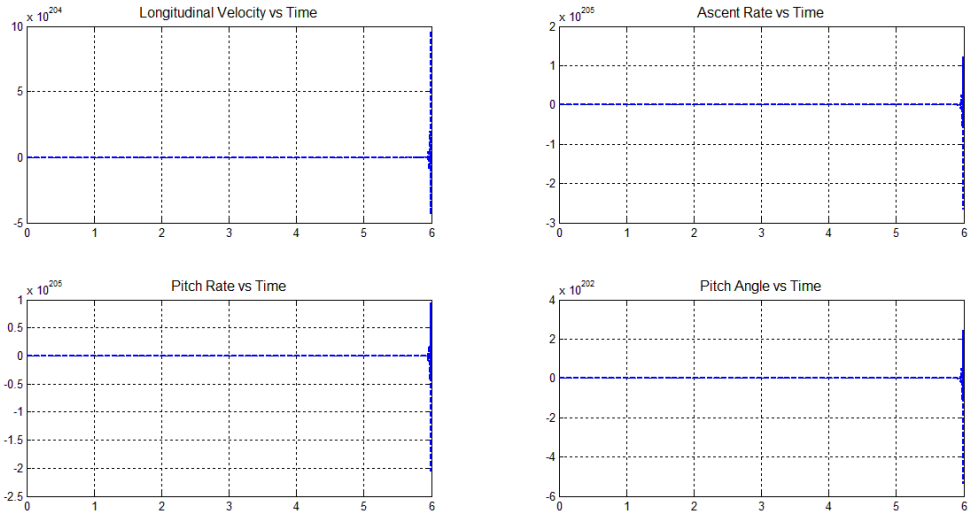

Fig.79 – Robust *LQR* (with Bryson's Rule) Longitudinal Response

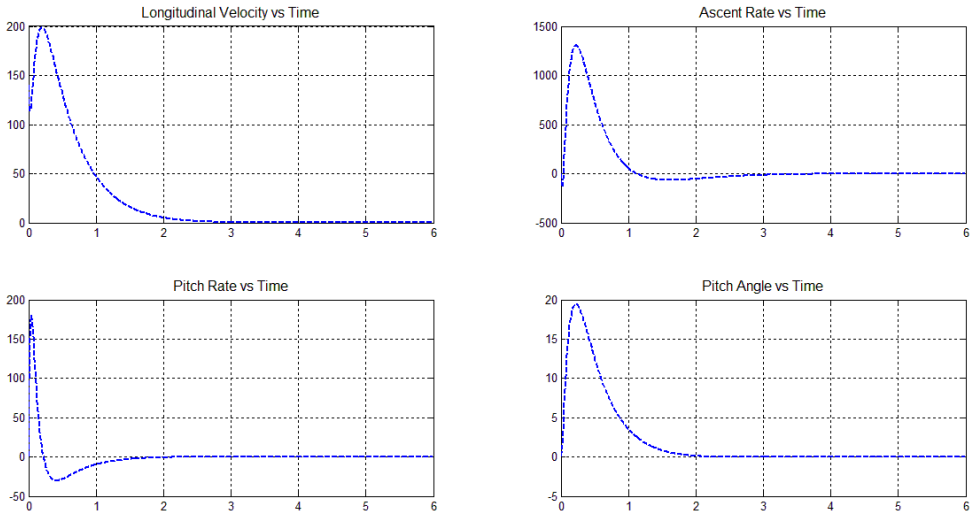

Fig.80 – Robust *LQR* (with Pole Assignment) Longitudinal Response

Lateral Simulation

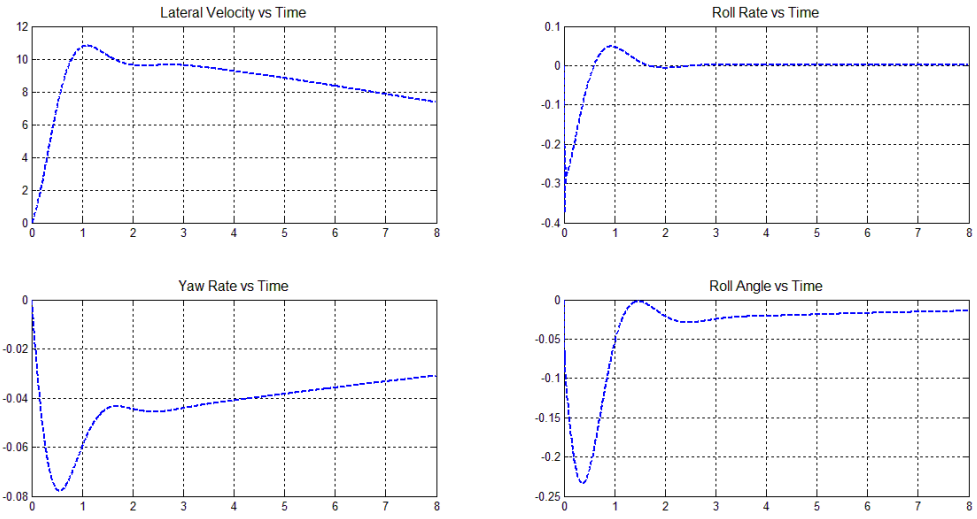

Fig.81 – *LQR* (with Bryson's Rule) Lateral Response

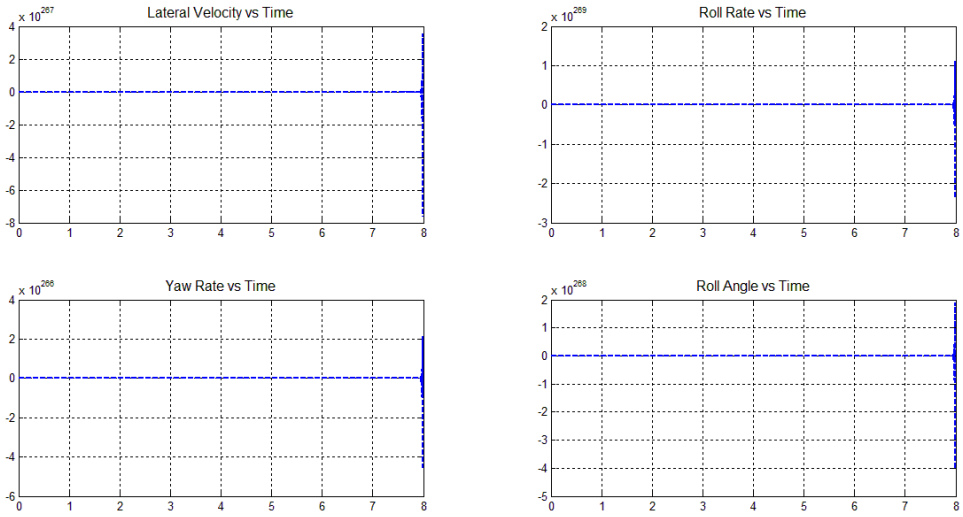

Fig.82 - *LQR* (with Pole Assignment) Lateral Response

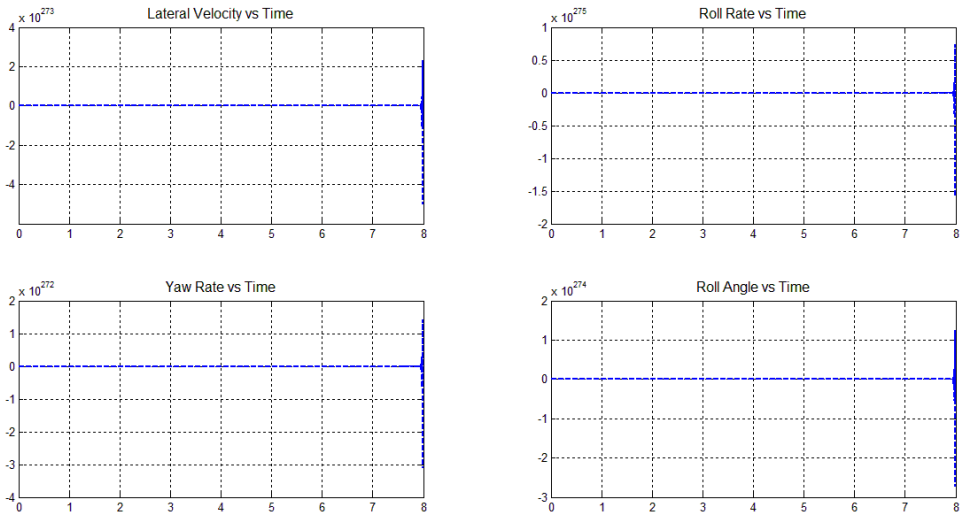

Fig.83 – Robust *LQR* (with Bryson's Rule) Lateral Response

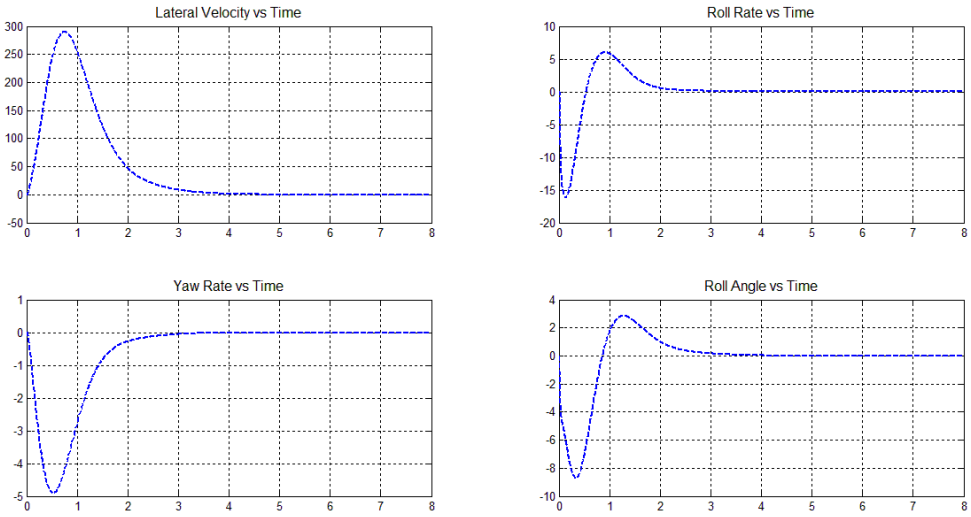

Fig.84 – Robust *LQR* (with Pole Assignment) Lateral Response